THESIS

DEVELOPMENT OF NOVEL RE-MINERALISING, ANTI-BACTERIAL DENTAL COMPOSITES

Thesis submitted by

Lama Ismat Dakkouri

DDS (Jordan), MFD (Ireland)

In partial fulfilment of the requirements for the Degree of

DENTAL DOCTORATE IN DENTISTRY (PAEDIATRIC DENTISTRY)

UNIVERSITY COLLEGE LONDON

Eastman Dental Institute

2015

Dedicated to

My Father

I offer my sincerest appreciation to my Father, Ismat Dakkouri, who has supported me throughout my life with his love and care whilst giving me the chance to achieve my own dreams. I attribute it all to his encouragement and effort and without him I will never be here. I recognise that this research would not have been possible without his financial assistance. One simply could not wish for a better father. This thesis, too, would not have been completed or written without the support of my lovely mother. It was through her, love, caring and kindness that I was able to accomplish my goals.

DECLARATION OF ORIGINALITY

I hereby declare that the work represented in this thesis is the result of my own investigations, except where otherwise stated. Information imitative from the published and unpublished work of others had been acknowledged in the text and the relevant references are included in this thesis.

Lama Ismat Dakkouri

Eastman Dental Institute, University College London

September 2015

ACKNOWLEDGMENT

First and foremost, I am grateful to God for the good health and wellbeing that were necessary to complete this thesis. Also, I would like to express my deepest gratitude to my supervisors Dr Anne Young and Dr Paul Ashley, for their excellent guidance, supervision, kindness, and patience. Their understanding and knowledge added considerably to my research experience.

I would also like to thank my lovely family and especially my parents for the support they provided me through my entire life. Thank you for all your motivation and guidance. I would also like to thank my youngest brother, Mohammed, for all his love and encouragement in my educational journey. I doubt that I will ever be able to convey my appreciation fully, but I owe him my eternal gratitude. I would also like to thank my elder sister, Maram, and her lovely family, my elder brother, Yazid, and my brother in law, Thaer. They were always supporting me and encouraging me with their best wishes.

A very special thanks goes out to the sweetest sister and best friend, Layan Mehyar, for her constant wishes and inspiration. She was always there cheering me up and stood by me through the good times and bad. I would also like to thank my friends, Fairouz, Zeena, Marry, and Salah for their constant wishes. I would never have been able to finish my thesis without their support and help. A big thanks to my colleagues at the paediatric department, thank you for Salwa, Khalefa, Nada, Abdulfattah, Shaima, Shaikha, May, and Albatool for their care and support.

I would like to thank Dr Wendy Xia, Nick Walters, Piyaphong Panpisut, Saad Liaqat, and Abeer Al Shami for all their help and assistance. They were always willing to help and give their best suggestions. In which their assistance helped me along the way. Many thanks to my friend Soha Alqadi for our exchanges of knowledge, skills, and venting of frustration during the research program, which helped enrich the experience, also it would have been a lonely lab without her. I would like to thank the other members of my group, for their assistance and guidance they provided at all levels of the research project.

Finally, I must also acknowledge every person who made my educational journey in London special and memorable. Special last thank you to Joao, Joy, Moutassum, Sireen, Hamsa, Sama, and Lino.

ABSTRACT

The most common current cause of composite restoration failure is bacterial micro-leakage. This is the passage of bacteria between the tooth and restoration and results in continuing dentine de-mineralisation and disease. The **aim** of this study was therefore to develop a dental composite with re-mineralising and anti-bacterial components.

Methods: Urethane dimethacrylate: poly(propylene glycol) dimethacryate (3:1) was mixed with 5 wt% 2-hydroxyethyl methacrylate, 1 wt% photoinitiator (camphorquinone), and 1 wt% accelerator (*N*(*p*-tolyl)glycine-glycidyl methacrylate). This was combined with dental glass particles mixed with anti-bacterial polylysine (0 or 5 wt%) and mono and tri calcium phosphate (each at 0 or 20 wt%) in a powder to liquid ratio of 4:1. Light cured composite discs (10 mm diameter, 1 mm thick, n=8) were prepared and stored dry, in distilled water (DW), simulated body fluid (SBF) or Artificial Saliva. Surfaces were examined by Scanning-electron microscopy (SEM), Energy-dispersive X-ray (EDX) spectroscopy and Raman microscopy after 7 days storage. Mass and volume changes in DW and SBF were determined gravimetrically at 12-weeks storage. Polylysine release into water was assessed using Trypan Blue dye and visible absorbance spectroscopy.

Results: Various calcium phosphates precipitated on the material surfaces and cores but apatite was found only on the surface of samples containing both calcium phosphates and Polylysine that were stored in SBF. This formula showed greater increase in mass and volume change, and the highest Polylysine release. Composite containing both calcium phosphates (MCPM and TCP) and polylysine showed the highest water sorption potential and therefore more precipitation and increase in volume. Also, adding both MCPM and TCP slightly enhanced the release of the anti-bacterial (polylysine).

Significance: Formulations with MCPM, TCP and polylysine through water sorption induced expansion; re-mineralisation and anti-bacterial release have potential to reduce recurrent caries.

Key words: composite, restoration, remineralisation, anti-bacterial.

Table of Contents

DECLARATION OF ORIGINALITY **3**
ACKNOWLEDGMENT **4**
ABSTRACT **5**
List of tables **8**
List of figures **10**
List of equations **14**
List of abbreviations **15**
Introduction **17**
1.1 Teeth: **18**
1.2 Importance of teeth: **19**
1.3 Caries: **19**
1.3.1 Histopathology of caries in enamel: 20
1.3.2 Histopathology of caries in dentine: 21
1.3.3 Recurrent caries: 22
1.3.4 Epidemiology of caries: 23
1.4 Caries management: **23**
1.4.1 Restorations: 23
1.4.2 New concepts in caries management (minimal intervention): 29
1.5 Composites with anti-bacterial and re-mineralising properties in literature: **29**
1.6 Novel Composite Formulations: **31**
1.7 Literature review on the materials used in the novel composite: **34**
1.7.1 Calcium phosphates: 34
1.7.2 Polylysine: 45
1.7.3 Monomers: 47
Summary: **53**
Hypothesis: **54**
Aim: **55**
Objectives: **55**
Materials and Methods **56**
2.1 Materials: **57**
2.1.1 Liquid phase components: 57
2.1.2 Powder phase components: 59
2.2 Methods: **61**
2.2.1 Specimen manufacture: 61
2.3 Microstructure analysis of the new mineral phases study: **67**
2.3.1 Analytical Techniques used in this study: 67
2.4 Effect of calcium phosphate and ε-poly(L-lysine) on composite mass and volume changes: **71**
2.5 Solubility and water content of the novel composite study: **72**
2.6 Anti-bacterial (polylysine) release study: **73**
2.7 Data analysis: **76**
Factorial analysis: 76
Error bar analysis: 77
Regression analysis: 78
Univariate Analysis of Variance: 79
One way analysis of variance: 79

Results 81
3.1 Identification of new mineral phases on the surfaces and in the bulk of the novel composites (Microstructure study analysis): 82
3.1.1 Effects of individual and combined calcium phosphates and polylysine on bulk and surface precipitations after storage in different fluids (SEM and Raman spectroscopy analysis): 87
3.1.2 EDX determination of calcium / phosphate ratios: 103
3.2 Effect of calcium phosphate and ε-poly (L-lysine) on composite mass and volume changes: 114
Mass Change increase after 12 weeks in simulated body fluid (SBF): 114
Mass Change increase after 12 weeks in distilled water: 118
Volume Change increase after 12 weeks in simulated body fluid (SBF): 126
Volume Change increase after 12 weeks in distilled water: 130
3.3 Solubility and mass loss/Vol (mg/cc): 138
3.4 Water content: 140
Comparisons between solubility and water content in SBF and water: 142
3.5 Anti bacterial (polylysine release) study: 144

Discussion and Conclusions 146
4.1 Identification of new mineral phase on the surface and in the bulk of the Novel composite: 147
4.2 Effect of calcium phosphate and ε-poly (L-lysine) on composite mass and volume changes: 153
Mass change and volume change: 153
Solubility and Mass loss/Vol (mg/cc): 157
Water Content: 158
Comparisons between solubility and water content in SBF and water: 159
4.3 Polylysine release: 160
4.4 Conclusions: 161

Future work and Summary 163
5.1 Future work: 164
· Adhesion properties of the experimental composite: 164
· Mechanical properties: 164
· Degree of conversion: 164
· Shelf life of the monomer: 165
· Aesthetics properties of the composite: 165
· Biocompatibility: 165
· Microstructure study of the novel composite: 166
· Water sorption study: 166
· Anti-bacterial study: 167
· Comparison to commercial composite: 167
· Final composition of the experimental composite: 167
5.2 Summary 168

References 169

Appendices 182

List of tables

Table 1.1: Summary of the properties of dental materials……**28**
Table 1.2: Summary of the composite's superior clinical outcomes……**31**
Table 1.3: Existing calcium orthophosphates and their major properties……**35**
Table 2.1: Liquid phase components of the experimented composite……**58**
Table 2.2: Powder phase components of the experimented composite……..**59**
Table 2.3: Re-mineralising agents used and the mineral precipitation name and chemical formula……**60**
Table 2.4: Liquid phase components and percentages by weight……**62**
Table 2.5: Composite powder compositions used in the studies. M is MCPM, T is β-TCP, and P is EPL……**63**
Table 2.6: Artificial saliva components……..**65**
Table 2.7: Simulated body fluid components……...**66**
Table 2.8: Factorial design of the formulae showing the percentages of the powder phase components……**76**
Table 3.1: Dominant components other than the polymer identified by Raman and/or SEM in the core of composites stored under different conditions……...**100**
Table 3.2: Dominant components other than the polymer identified by Raman and/or SEM on the surfaces of composites stored under different conditions……..**100**
Table 3.3: Calcium phosphate resultant precipitant on the core of the composites when stored in AS and SBF……**101**
Table 3.4: Calcium phosphate resultant precipitant on the surfaces of the composites when stored in AS and SBF……..**102**
Table 3.5: Ca/P ratio in the surface and core of samples G ($M_{20}T_{20}P_0$) after immersion in artificial saliva at multiple different points and identification of the probable component……...**105**
Table 3.6: Ca/P ratio in the surface and core of samples H($M_{20}T_{20}P_5$) after immersion in artificial saliva showing several spectrums in both surface and core.....**107**
Table 3.7: Ca/P ratio in the core and surface of samples G after immersion in SBF from several points in both surface and core……..**110**
Table 3.8: Ca/P ratio in the core and surface of samples H ($M_{20}T_{20}P_5$) after immersion in SBF showing several spectrums in both surface and core……..**113**
Table 3.9: The novel composite maximum increase in mass and gradient during early (2 weeks) and late time (10 weeks) when immersed in SBF…….……..**116**

Table 3.10: The novel composite maximum increase in mass and gradient (wt%/hr$^{0.5}$) during early (2 weeks) and late time (10 weeks) when immersed in water……..……**120**

Table 3.11: The % mass increase of formulae A ($M_0T_0P_0$), C ($M_{20}T_0P_0$), G ($M_{20}T_{20}P_0$) and H ($M_{20}T_{20}P_5$) after 1 week in SBF or water. Same letters indicate no significant differences at p = 0.05……..……..**125**

Table 3.12: The novel composite maximum increase in volume and gradient (wt%/hr$^{0.5}$) during early (2 weeks) and late time (10 weeks) when immersed in SBF……**128**

Table 3.13: The novel composite maximum increase in volume and gradient (wt%/hr$^{0.5}$) during early (2 weeks) and late time (10 weeks) when immersed in water……..……**132**

Table 3.14: The % volume increase of formulae A ($M_0T_0P_0$), C ($M_{20}T_0P_0$), G ($M_{20}T_{20}P_0$) and H ($M_{20}T_{20}P_5$) after 1 week in SBF or water. Same letters indicate no significant differences at p = 0.05……..……..**136**

Table 3.15: The gradient of the early (2 weeks) and late release (10 weeks) of polylysine from experimental composite upon immersion in water for 12 weeks. ……**145**

List of figures

Figure 1.1: Tooth structure…..……..**18**

Figure 1.2: The solubility isotherm of calcium phosphate phases at 25^{o}C……**36**

Figure 1.3: Chemical structure of monocalcium phosphate monohydrate (MCPM)……...**38**

Figure 1.4: Chemical structure of beta-tricalcium phosphate (β-TCP)……....**39**

Figure 1.5: Chemical structure dicalcium phosphate dihydrate (DCPD), also known as Brushite……....**40**

Figure 1.6: Chemical structure dicalcium phosphate anhydrous (DCPA), also known as Monetite……....**40**

Figure 1.7: Chemical structure Chemical structures of hydroxyapatite (HA)…….**43**

Figure 1.8: Crystalline structure of hydroxyapatite (HA)……**43**

Figure 1.9: The chemical structure of Polylysine……**45**

Figure1.10: Chemical structure of a) the two conformations of urethane dimethacrylate (UDMA) b) bisphenol-A glycidyl methacrylate (Bis-GMA)……..**47**

Figure1.11: Chemical structure polypropylene-glycol-dimethacrylate (PPGDMA)…**48**

Figure 1.12: Chemical structure of TEGDMA……..**48**

Figure 1.13: The chemical structure of HEMA……**49**

Figure 1.14: Chemical structure of CQ……**50**

Figure 1.15: Chemical structure of NTG-GMA-Na……..**52**

Figure 1.16: Chemical structure of DMPT……**52**

Figure 2.1: Example of sample preparation……**64**

Figure 2.2: EPL calibration curve in distilled water……**74**

Figure 2.3: Centrifuge used in the EPL release experiment……..**74**

Figure 2.4: Flowchart of the studies done in the experimented composite……**80**

Figure 3.1: Raman spectra of powder phase components……**82**

Figure 3.2: Raman spectra of polylysine (EPL)……...**83**

Figure 3.3: Raman spectra of monomer components before and after polymerisation and of UMDA monomer……**84**

Figure 3.4: Raman spectra for various calcium phosphates……**85**

Figure 3.5: Raman spectra of artificial saliva components……**86**

Figure 3.6: Formula A a) SEM of dry sample's surface b) SEM of core after 7 days in SBF showing no precipitation and c) Example Raman spectrum of the core showing glass peaks around 1400 cm^{-1}……**88**

Figure 3.7: Formula B a) SEM of the surface after 7 days in AS b) SEM of core after 7 days in AS with no precipitation but some un-dissolved EPL. c) Raman spectra of

the core showing a high peak at 1400 cm^{-1} due to glass in addition to monomer / polymer peaks at higher wavenumbers……**89**

Figure 3.8: Surface of formula B at a) 250X, b) at 1000X after 7 days in SBF with no precipitation. c) Raman spectrum of the surface of formula B after 7 days in SBF……**90**

Figure 3.9: a) SEM of the surface of sample C after 7 days in AS with no precipitation, b) SEM of core after 7 days in AS showing crystal precipitation and c) Raman of crystals in core showing Monetite peaks……**91**

Figure 3.10: Sample C a) surface after 7 days in SBF. b) The core after 7 days in SBF with crystal precipitation. c) Raman spectrum shows high Brushite peak at 989 cm^{-1}……**92**

Figure 3.11: a) The surface of formula E in SBF b) The core of formula E in SBF with no precipitation, c) Example of β-TCP's dominant peaks at 943 cm^{-1} and 968 cm^{-1} seen in surface and core……**93**

Figure 3.12: a) The surface of formula G ($M_{20}T_{20}P_0$), after 7 days in SBF at 80X magnification. B) at 1000X showing calcium phosphate precipitations c) Raman shift of the formula's surface after 7 days in SBF with a high peak at 989 cm^{-1}……**94**

Figure 3.13: SEM of formula G ($M_{20}T_{20}P_0$) core when kept dry and showing no any crystal precipitation……**95**

Figure 3.14: SEM of formula G ($M_{20}T_{20}P_0$), core a) in distilled water, c) in AS, e) in SBF with different crystals precipitations and Raman spectra of formula G ($M_{20}T_{20}P_0$) core showing b) Monetite in distilled water, d) Monetite in AS, f) Brushite in SBF……**96**

Figure 3.15: a and b) Surface of formula H ($M_{20}T_{20}P_5$) at 1000X.Both images are for the sample after 7 days in SBF showing crystal precipitations. c) Raman mapping of the surface of the sample after 7 days in SBF showing one HA single peak at 960 cm^{-1}……**97**

Figure 3.16: The surface of sample H ($M_{20}T_{20}P_5$) upon immersion in SBF for 4 weeks showing calcium phosphate precipitation layer formation, a) at 800X b) at 4548X c) at 2000X d) Raman mapping of the surface of the sample after 1 month in SBF showing one HA single peak at 960 cm^{-1}……**98**

Figure 3.17: a and b) SEM image of the core of formula H ($M_{20}T_{20}P_5$) after 7 days in SBF at 2000X and 3500X respectively with crystal precipitations. c) Raman shift of the surface showing a Brushite high peak at 989 cm^{-1}……**99**

Figure 3.18: sample G ($M_{20}T_{20}P_0$) a) surface and b) core after 7 days in artificial saliva……**104**

Figure 3.19: sample H ($M_{20}T_{20}P_5$) a) surface and b) core after 7 days in artificial saliva……**106**
Figure 3.20: sample G ($M_{20}T_{20}P_0$) a) surface and b) core after 7 days in simulated body fluid……**109**
Figure 3.21: sample H ($M_{20}T_{20}P_5$) a) surface and b) core after 7 days in simulated body fluid……**112**
Figure 3.22: Mass changes against SQRT (time/hours) of each formulation in SBF in different time periods at 37°C: a) formulations with 0% EPL and. b) with 5 wt% EPL during 12 weeks. ……**114**
Figure 3.23: Gradient of early increase in mass (2 weeks) for the 8 formulae when immersed in SBF ……**117**
Figure 3.24: Mass changes against SQRT (time/hours) of each formulation upon immersion in water at different time periods at 37°C: a) formulations with 0% EPL and b) with 5 wt% EPL. ……**118**
Figure 3.25: The initial gradient of early increase in mass (2 weeks) for the 8 formulae when immersed in water……**121**
Figure 3.26: The factorial analysis of the effect of TCP, MCPM, and EPL on the increase in mass after 12 weeks for the samples when immersed in SBF and water, where: a_1, a_2, a_3 are the level of effects of TCP, MCPM, and EPL respectively. ……**122**
Figure 3.27: The factorial analysis of the effect of TCP, medium, and EPL on the increase in mass after 12 weeks for the samples when immersed in SBF and water, where: $a_1$is the effect of TCP, a_2 is the effect of the medium (SBF or water), and a_3 is the effect of EPL……**123**
Figure 3.28: Average effects of TCP, MCPM and EPL on final mass change in both water and SBF……**124**
Figure 3.29: The % difference in mass increase in SBF vs. water during 12 weeks (Difference%= %mass in SBF - %mass in water)……**125**
Figure 3.30: Volume changes against SQRT (time/hours) of each formulation in SBF in different time periods at 37°C: a) formulations without EPL and b) with 5 wt% EPL during 12 weeks……**126**
Figure 3.31: Gradient of initial increase in volume (2 weeks) for 8 formulae when immersed in SBF……**129**
Figure 3.32: Volume changes against SQRT (time/hours) of each formulation after immersion in distilled water at different time periods at 37°C: a) formulae without EPL and b) with 5 wt% EPL during 12 weeks.....……**130**

Figure 3.33: The initial gradient of early (2 weeks) increase in volume for 8 formulae when immersed in water……**133**

Figure 3.34: The factorial analysis of the effect of TCP, MCPM, and EPL on the increase in volume after 12 weeks for the samples when immersed in SBF and water, where: a_1 a_2 and a_3 indicate the level of effect of TCP, MCPM and EPL respectively……..……...**134**

Figure 3.35: Average effects of TCP, MCPM and EPL on volume change in both water and SBF……**135**

Figure 3.36: The % difference in volume increase in SBF vs. water during 12 weeks (Difference%= %volume in SBF - %volume in water)……...**136**

Figure 3.37: Mean of solubility % of experimental dental composites after 12 weeks in SBF and water. Samples from left to right are in alphabetical order A through to H. ……**138**

Figure 3.38: Mean of mass loss/ Vol (mg/cc) of experimental dental composites after 12 weeks in SBF and water. Samples from left to right are in alphabetical order. ……**139**

Figure 3.39: Mean of water sorption of experimental dental composites after 12 weeks in SBF and water. Samples from left to right are in alphabetical order. ……**140**

Figure 3.40: Mean water sorption % and solubility % of experimental dental composites after 12 weeks in SBF. Samples from left to right are in alphabetical order……**142**

Figure 3.41: Mean of water sorption % and solubility % of experimental dental composites after 12 weeks in distilled water. Samples from left to right are in alphabetical order……..**143**

Figure 3.42: Polylysine release from novel composite containing 5% EPL during 3 months (12 weeks) in distilled water…..……**144**

List of equations

Equation 1	Page 68
Equation 2	Page 68
Equation 3	Page 68
Equation 4	Page 71
Equation 5	Page 71
Equation 6	Page 71
Equation 7	Page 71
Equation 8	Page 72
Equation 9	Page 72
Equation 10	Page 72
Equation 11	Page 75
Equation 12	Page 75
Equation 13	Page 76
Equation 14	Page 76
Equation 15	Page 77
Equation 16	Page 77
Equation 17	Page 77
Equation 18	Page 77
Equation 19	Page 78
Equation 20	Page 78
Equation 21	Page 78

List of abbreviations

ACP	Amorphous calcium phosphate
AS	Artificial Saliva
α-TCP	α- Tricalcium phosphate
β-TCP	β-Tricalcium phosphate
Bis-GMA	bisphenol-A glycidyl methacrylate
BCA	Bicinchoninic acid assay
CHX	Chlorhexidine diacetate
CQ	Camphorquinone
Cap	Reactive calcium phosphate (MCPM, β-TCP)
CDHA	Calcium – deficient hydroxyapatite
CI	Confidence interval
CEJ	Cemento-enamel junction
CDJ	Cemento-dentinal junction
Cm	Centimeter
DCPD	Dicalcium phosphate dihydrate (Brushite)
DCPA	Dicalcium phosphate anhydrate (Monetite)
DMPT	N,N-dimethyl-p-toludine
DEJ	Dentino-enamel junction
pDNA	plasmoid Deoxyribonnucleic acid
DW	Distilled water
EDX	Energy-dispersive X-ray
EPL	ε-polylysine
FA	Fluoroapatite
FTIR	Fourier transform infrared spectroscopy
GIC	Glass ionomer cement
g	gram
HA	Hydroxyapatite
HEMA	2-Hydroxyethylmethacrylate
LED	Light emitting diode
L	Litre
MCPA	Monocalcium phosphate anhydrate
MCPM	Monocalcium phosphate monohydrate
MIC	Minimum inhibitory concentration
Mm	Millimeter

nm	Nanometer
mL	Millilitre
NTG-GMA	N(p-tolyl)glycine-glycidyl methacrylate
NHS DEP	NHS Dental Epidemiology Programme
OCP	Otacalcium phosphate
OPA	Orthophthalaldehyde assay
µm	micrometre
RMGICs	Resin modified glass ionomer cements
SEM	Scanning Electron Microscopy
SQRT	Square root of time
SD	Standard deviation
SE	Standard error
SBF	Simulated body fluid
TB	Trypan Blue
TNBS	2,4,6-trinitrobenzene sulfonate
TEGDMA	Triethylene glycol dimethacrylate
TetCP or TTCP	Tetracalcium phosphate
PLR	Powder monomer liquid phase mass ratio
PPGDMA	Poly(propylene glycol) dimethacrylate
ppm	part per million
UDMA	Urethane dimethacrylate
UV	Ultra violet

Chapter I

Introduction

1.1 Teeth:

Humans have two sets of teeth during their lifetime, primary (deciduous) and permanent teeth. Each tooth has a crown and a root portion. The crown is covered with enamel and the root is covered with cementum. These two portions meet at the cemento-enamel junction (CEJ) which is also called the cervical line (Nelson, 2009). Dentine forms the bulk of the teeth and it covers the pulp which is covered by cementum in the root and enamel in the crown (Scully and Al-Bayaty, 2002). Enamel and dentine meet in a joint called the dentino-enamel junction (DEJ) while the dentine meet with the cementum in a joint called cemento-dentinal junction (CDJ) (Berkovitz et al., 2002) (see Figure 1.1).

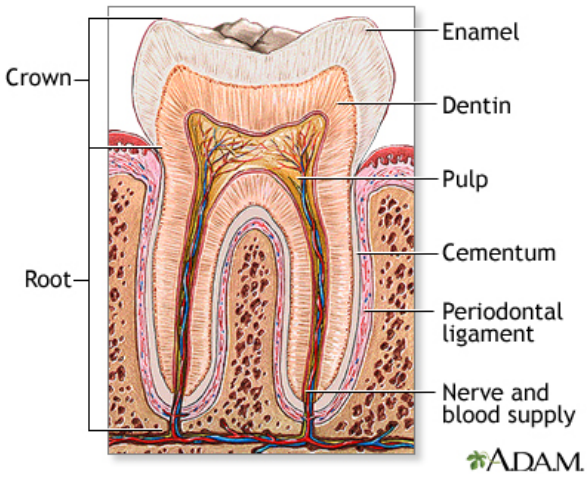

Figure 1.1: *tooth structure*

(Taken from Medline Plus a service of the U.S national library of Medicine National Institute of Health (MedlinePlus.gov)) (Updated by: Ilona Fotek).

Enamel is the part of tooth structure that covers the crown and it is considered to be the hardest structure in the human body (Nelson, 2009). It is epithelially derived hard, protective dental tissue, which is highly mineralized. Enamel consists of approximately 96% of inorganic materials and 4% of organic material and water by weight (Berkovitz et al., 2002).

Dentine is the most abundant tissue in the teeth. It is produced by odontoblasts, which differentiate from the mesenchymal cells of the dental papilla. Dentine by weight compromise of 70% mineralised inorganic materials, 20% organic materials, and 10% water (Scully and Al-Bayaty, 2002).

Cementum covers the root of the tooth and overlies the dentine. Its main function is to anchor the tooth to its socket. The dental pulp is a connective tissue organ that contains structures like nerves, veins, arteries, and lymphatic system. Its primary function is forming the dentine of the tooth (Nelson, 2009, Berkovitz et al., 2002).

1.2 Importance of teeth:

Having bright and healthy teeth is an appealing advantage. Not only for appearance, but, scientific research has shown that healthy teeth have an important effect on individual's diet, general health and overall sense of wellbeing. They enhance confidence and improve quality of life (Gerritsen et al., 2010). Oral diseases can cause considerable pain and other problems. They can also affects one's diet, speech and quality of life (Sheiham, 2006). In children the literature shows that caries increases the risk of hospitalization, requires higher cost of treatment and causes school absence with reduced ability to learn. Studies showed that children with caries have a mean weight about 1 kg less than control children as it can affect nutrition, growth, and metabolic processes (Sheiham, 2005).

Oral diseases are considered the fourth most expensive disease to treat. This is a serious problem especially in developing countries where there is an accumulation of untreated oral diseases (Sheiham, 2005). Health promotion planners overlook oral diseases even if they have high impact on quality of life. This can lead to extensive decay and higher treatment expenses.

Oral diseases include dental caries, periodontal disease and oral cancer. Of these, dental caries is probably the most common.

1.3 Caries:

Dental decay or caries is a complex disease and is called "caries" taken from the Latin word that means "rottenness" (Ismail et al., 2007, Rugg-Gunn, 2013).

"Caries" is a term used for both the process and the final lesions that form as a result of caries formation (Kidd and Fejerskov, 2004). Dental caries is caused by presence of a biofilm, known as dental plaque (Fejerskov et al., 1990, Fejerskov and Thylstrup, 1994, Manji et al., 1991, Kidd and Fejerskov, 2004). The biofilm can be formed on any exposed surface where water and nutrients are present (Wimpenny, 1994, Kidd and Fejerskov, 2004). The dental tissues such as enamel, dentine and cementum can be coated by pellicle where microbial cells attach to them and a colonization of

organisms is formed (Kidd and Fejerskov, 2004).

The bacteria that form the biofilm are metabolically active and able to cause fluctuation in the pH of the oral cavity (Kidd and Fejerskov, 2004). These pH fluctuations can cause loss of dental tissue minerals when the pH is low and gain of minerals when the pH is high (Manji et al., 1991, Kidd and Fejerskov, 2004). When de-mineralisation exceeds re-mineralisation, the result is a net loss of dental tissue and cavity formation. Dental biofilm contains group of microorganisms found on a tooth surface, surrounded in a matrix of polymers of host and bacterial origin. The main bacteria associated in the carious process are S. *mutans,* S. *sanguis,* S. *salivarius, Actinomyces viscosus,* A. *naeslundii* and *Lactobacillus* species (Yip and Smales, 2012).

The biofilm pH fluctuations are a natural phenomenon that occur at any time during the day and the night (Kidd and Fejerskov, 2004). The results of these fluctuations might be at a subclinical level and the tooth will be intact clinically. On the other hand, loss of minerals can lead to de-mineralization of dental hard tissue and subsequently the clinical carious lesion. This means that the carious lesion is a reflection as to what is happening in the biofilm.

1.3.1 Histopathology of caries in enamel:

Early carious lesions in enamel might not be obvious clinically. However, sub-clinically at the ultra-structural level there will be sign of dissolution of the enamel, which is seen as enlargement of the inter-crystalline spaces resulting from the dissolution of the crystal peripheries (Kidd and Fejerskov, 2004). These inter-crystalline spaces increase when the lesion is more active. Active enamel lesion represents surface erosion and subsurface porosity. This is called subsurface demineralization or the white spot lesion (Holmen et al., 1985). The histological zones of the white lesion (Silverstone, 1973) are the surface zone, body of the lesion, dark zone and the translucent zone.

As a result, enamel active lesions show surface erosion and subsurface porosity. While inactive or arrested enamel lesions may be harder than sound enamel. However, arresting the progression of caries can leave some interior opacity even after re-mineralising of the sub-surface (Kidd and Fejerskov, 2004, Thylstrup et al., 1994, Koulourides et al., 1980).

The shape of the white spot is determined by both the distribution of the biofilm and

the direction of the enamel prisms (Kidd and Fejerskov, 2004). In proximal surfaces it has a kidney shape, while in the smooth surfaces it is conical and this conical shape represents the lesion progression stage (Bjørndal and Thylstrup, 2007). In occlusal surfaces it has a conical shape but the base of the cone is toward the dentinal enamel junction. Ultra structural studies have revealed that the deepest point in the fissures of the occlusal surfaces contains non-vital bacteria and calculus. This has an important clinical impact in preventing biofilm formation on the occlusal surfaces by the application of fluoride toothpaste on erupting molars (Carvalho et al., 1992, Theilade et al., 1976, Kidd and Fejerskov, 2004).

1.3.2 Histopathology of caries in dentine:

Dentine represents the main bulk of the tooth and it encloses the pulp (soft tissue). Together, the pulp and dentin forms a functional unit and a defence system called the “pulp-dentin complex” (Scully and Al-Bayaty, 2002). Dentine consists of 70% inorganic material, 20% organic and 10% water (by weight). The inorganic component is mainly hydroxyapatite crystallites which are embedded in the organic extra-cellular matrix (ECM), which consists mainly of collagen type 1 (Berkovitz et al., 2002).

Enamel is made by ameloblast cells, which are derived from the ectoderm that vanishes after the hard tissue formation is completed. In contrast, dentine is formed by odontoblasts, which remain at low levels in the pulp tissue for a life span and are capable of a very limited amount of dental tissue regeneration and repair (Huang, 2011). Therefore, dentine is considered a vital tissue. It is also capable of transmitting signals from the oral cavity to the dental pulp tissue through the micro porous enamel.

The deposition of minerals in the dentinal tubules is the first defence reaction, which is the “pulp-dentine complex” (Massler, 1967, Levine, 1974, Johnson et al., 1969), which, react against bacterial invasion. This is called the “tubular sclerosis” or “translucent dentine”, since the tissue appears histologically translucent due to low light scattering when examined in transmitted light.

In dentine, tubular sclerosis is visible before caries advances to the enamel-dentine junction through the enamel. Therefore, once the lesion has reached the enamel-dentine junction, a brownish discoloration of the dentine occurs. This is the first sign of the dentin demineralisation, and it is the reaction of the biofilm in tooth structure (Bjorndal et al., 1999, Bjørndal and Thylstrup, 2007, Kidd and Fejerskov, 2004).

The second important defence reaction by the “dentine-pulp complex” is the formation of tertiary dentine or reactionary dentin (Massler, 1967, Silverstone, 1973, Kidd and Fejerskov, 2004). This is produced by the odontoblasts in response to dental caries, cavity formation or enamel fracture and it contains sparse, irregular dentinal tubules (Scully and Al-Bayaty, 2002).

Non-cavitated lesions have less bacterial invasion than cavitated lesions, even though the dentine in the un-cavitated lesions is lightly infected and soft (Ratledge et al., 2001). Once the enamel is chipped due to different forces such as mastication, trauma or improper probing by dentists, the cavity is exposed directly to bacteria. The bacteria then invade the tubular dentine and the superficial dentine is decomposed due to acidic and proteolytic enzymes. This is called the “zone of destruction”. Underneath it there is frequent invasion of the dentinal tubules by bacteria. If there is rapid progression of bacteria, the odontoblasts are unable to produce tubular sclerosis because they are rapidly destroyed and form dead tracts in the dentine. In this situation, the bacteria invade empty tubules and these tubules coalesce together to form “liquefaction foci”. The area formed by this process is known as the bacterial penetration zone. While in sclerotic dentin, acid de-mineralization will produce what is called the “ translucent zone” (Thylstrup and Qvist, 1987, Kidd and Fejerskov, 2004).

Once the cavity is directly exposed to the bacterial biomass, superficial tubular invasion occurs. The most superficial part of the dentine becomes decomposed due to the action of acid and proteolytic enzymes. This is called the “zone of destruction". Beneath this zone, tubular invasion of bacteria is frequently seen. With rapid lesion progression, the odontoblastic processes are destroyed without having produced tubular sclerosis. These are called dead tracts in the dentine. Bacteria invade these empty tubules, and groups of tubules may coalesce to form liquefaction foci. This area is called the zone of bacterial penetration. In the sclerotic dentin, the translucent zone is a zone of demineralization resulting from acid demineralization (Kidd and Fejerskov, 2004).

1.3.3 Recurrent caries:

Recurrent (secondary) caries are believed to be primary caries at the edges or margins of a failed restoration (Mjor and Toffenetti, 2000). Micro-leakage is one of the reasons for secondary caries. It is enhanced by polymerisation shrinkage, which occurs upon curing of resin-based dental restorative materials.

Generally recurrent caries are new lesions existing at the margins of previously placed restorations (Kirkevang et al., 2011). In the United States, replacing failed restorations accounts for around 60% of the total number of restorations performed each year with an annual cost of approximately US$5 billion (Melo et al., 2013). Prevention of recurrent caries requires either; inhibition of the bacteria in the dental plaque formed around the restoration and/or interfering with the metabolism of caries related bacteria. Another approach could be by inhibiting the demineralisation and enhancing the remineralisation of dental hard tissues. As a result researchers are focusing now a days on adding anti-caries substances in restorative materials (Melo et al., 2013).

1.3.4 Epidemiology of caries:

NHS Dental Epidemiology Programme (NHS DEP) for England in 2012 showed that the distribution of caries is skewed. 27.9% of 5 years old age group have dentine caries with an average of 3.38 of the teeth were decayed, filled or missing. Also, according to the Adult Dental Health survey 2009, 31% of adults have obvious tooth decay in either the crowns or roots of their teeth. This means that almost below one third of the adult have dental decays and the average number of teeth affected was 2.7, compared with an average of 0.8 within all dentate adults.

1.4 Caries management:

Conventional concepts of caries management were to restore cavities after complete removal of caries. Modern approaches now advocate a ‘minimal intervention’ approach where caries is sealed in.

1.4.1 Restorations:

Dental restorative materials are used to restore damage to teeth, usually resulting from oral diseases or trauma. Untreated dental diseases have adverse effects on the wellbeing of the patient, such as pain, further progression of caries and infections. Therefore, restoration of the teeth is of primary importance.

Providing restorative treatment to children and anxious patients is challenging. A study in the USA rated dental anxiety about dental treatment as 4th behind snakes, heights and storms (Agras et al., 1969). Also, anxiety related to dentistry occurs in 10% of 5-years- old children (Vassend, 1993). Moreover, 35% of 5 year old and 21% of 12 year olds children are fearful and anxious about dental treatment before visiting

the dentist (Bolin, 1996). As a result, dental anxiety is a significant barrier to treatment uptake and eventually anxious patients requires more chair time and thus complicates the dental restorative treatment.

In addition, restorative materials must exhibit good biocompatibility. This is because toxicity to surrounding tissues, clinicians handling the materials and to the environment during production and disposal of the materials could happen and should be minimised (Schedle et al., 1998).

It is important to understand the physical, and mechanical properties of any materials used in dentistry. These materials are replacing tooth structure so they are exposed to the oral environment and subjected to different types of forces. Therefore they should possess characteristics that mimic the natural dental tissues including, dimensional stability, thermal conductivity, electrical properties, and solubility, wetting ability, hardness and elastic modulus, which indicates stiffness. Yield strength, ultimate strength, and toughness are also other important properties for a dental material that must be taken into consideration to withstand masticatory and functional forces (Craig et al., 2004).

Unrestored primary teeth have an adverse effect on the quality of life in children as stated by Sheiham (Sheiham, 2006). As a result, restoring primary teeth is essential to maintain quality of life and prevent subsequent pathological outcomes.

Current restorative materials:

Several restorative materials are available to restore carious teeth such like amalgam, dental composites, and glass ionomer cements. Table 1.1 summarise the properties of several dental restorative materials. Aesthetics are becoming more important for patients and clinicians. Therefore, producing an aesthetic restorative material with favourable properties that overcomes some of the problems associated with them is essential.

Amalgam:

Despite the concerns raised regarding the safety of amalgam, it is one of the most used restorative treatments historically (Berry et al., 1998). It is made of mercury and different alloys (silver, zinc, tin, and copper) (Schmalz and Arenholt-Bindslev, 2009).

Amalgam is considered to have high strength, high fracture toughness, good wear resistance and low micro-leakage (Sakaguchi and Powers, 2012b) but it is unable to bind to tooth structure or induce tooth-restoration remineralisation. Therefore, it necessitates the removal of sound tooth structure in order to gain mechanical retention of the restoration (Görücü et al., 1997).

Amalgam can corrode to seal the tooth-restoration interface and thus reduce micro-leakage. This property occurs gradually and may lead to discolorations. In addition, other reported complications of Amalgam are tooth and bulk fracture, marginal ditching, and overhanging with eventually secondary caries initiation (Burke et al., 1999).

Moreover, Amalgam's major failure is its lack of aesthetics properties. Not withstanding this, amalgam is considered to have excellent longevity, strength, and cost. As a result it has been used for more than 150 years (Berry et al., 1998).

However this may change with signing the Minamata agreement. The Minamata convention is a worldwide agreement to protect the environment and the human health from the use of Mercury. This convention was named after the Japanese city Minimata that passed through a harmful incident of mercury poisoning. This agreement was launched after 3 years of negotiations and agreements to limit the exposure to mercury (Mercuryconvention.org). And due to the fact that Amalgam consists of Mercury, its application in many countries gained a significant attention and restrictions. It is likely that amalgam use for dental restorations will be increasingly restricted in the future.

Glass ionomer cements (GICs):

Glass ionomer cements consist of organic acids and silicate glass powders. They react chemically with the tooth via acid-base reaction. Glass Ionomer adheres to the tooth surface by a combination of micro- mechanical attachment and chemical bonding. Glass ionomer cements have the property of fluoride release so this can help in producing fluoroapatite that is more resistant to dental caries (Van Meerbeek et al., 2002). In literature, generally there is a debate on the effect of the fluoride

release from GIC. This is because GIC's fluoride release declines with time. It also causes increase in material roughness. Potentially GICs reduce bacterial micro-leakage by several ways; firstly the initial low pH of the freshly mixed cement, the less dimensional change during material setting, and the fluoride and other element release and adhesion to tooth structure (Mehdawi and Young, 2012). The aesthetic properties of glass ionomer is superior to amalgam but less than composite.

However, glass ionomer cements have low mechanical properties, poor longevity and poor wear resistance (Piwowarczyk et al., 2002). Therefore, they are not ideal in stress bearing cavities (Mehdawi and Young, 2012).

Hybrid restorative materials:

Hybrid restorative materials are a mixture between composites and glass ionomers (GIC). They mainly divide into Resin modified Glass ionomers (RMGICs) and compomers.

Resin- modified glass ionomer cements (RMGICs):

RMGICs are chemically similar to GICs, but with the addition of photopolymerisable monomer. Often the monomer is 2-hydroxyethylmethacrylate (HEMA) (Piwowarczyk et al., 2002).

With regards to the properties of RMGICs, they show similar adverse properties to other resin based materials (e.g composites) such as polymerisation shrinkage and heat generation but also poorer mechanical properties than those of composites. On the other hand, RMGICs have bonuses such as fluoride release and the ability to adhere to tooth structure chemically therefore requiring less sound structure removal. Despite the fact that RMGICs are not suitable for stress bearing areas, it is now used in many clinical implications instead of GICs (Mehdawi and Young, 2012).

Compomers:

Compomers' components are generally similar to the composites but in addition they contain monomer/polymer with an acidic chemical group that is able to attract water from the surroundings therefore react with inorgainc particles containing fluoride (Nicholson, 2007).

Polymerisation shrinkage is also a major problem in compomers. However, water sorption potential of compomers has been suggested to compensate for polymerisation shrinkage (Huang et al., 2002). But, this water sorption potential

doesn't initiate significant glass/acid reaction in the bulk of the material which is required to promote fluoride release (Young et al., 2004).

Compomers present with lower mechanical properties compared to composites. This is because of water sorption properties and fluoride release that eventually will affect the mechanical properties of the material. As a result, they are more indicated in primary teeth and non-stress bearing areas (Mehdawi and Young, 2012). But, compomers generally release less fluoride than GIC and therefore, they are not the solution to bacterial micro-leakage and secondary caries.

Composite:

As aesthetics are of great importance to clinicians and patients, composites with the best aesthetics and are often chosen. Composites generally consist of two phases: a resin-based liquid phase and a filler phase, typically consisting of glass particles (Craig et al., 2004). The glass particles are treated with a silane, which contains methacrylate groups and forms a chemical bridge between the filler and the polymer that forms upon curing.

The most commonly used monomers in commercial composites are urethane dimethacryate (UDMA) and bisphenol A glycidyl methacrylate (Bis-GMA). A diluent monomer such as TEGDMA is used to reduce the viscosity of the liquid phase. The liquid phase also contains a photo-initiator and accelerator (Craig et al., 2004).The components of the filler phase can be varied in order to increase the abrasion resistance, modulus of elasticity, compressive strength, fracture toughness, setting contraction and thermal expansion and aesthetic properties of the composite. Composites may be classified as macro-filled (conventional), micro-filled or hybrid, which is a mixture of both macro-filled and micro-filled composite, depending upon the particle size of the bulk filler component (Mitchell and Mitchell, 2009).

It is important to illustrate some properties of commercial composites. Composites suffer from volumetric polymerisation shrinkage of 1 – 4% and thermal expansion greater than that of enamel and dentin. Therefore bacterial micro-leakage often results and leads to failure of the restoration. Composites also tend to have a high elastic modulus or low elasticity, which results in brittleness and a high tendency to fracture. However they have the best wear resistance of the aesthetic materials and are radio-opaque which is a particularly useful clinical property to detect a recurrent caries and overhangs in radiographs (Craig et al., 2004, Mitchell and Mitchell, 2009).

Composites generally have good wear and mechanical properties but their main reason for failure and replacement is bond damage. Whereas GICs undergo an acid-base reaction with the tooth mineral, forming a chemical ionic bond, composites bind purely by micromechanical interactions between the demineralised collagen and the polymer in the composite. Damage to this bond enables micro-leakage and furthermore bacterial penetration between the tooth and the restoration and hence secondary caries. Because the composite doesn't have anti-bacterial action a re-infection can occur. This problem is exaggerated by the degradation of the collagen and the adhesive by the bacterial enzymes as well as the polymerisation shrinkage of the composite during the setting process (Young et al., 2004, Leung et al., 2005, Bernardo et al., 2007). Table 1.1 summarises the properties of the most common used restorative materials.

Property	**Amalgam**	**GIC**	**Resin based composite**
Strength	Excellent	Poor	Good
Aesthetics	Very poor	Satisfactory	Excellent
Longevity*	Excellent	Poor	Good
Anti bacterial	Yes	No	No
Remineralisation	No	Yes	No

Table 1.1: Summary of the properties of dental materials.

1.4.2 New concepts in caries management (minimal intervention):

Partial caries removal is preferable to complete caries removal (Ricketts et al., 2006). In this concept a reduction of the risk of pulpal involvement can be achieved. Furthermore, a well conducted trial showed that sealing caries in primary teeth showed significantly less major failures and was preferred by both dentist and patients (Innes et al., 2011). Since children present a barrier to treatment due to fear and anxiety, restorations and fillings with easier techniques should be considered (Yengopal et al., 2009) as the traditional way of restorative care might be difficult to apply.

For all there is a great interest to develop alternative means of providing restorative care, which are more conservative and result in less pain for the patient. In particular, developing a new filling material that is able to re-mineralise the affected tissue and has anti-bacterial effect will aid the success of this approach. This project is looking at modifying a composite to this end.

1.5 Composites with anti-bacterial and re-mineralising properties in literature:

The interface between tooth and fillings is exposed continually to de-remineralisation and remineralisation (Gao et al., 2001). When an imbalance between the mineralisation processes of the tooth structure due to acid production of the cariogenic bacteria occurs, more demineralisation of tooth structure and the formation of tooth cavity results (Aoba, 2004). On the other hand, if remineralisation exceeds the mineral loss a re-precipitation of mineral contents can be achieved by crystal growth formation (Featherstone, 2009). So, the remineralisation and demineralisation process is a continuous process that affects the tooth according to the surrounding oral environment.

The degree of saturation (DS) as shown by several crystals growth studies is the controlling factor for the balance between the remineralisation and demineralisation process. As a result the interface between the tooth structure and the dental filling should be saturated with minerals that enhance the remineralisation (Aoba, 2004). So supplementation of calcium and phosphate ions in the restorative materials is needed to enhance the remineralisation property of the filling (Reynolds, 2009).

Dicalcium phosphate dihydrate (DCPD or Brushite), octacalcuim phosphate (OCP) and hydroxyapatite (HA) can all be produced by precipitation of calcium phosphate in aqueous solutions (Koutsoukos and Nancollas, 1981, Lu and Leng, 2005). At neutral

pH HA is the most stable crystal formed, while OCP and DCPD may be precursors of it. Brushite (DCPD) becomes more stable when the pH drops below 3.

The idea of anti-bacterial dental materials has been highlighted in several studies. For example, fluoride containing components and gluteraldahyde has been added in some dental adhesives. Despite the fact that this effect will fade away as soon as the material is cured, the acidic monomers can initially be anti-bacterial (Imazato, 2003). Triclosan (2,4,4-trichloro-2-hydroxidiphenilethere), Benzalkonium chloride (BAC), and Chlorhexidine (CHX) are examples of anti-bacterial components added in several dental materials (Mehdawi and Young, 2012).

With regards to the re-mineralising potential of dental materials, many studies have added calcium phosphate particles into the dental materials. Soluble components such as calcium fillers added to the powder phase instead of hydroxyapatite crystals can be released and precipitate within the tooth structure (Mehdawi and Young, 2012). In particular, adding amorphous calcium phosphate (ACP) has been widely investigated (Skrtic et al., 1996).

Composites containing, monocalcium phosphate monohydrate (MCPM), dicalcium phosphate anhydrate (DCPA), and tetracalcium phosphate (TetCP) have been studied and considered (Dickens et al., 2003, Xu et al., 2007b). The most demanding issue with regard to adding calcium phosphate into the novel composites was the reduction in mechanical strength (Mehdawi and Young, 2012). Therefore, many studies aimed to improve the mechanical properties by various methods. For example, reducing the water sorption potential of the material (Antonucci et al., 2008), lowering filler particle size (Lee et al., 2007), enhancing the interaction between resin matrix and filler, and ACP hybridisation with glass fillers (Skrtic et al., 2003). As a result of low strength, composites containing ACP cannot be used in stress bearing areas and only as a cavity liner/base or adhesive material (Mehdawi and Young in 2012). This is due to the fact that the bond strength of it is around 18 MPa and the maximum biaxial flexure strength of composite with ACP to date is approximately only 50MPa which is in a similar range to GICs (Mehdawi and Young, 2012).

Dickens in 2003 added dicalcium phosphate anhydrate (DCPA) and tetracalcium phosphate in dental resin and showed release of calcium and phosphate ions. In vitro this composite was able to achieve remineralisation of tooth structure (Dickens et al., 2003). Another study also compared a similar composite to light cure calcium hydroxide cavity liner. In this case the composite had less micro-leakage and higher

bond strength properties (Dickens et al., 2004). Also, another study showed that replacing DCPA with more soluble calcium phosphate particles such as MCPM nanoparticles resulted in higher levels of calcium and phosphate and an acceptable flexural strength (Xu et al., 2007a).

1.6 Novel Composite Formulations:

The aim of this multidisciplinary project involving clinicians, chemists, materials scientists, micro-biologists, cell-biologists and a dental supplier, Schottlander is to produce a dental composite with several novel features that do not exist in current commercial materials. The resin-based composites incorporate monomers that theoretically shrink less upon curing, fibres that act as a toughening agent, calcium phosphates (CaP) that act as re-mineralising agents and anti-microbial agents that prevent formation of caries. This should enable a less aggressive approach and more conservative tooth preparation. Consequently children, anxious patients and less developed areas with few dental facilities will particularly benefit from this composite.

Table 1.2 summarises the proposed superior clinical outcomes promised by the objectives of producing this novel composite.

Objective	**Clinical outcomes**			
Re-mineralising	Reduced micro-leakage	Reduced recurrent caries	Reduced failure rate	Self- repair
Low shrinkage				
Anti microbial				
Less small molecules	Reduced toxicity for patients and allogenicity for clinician		Prolonged shelf-life	

Table 1.2: summary of the composite's superior clinical outcomes.

The new material features include:

1) Re-mineralising properties

Calcium phosphates (CaP) are added that may react in the presence of water and form Brushite mineral. β-tricalcium phosphate and monocalcium phosphate monohydrate have the ability to release upon absorption of water into the microscopic gaps between the tooth and the restoration, creating mineral and blocking bacterial micro-leakage. This property helps to improve the self-repair potential of the material (Reynolds, 2009, Cheng et al., 2012c, Cheng et al., 2012a, Combes and Rey, 2010).

2) Polymerisation shrinkage compensation

Producing a restorative material, which is capable of absorbing water and swelling to compensate for polymerisation shrinkage, is another point targeted in this project. Adding soluble material into the material components should promote more water sorption.

3) Anti-microbial agents

Poly (L-lysine) has also been incorporated and as it has antimicrobial properties. This can help in providing protection against infection. Furthermore it can promote remineralisation and expansion.

4) Biocompatibility and Shelf life properties

Biocompatibility may be improved by using:

i. UDMA instead of Bis-GMA as a bulk monomer. In fact, both are used commercially but UDMA has better handling since it is less viscous. Bis-GMA also may contain traces of precursor molecular Bisphenol-A which mimics oestrogen so UDMA is used instead of it (Van Landuyt et al., 2007, Leung et al., 2005).

ii. PPGDMA instead of TEGDMA as a diluent monomer. PPGDMA is higher in molecular mass. As a result, PPGDMA has lower potential for penetrating cells and leeching into plastic that should improve shelf life. PPGDMA has lower double bond concentration so this may lower polymerisation shrinkage. Its high flexibility should

as well improve the composite cure rate. PPGDMA should theoretically cure more completely, which would leave less of it free to leech out of the material and penetrate cells (Lee et al., 2004) (Van Landuyt et al., 2007).

iii. NTG-GMA-Na instead of DMPT as accelerator. NTGGMA again has higher molecular mass and so is also less able to penetrate cells that may improve biocompatibility and less able to leech into plastic that should improve shelf life. NTG-GMA-Na is a monomer as well as accelerator, unlike DMPT. It potentially therefore becomes incorporated into the polymer so further reducing the leeching. NTG-GMA may have the additional property of acting as an adhesive agent to some degree, by binding to the calcium in dentine (Van Landuyt et al., 2007).

Additional promising properties:

5) Low shrinkage

Production of a material with minimal polymerisation shrinkage is a major target of this project. Both, urethane dimethacrylate (UDMA) and poly (propylene glycol) dimethacrylate (PPGDMA) have low double bond concentration and high molecular mass (Mr). Therefore, they were used in order to minimise polymerisation shrinkage (Leung et al., 2005).

6) Excellent aesthetics and wear resistance

Composites are favoured over GICs by both clinicians and patients because of their superior aesthetic properties, especially for anterior dental restorative fillings. This composite should have excellent aesthetics and wear resistance, although re-mineralising and anti-microbial agents that might cause some discolouration.

1.7 Literature review on the materials used in the novel composite:

1.7.1 Calcium phosphates:

Calcium phosphate has been widely used in various applications. For example it has been used in drug delivery, bone cements, wastewater remediation, gene therapy, chromatography and in dental purposes. This is owing to the fact that calcium phosphate is generally considered bioactive and biocompatible (Ahmad Salimi, 2013).

Several types of calcium phosphate have been studied and investigated in multiple fields. For example amorphous calcium phosphate (ACP) as mentioned earlier has been added to dental materials to aid in remineralisation potential of restorative materials (Skrtic et al., 2004). Also, dicalcium phosphate anhydrous (DCPA), dicalcium phosphate dehydrate (DCPD), otacalcium phosphate (OCP) and other calcium phosphate particles have been used or formed as products of calcium phosphate bone cements (Brown, 1987, Mejdoubi et al., 1994, Bermudez et al., 1994a, Ginebra et al., 1997, Lee et al., 1999). In addition, hydroxyapatite was also used in bone as a substitutes and coating agent in implants (Sun et al., 2001, LeGeros, 1990).

Calcium phosphates have three major elements; phosphorus (oxidation state +5), calcium (oxidation state +2), and oxygen (reduction state -2). There are various calcium phosphate types available and the type of phosphate anion differentiates these. For instance, ortho- (PO_4^{3-}), meta- (PO_3^{-}) or pyro- ($P_2O_7^{4-}$) and poly- ($(PO_3)_n^{n-}$). In addition, according to temperature, presence of water, and impurities, several phases of calcium phosphate crystallization can be formed (Ahmad Salimi, 2013).

A summary of the different phases of calcium phosphate phases is provided in table (1.3).

Ca/P ionic ratio	**Compound**	**Chemical formula**	**Aqueous solubility at 25 °C, -log (K_S)**	**pH stability range in aqueous solutions at 25 °C**
0.5	MCPM	$Ca(H_2PO_4)_2.H_2O$	1.14	0.0-2.0
0.5	MCPA	Ca(H2PO4)2	1.14	[c]
1.0	DCPD, mineral Brushite	$CaHPO_4.2H_2O$	6.59	2.0-6.0
1.0	DCPA, mineral Monetite	$CaHPO_4$	6.90	[c]
1.33	OCP	$Ca_8(HPO_4)_2(PO_4)_4.5H_2O$	96.6	5.5-7.0
1.5	α-TCP	α-$Ca_3(PO_4)_2$	25.5	[a]
1.5	β-TCP	β-$Ca_3(PO_4)_2$	28.9	[a]
1.2-2.2	ACP	$Ca_xH_y(PO_4)_z.nH_2O$, n = 3 – 4.5; 15 – 20% H2O	[b]	~ 5 – 12
1.5-1.67	CDHA [d]	$Ca_{10-x}(HPO_4)_x(PO_4)_{6-x}(OH)_{2-x}$ (0<x<1)	~ 85.1	6.5-9.5
1.67	HA	$Ca_{10}(PO_4)_6(OH)_2$	116.8	9.5-12
1.67	FA	$Ca_{10}(PO_4)_6F_2$	120.0	7-12
2.0	TTCP, mineral hilgenstockite	$Ca_4(PO_4)_2O$	38-44	[a]

[a] These compounds cannot be precipitated from aqueous solutions. [b] Cannot be measured precisely. However, the following values were found: 25.7 ± 0.1 (pH = 7.40), 29.9 ± 0.1 (pH = 6.00), 32.7 ± 0.1 (pH = 5.28). [c] Stable at temperatures above 100 °C. [d] Occasionally, CDHA is named as precipitated HA.

Table 1.3: Existing calcium orthophosphates and their major properties [reproduced from (Dorozhkin, 2009)].

Generally the lower the Ca/P ratio in the phase of calcium phosphate, the lower the pH and the more soluble it is. This is because of the solubility conditions and the kinetics of precipitation formation and transformation (Elliott, 1994).

In figure 1.2 the profile solubility isotherm demonstrates the favored conditions needed for the formation of the several types of calcium phosphate. The curve in each kind of calcium phosphate shows the saturation boundary needed for the formation of the various types of calcium phosphate. Therefore, any calcium phosphate composition below the curve is considered supersaturated. Whereas, above the curve is under-saturated. Hydroxyapatite (HA) compositions are the least soluble calcium phosphate phase when the pH value is of >4.2 therefore, it is considered the most stable phase. As a result, any calcium phosphates above this pH may hydrolyse into HA. Depending on the pH of the environment the different phases of calcium phosphate can eventually precipitate (Lynn and Bonfield, 2005).

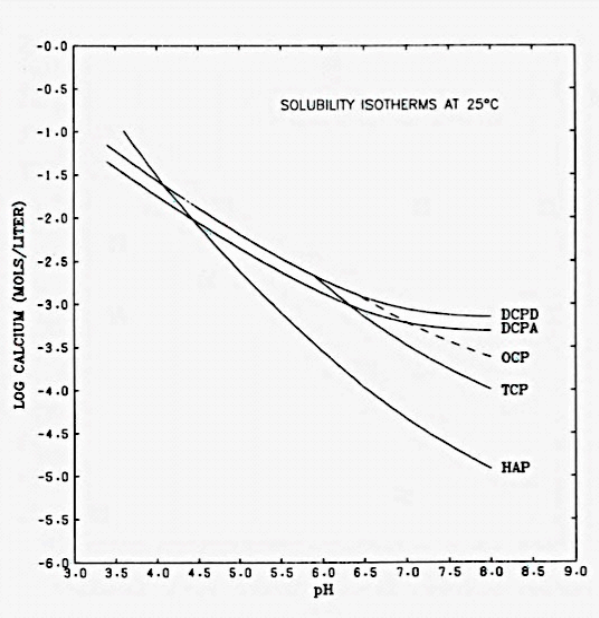

Figure 1.2: *The solubility isotherm of calcium phosphate phases at 25^{o}C* [replicated from (Gregory, 1974) Vol 78A, No. 6, p. 673].

Amorphous calcium phosphate:

The term amorphous calcium phosphate (ACP) has several different meanings. For example, it was firstly used to indicate amorphous calcium orthophosphate phase. In addition the term ACP was used to refer to micelles of calcium phosphate in milk and cheese. Also to refer to poorly defined domains in apatite nanocrystals and apatite ceramics (Combes and Rey, 2010). Accordingly, ACP is an important phase in the mineralised tissues and considered the first commercial product as synthetic HA. It can additionally easily transfer to crystalline phases such as apatite and octacalcium phosphate by the microcrystalline growing potential of ACP (Zhao et al., 2011).

ACP is considered as one of the most frequent forms of calcium phosphate (CaP) mineral in biological organisms. For instance, it has been found in the mitochondria of prokaryote and eukaryote cells and is also considered a precursor phase of bone mineral in vertebrates. ACP was found abundantly in tooth structures and in the exoskeletal structure of marine invertebrates (Combes and Rey, 2010).

ACP is an intermediate phase in several calcium precipitation phases. Therefore, it has been used in several biomaterials applications and preparations. For example, it was used as a coating for metallic endoprothesis and as self-setting injectable cements. Dentally, ACP has been used as a component in dental composites to aid in remineralisation properties with enamel and dentine (Zhao et al., 2011) . ACP was also included in toothpastes as a re-mineralising agent (Combes and Rey, 2010).

From the literature, there has been growing interest in ACP biomaterials since 1970's. The literature showed that there are different types of ACP according to the Ca/P atomic ratio. In an alkaline medium with a pH ranging from 9-11, ACP with an atomic Ca/P ratio of 1.5 with the chemical formula $Ca_3(PO_4).nH_2O$ is the most precipitated type (Combes and Rey, 2010).

(Regnault et al., 2008) showed that when ACP was included in methacrylate monomers and placed in aqueous fluids, calcium and phosphate could be released. When medium is acidic the release can be higher. However, this composite showed lower strength properties (Cheng et al., 2012b, Skrtic and Antonucci, 2007) indicated that the levels of calcium and phosphate released from ACP composites are sufficient to promote tooth remineralisation in vitro (Lee et al., 2007).

As a result, several studies have been carried out to try to improve the mechanical properties of the ACP dental composites. Some studies tried enhancing the interaction between the resin and filler matrix. Others tried to hybridize the ACP with

glass fillers or reducing the water sorption potential (Skrtic and Antonucci, 2007). In fact, the maximum biaxial flexural strength of these composites achieved to date is around 50 MPa. Thus, it is not aplicable as a restorative material in areas with high occlusal demands and load bearing areas.

Monocalcium phosphate monohydrate (MCPM):

Mono calcium phosphate can be either MCPM, which is the monocalcium phosphate monohydrate (its correct chemical name is calcium dihydrogen phosphate monohydrate) or the MCPA, which is the monocalcium phosphate anhydrous salt (its correct chemical name, is calcium dihydrogen phosphate anhydrous). The chemical formula of the first is $Ca(H_2PO_4)_2.H_2O$, whereas for the second is $Ca(H_2PO_4)_2$. MCPM and MCPA are the most acidic calcium phosphates and also have the lowest Ca/P ratio as seen in table 1.1. As a result they are the most soluble phase (Ahmad Salimi, 2013, Dorozhkin, 2009).

A procedure called triple superphosphate for phosphorus-containing fertilizer production is the reaction that occurs for the construction of MCPM. In this reaction the powder phosphate rock reacts with concentrated phosphoric acid to produce the MCPM. In this process MCPM releases a molecule of water and transforms to MCPA when the temperature is above 100^{o}C (Becker, 1989).

The peaks of an XRD pattern and FTIR spectrum can differentiate the MCPM and MCPA. Both have the structure of crystallographic triclinic space group (Ahmad Salimi, 2013). Despite the fact that MCPM is not considered to be biocompatible due to the fact of its acidity it is still used in medicine as an element in self-hardening calcium phosphate cements (Bermudez et al., 1994b). On the other hand, in literature there was no current medical application of MCPA (Ahmad Salimi, 2013).

See figure 1.3 for the chemical structure of MCPM.

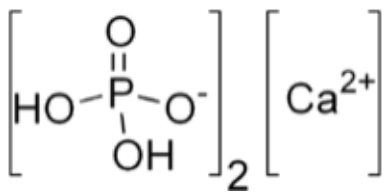

Figure 1.3: Chemical structure of monocalcium phosphate monohydrate (MCPM).

Tri-calcium phosphates (TCP):

TCP can exist in two forms; α-TCP or β-TCP crystal forms. β-TCP cannot precipitate from aqueous solutions. However, it can be prepared by adding $CaCl_2$ solution to Na_3PO_4 solution at 1.5 Ca/P ratios. This can happen at pH value of 9 and 5^0C temperature conditions (Ahmad Salimi, 2013). It has the chemical formula of $Ca_3(PO_4)_2$.

β-TCP can be prepared chemically by calcium deficient HAp (CDHAp) thermal decomposition at temperatures above 800^0C or by interactions of acidic calcium phosphates in a solid-state phase. For example if DCPA is added to CaO which is a base. Also calcining bones can form ion-substituted β-TCP. This type of β-TCP is called "bone ash" as reported by Dorozhkin in 2009 (Dorozhkin, 2009).

α-TCP is formed by the phase transformation of β-TCP and is considered to be stable at temperatures ranging between 1180 and 1400°C. If the temperature increases to above 1125°C then β-TCP can transform into α-TCP. α-TCP and β-TCP have similar chemical composition, but differ in their solubility properties and β-TCP is more stable. α-TCP was reported to have higher specific energy, to be more reactive in aqueous solutions, and to be able to transform into other combinations of calcium phosphates by hydrolyzing. With regards to the structures of α-TCP and β-TCP, β-TCP has a crystallographic structure of rhombohedral space group and α-TCP has monoclinic space group crystallographic structure (Yin et al., 2003, Ahmad Salimi, 2013).

In literature, β-TCP has been more commonly used; for example as calcium phosphate bone cements (Mirtchi et al., 1990), the development of multivitamins, and as an agent in the ingredients of toothpastes. α-TCP is mostly used in calcium phosphate cements as reported by Bermudez in 1994 (Bermudez et al., 1994a). The two phases of TCP can be differentiated by FTIR and XRD spectrum analysis (Ahmad Salimi, 2013). See figure 1.4 for the chemical structure of β-TCP.

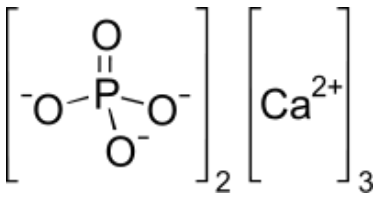

Figure 1.4: Chemical structure of beta-tricalcium phosphate (β-TCP).

Dicalcium phosphate (dehydrate - Brushite and anhydrate - Monetite):

Dicalcium phosphate dihydrate (DCPD) is known as the mineral Brushite. It is easily formed by crystallization from aqueous solution in pH conditions of <6.5. It consists of $CaHPO_4$ chains that are arranged in a parallel way to each other with lattice water molecules layering in between. At room temperature if mixing phosphoric acid (H_3PO_4) solutions in equimolar amounts with calcium hydroxide suspensions $Ca(OH)_2$, Brushite (DCPS) will be formed (Oliveira et al., 2007).

In 1955 Pierre was able to form DCPD by neutralizing dilute H_3PO_4 when adding calcium surcate (calcium carbonate and sucrose) (Pierre, 1955).

DCPD is able to transform to DCPA when the surrounding temperature is above 80^{o}C. DCPD was widely used in medicine; it was used in calcium orthophosphate cements (Bermudez et al., 1994b), toothpaste ingredient to act as caries protection agent when coupled with fluoride or as a polishing agent in the toothpaste. Also, it was added as an intermediate for tooth remineralisation (Crall and Bjerga, 1987). In addition DCPD has the crystallographic structure on monoclinic space group (Ahmad Salimi, 2013).

Monetite is the anhydrous form of DCPD. Water is absent in the inclusion of Monetite, therefore; it is less soluble. It has various uses, for example, as calcium phosphate cement (Takagi et al., 1998), a polishing agent, a nutrients supplement to act as a source of calcium and phosphate, and as a toothpaste ingredient (O'Neil, 2013). Also, DCPA has the crystallographic structure of triclinic space group and doesn't occur in either normal or pathological calcifications (Ahmad Salimi, 2013). See figures 1.5 and 1.6.

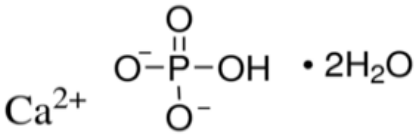

Figure 1.5: Chemical structure dicalcium phosphate dihydrate (DCPD), also known as Brushite.

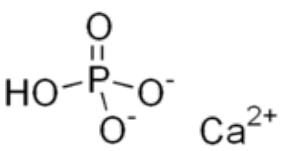

Figure 1.6: Chemical structure dicalcium phosphate anhydrous (DCPA), also known as Monetite.

Octacalcium phosphate (OCP):

Octacalcium phosphate (OCP) is usually found as an intermediate unstable calcium phosphate phase. It occurs during the formation and precipitation of the more stable phase of calcium phosphate (HA) in an aqueous solution. The chemical formula of OCP is $Ca_8(HPO_4)_2(PO_4)_4.5H_2O$. Similarly to HA, OCP has apatite layers divided and disjoined by hydrated layers (LeGeros, 1985, LeGeros, 1990, Elliott, 1994, Ahmad Salimi, 2013).

Shelton et al in 2006 showed that OCP could be synthesised by homogeneous crystallisation. In this, a solution of disodium hydrogen orthophosphate and calcium nitrate tetrahydrate are mixed together at pH between 6.49 and 7.15 and temperature ranging between 45 and 55^{o}C for 48 hours (Shelton et al., 2006). When equal volume of sodium and phosphate is added to calcium acetate, pure OCP can be precipitated at pH 4-4.5 and 70-80^{o}C during 1-hour duration (LeGeros, 1985).

The following equation explains how OCP can hydrolyse into HA in water and according to the availability of calcium ions (Elliott, 1994):

$$Ca_8H_2(PO_4)_65H_2O + 2Ca^{2+} \rightarrow Ca_{10}(PO_4)_6(OH)_2 + 3H_2O + 4H$$

With regards to the crystallographic structure of OCP, it has a triclinic space group structure and can also be distinguished using XRD pattern and FTIR spectra (Ahmad Salimi, 2013).

Hydroxyapatite (HA):

The chemical formula of HA is $Ca_5(PO_4)_3(OH)$, but because usually the crystal unit cell comprises of two molecules it is most often written as $Ca_{10}(PO_4)_6(OH)_2$.

After fluoroapatite, HA is the second most stable and least soluble calcium phosphate in water with K_s of –log 116.8 as seen in table 1.1.

The Ca/P ratio of pure HA is 1.67. If the ratio is above 1.67 it is considered calcium rich HA or maybe carbonated HA. If the Ca/P ratio is below 1.67, it means that it contains other impurity phases or calcium deficient HA (Hench et al., 1993). HA is very similar to bone minerals, hence, it gained a lot of attention as a biomaterial substance (Shi, 2004).

Techniques to prepare HA can be simply divided into either solid-state (material chemistry) reactions or wet methods (El Briak-BenAbdeslam et al., 2008). The wet method consists of precipitation, hydrothermal, and hydrolysis of calcium phosphates. One method explained by LeGros in 1993 is to mix equal amounts of solutions containing Ca and PO_4 at pH more than 9, then boil it for few days in an atmosphere free of CO_2 (maturation or aging stage), then filter the solution, dry it, and then sinter it to about 1000^{o}C.(LeGeros and LeGeros, Ahmad Salimi, 2013)

In order to precipitate HA directly, the reactant must contain salts of calcium and phosphate, or must be H_3PO_4 and $Ca(OH)_2$. Calcium and phosphates needed to form HA must be with ions such as nitrates or ammonium that are usually unlikely to be part of the apatite phase. Also, if the calcium and phosphate have similar correct molar value e.g 5:3 in the medium, pure HA can be formed (Ahmad Salimi, 2013).

Another way of preparing HA is the sol-gel technique. In this technique the HA powder is formed by reacting calcium nitrate tetrahydrate ($Ca(NO_3)_2.\ 4H_2O$) and phosphoric pentoxide (P_2O_5). Also a sintering step to 600^{o}C is used in this technique to form the HA (Feng et al., 2005). Another method of preparing HA is the hydrothermal precipitation. In this method HA whiskers are formed by hydrolysis method in a moderate acid solution at temperature ranging between 85 and 95^{o}C for approximately 48 to 120 hours (Zhang et al., 2003).

More methods have been reported in the literature regarding preparing HA. For example the emulsion method as reported by Sonoda in 2002. In this method, potassium dihydrogenphosphate (KH_2PO_4) is mixed with calcium hydroxide $Ca(OH)_2$ for 24 hours at 50^{o}C at intense agitation then calcined at 650^{o}C for another 1 hour

(Sonoda et al., 2002). Whereas for the solid-state reaction method of preparing HA, calcium carbonate ($CaCO_3$) is mixed with calcium pyrophosphate ($Ca_2P_2O_7$) in an acetone and water solutions. Then HA production was noted after heating treatment at 1100^{o}C for 1 hour (Rhee, 2002).

Metastable synthetic body fluids made of inorganic salt composition are used to deposit HA coatings onto prosthesis surfaces as described by Ferraz in 2004 (Ferraz et al., 2004). The coating's thickness of HA ranges between 200 to 400 µm. Plasma spraying, laser deposition, sputter coating, and sol-gel processing are other methods mentioned in literature in HA coating procedures. Therefore, HA can be used as a coating material in multiple orthopaedic prosthesis. Also, it was reported that HA was used in drug delivery because it is very similar to bone and tooth structure, thus, it was considered a biological components such as the pDNA (Dorozhkin, 2007, Ahmad Salimi, 2013).

Describing the crystallographic structure of HA, it can be either hexagonal or monoclinic space group structure. In addition, Elliot mentioned in 1994 that HA can be distinguished using FTIR analysis (Elliott, 1994). See figure 1.7 and 1.8.

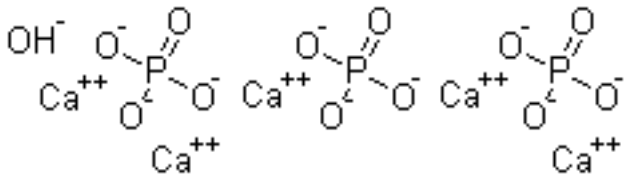

Figure 1.7: Chemical structure Chemical structures of hydroxyapatite (HA).

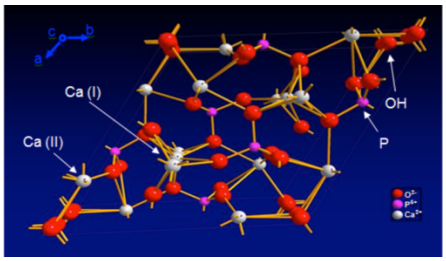

Figure 1.8: Crystalline structure of hydroxyapatite (HA) (Fazel-Rezai, 2011).

Tetracalcium phosphate (Hilgenstockite):

This calcium phosphate (TTCP or TetCP) phase has a Ca/P ratio of 2 and is the most alkaline phase of all the calcium phosphate phases. Yet, the solubility in water of TTCP is higher than HA. In addition, TTCP has an oxygen atom in its formula ($Ca_4(PO_4)_2O$, and in basic solutions precipitates formed will incorporate with the hydroxyl ion; as a result it cannot be synthesised in aqueous conditions because it always consist of apatite containing carbonate- and/or hydroxyl ions (Jalota et al., 2005).

So, synthesizing TTCP is somewhat limited. Common methods to produce TTCP are solid-state reactions in high temperature conditions. In these methods, calcium carbonate ($CaCO_3$) and dicalcium phosphate anhydrate ($CaHPO_4$) are mixed then heated to 1400-1500^oC for 6 to 12 hours (Ahmad Salimi, 2013). The following equation illustrates the reaction:

$2CaHPO_4 + 2CaCO_3 \rightarrow Ca_4(PO_4)_2O + 2CO_2 + H_2O$

Following heating, the mixture is cooled to room temperature to form undesired secondary phases. These phases are; HA, CaO, $CaCO_3$, and β-TCP. Looking at the crystallographic structure of TTCP, it has a monoclinic space group structure. Furthermore, Mia et al used TTCP in 2004 as a scaffold in tissue engineering (Miao et al., 2004, Ahmad Salimi, 2013).

1.7.2 Polylysine:

Hiraki in 1999 reported the antimicrobial effect of (e poly-L-lysine, (EPL)). It was mentioned that it is effective against various microorganisms such as; Gram-positive and Gram-negative bacteria which are responsible for caries formation, yeast, fungi, and moulds at a pH of 4-10 (Hiraki and Suzuki, 1999). As Polylysine is a cationic surface active agent it is positively charged and can act as antimicrobial against fungi and bacteria (Hiraki, 2000, Shukla et al., 2012b, Shukla et al., 2012a).

In addition, the US Food and Drug Administration approved the use of ε-poly(L-lysine) (EPL) in food as an anti-microbial agent (Hiraki, 2000). Also, it is used commonly in cosmetics as a preservative in low concentrations of 50-250 ppm (Hiraki, 2000). However, in dentistry, polylysine (e poly-L-lysine) was rarely used and its application in any dental literature was challenging to find.

For commercial and scientific purposes, polylysine was produced using Streptomyces albulus. It is a homo-polypeptide with 25-30 L-lysine residues. The linkage between ε amino groups and carboxyl groups of its monomers refers to "ε" while the lysine's chirality in three-dimensional orientation refers to "L". The carboxyl and the e-amino groups of L-lysine are linked molecularly by peptide bonds. Figure 1.9 shows the chemical structure of polylysine.

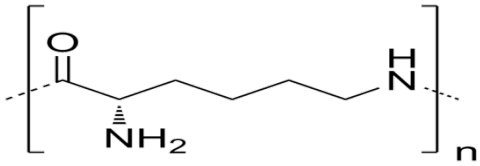

Figure 1.9: The chemical structure of Polylysine.

It is a highly soluble molecule with hydrophilic amino groups that contribute to its surfactant properties. It is used as a coating to facilitate the attachment of cells and proteins to solid surfaces in biological applications and cell culturing. Therefore, it might improve the bonding and adhesive stability of the composite (Li et al., 2012).

Looking at the anti-bacterial potential of polylysine; in bone infections, the minimum inhibitory concentration (MIC) of polylysine is 12 µg/ml against streptococcus aureus (Hai-tao, 2008). In pH conditions ranging between 5 and 8, polylysine showed the strongest anti-bacterial activity (Benji, 2008). The outer bacterial membrane is

stripped by the polylysine due to the electrostatic adsorption and leads to subsequent disorganisation of its cytoplasm, causing cell death (Shih et al., 2006).

Medically, It was used in various fields; for example, it was used in drug delivery in cancer therapy, as an anti-obesity agent being an anti-lipase inhibitor (Tsujita et al., 2003), and an interferon inducer by acting as anti-viral and anti-tumour agent. In addition, it also showed the ability to remove Endotoxin (natural lipopolysaccharide) from cell products (Hirayama et al., 1999).

According to literature, Hiraki in 2000 showed that polylysine is considered to be a stable material under acidic and basic conditions at high temperatures. When it is heated in water at 100^{o}C for 30 minutes or autoclaved at 121^{o}C for 20 minutes it showed high degradation boiling resistance and high solubility in water (Hiraki, 2000).

So this certainly clarifies its safety characteristics because it is stable under high temperatures, it lacks toxicity, and active antimicrobial agent.

1.7.3 Monomers:

Urethane Dimethacrylate (UDMA):

UDMA is the bulk monomer of the liquid phase in a light-cured composite. This is a viscous material and might cause some difficulty during mixing. However, comparing it to bisphenol-A glycidyl methacrylate (Bis-GMA), it is considered to have lower viscosity and a more flexible urethane linkage. This can help in improving the resin composites' mechanical properties and durability. Yet, the viscosity is still quite high; therefore, a diluent monomer such as tri(ethylene glycol) dimethacrylate (TEGDMA) or poly(propylene glycol) dimethacrylate (PPGDMA) must be added.

UDMA can be used as an alternative to Bis-GMA or in conjunction with it and has been more popular lately. The reactive carbon double bond at each end enables polymerisation by free radical initiation. UDMA is an aliphatic high molecular weight monomer containing two (-NH-) amine groups that can associate with carbonyl groups (C=O) by intermolecular hydrogen bonds. These interactions explain the high viscosity and glass transition temperatures properties of the monomer and the resultant polymer. However, comparing these amine groups to the hydroxyl group (-OH-) of Bis-GMA, they provide weaker hydrogen bonds (Sakaguchi and Powers, 2012a) (Anusavice et al., 2012, Vallittu, 2012). See figure 1.10 for the chemical structures of UDMA and Bis-GMA.

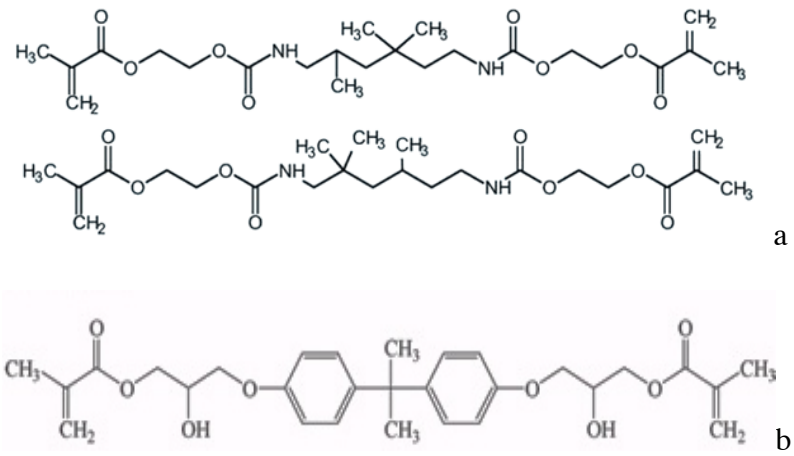

Figure 1.10: Chemical structure of a) the two conformations of urethane dimethacrylate (UDMA). b) bisphenol-A glycidyl methacrylate (Bis-GMA) (Floyd and Dickens, 2006).

Poly(propylene glycol dimethacrylate (PPGDMA):

Adding a diluent monomer will help in material handling. TEGDMA is the diluent used in the commercial composite. It has a low molecular mass, which can make methacrylates more cytotoxic. PPGDMA was used in preparing the experimental composite in this study. PPGDMA has double the molecular weight of TEGDMA and lower double bond concentration as shown in figure 1.11. A higher molecular weight indicates a higher chance of biocompatibility, as larger molecules are less able to penetrate cells and alter their normal physiological function. A lower double bond concentration could enable less shrinkage due to less polymerisation in a given volume of the material. PPGDMA would have two-thirds the shrinkage of TEGDMA if both are fully cured. PPGDMA, however, reacts quicker, which may give higher final conversion potentially cancelling the effect of higher molecular weight (Poorsattar Bejeh Mir and Poorsattar Bejeh Mir, 2012, Leung et al., 2005). Higher conversion of PPGDMA is an advantage as it reduces toxicity. Furthermore, composites with PPGDMA have a longer shelf life compared to composites containing TEGDMA as a diluent monomer (Zimmerli et al., 2009, Leung et al., 2005, Van Landuyt et al., 2007, Furuse et al., 2011). See figure 1.11 and 1.12 for the chemical structures of PPGDMA and TEGDMA respectively.

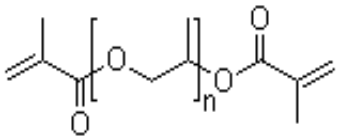

Figure1.11: Chemical structure polypropylene-glycol-dimethacrylate (PPGDMA) (Lee et al., 2004).

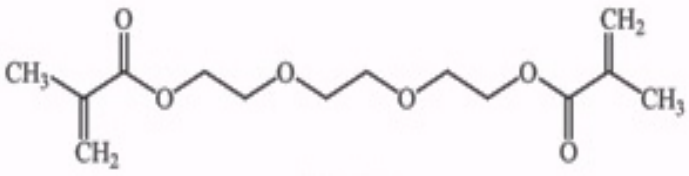

Figure 1.12: Chemical structure of TEGDMA
(Floyd and Dickens, 2006).

2-Hydroxyl ethyl methacrylate (HEMA):

HEMA has several biomedical uses. It is a monomer that has a low molecular weight. In dentistry it has been used as an adhesive and solvent. Also it is able to bind to tooth hard tissues. It is an aliphatic hydrophilic monomer. It has the ability to interact with water due the (-OH) group. It was also reported that when HEMA was added in low quantities it could help in achieving better bonding properties (Morra, 1993).

Figure 1.13 shows the chemical structure of 2-hydroxy ethyl methacrylate (HEMA).

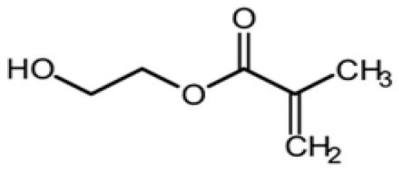

Figure 1.13: The chemical structure of HEMA.

Camphorquinone (CQ):

Camphorquinone (CQ) is used as photo-initiator to start the polymerisation reaction of monomer into polymer. When it is exposed to blue lights it breaks down and releases free radicals. These free radicals are unpaired electrons with short half-life. It was reported that CQ works most efficiently at wavelength ranging between 460 to 480 nm. However, CQ works in a dual system and in conjunction with the amine accelerator. The amine accelerator helps in stabilising the free radicals, and the CQ induces the free radicals. The free radicals already induced by the photo-initiator (CQ) will start the polymerisation chain reaction by breaking the C=C bond of the methacrylate group of the monomer. This is considered to be a reactive monomer that will eventually react with the terminus of the growing polymer molecule. CQ has a high molecular weight of approximately 166 and it is the most used photo-initiator (Yagci et al., 2010, Jandt et al., 2000, Odian and Odian, 2004).

Thus, the accelerators such as DMPT and NTG-GMA are to stabilize the free radicals in order to allow longer and complete polymerization, which means less toxicity.

Figure 1.14 shows the chemical structure of CQ.

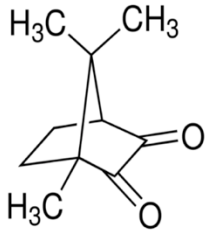

Figure 1.14: Chemical structure of CQ.

N(p-tolyl)glycine-glycidyl methacrylate (NTG-GMA):

As described earlier, amine accelerators are used to stabilise free radicals. In dental adhesives two types of amine accelerator are often used; N,N-dimethyl-*p*-toluidine (DMPT) and N(p-tolyl)glycine-glycidyl methacrylate (NTG-GMA).

NTG-GMA is considered as being a surfactant because of the hydrophilic head (aromatic ring) and the hydrophobic end. So, it can act as a bridge between hydrophilic and hydrophobic substances. Thus, it is used in dental adhesives, as it is able to show good wetting and filling properties. In addition it contains a CO^{2-} ion that is able to bind to the calcium phosphate of the hydroxyapatite in dentine.

DMPT is more commonly used as an amine accelerator, but growing concern is noted with regard to its toxicity. This is due to the fact that DMPT has a low molecular mass compared to NTG-GMA. It is reported that the molecular mass of DMPT is 2.5 times less than NTG-GMA. Furthermore, NTG-GMA is less able to leach as it contains a methacrylate group that incorporates it into the polymer. Also, it has the amine group that stabilise the free radicals and as a result reduce the shrinkage (Van Landuyt et al., 2007, Furuse et al., 2011).

The accelerator contributes about 1% of the monomer in the experimental composite and it is *N*(*p*-tolyl)glycine-glycidyl methacrylate (NTG-GMA-Na). As explained above accelerators often have an amine group that stabilizes free radicals and because DMPT is considered toxic due to its small size. Conversely, NTG-GMA-Na is double the size of DMPT so eventually should be less toxic and favoured to be used. Also, NTG-GMA-Na has a methacrylate group. Its reaction with other monomers will bind this molecule reducing its toxicity. The group can also bind to tooth structure, making NTG-GMA-NA act as adhesive. Moreover, 1% of NTG-GMA-NA will not act as adhesive but if it is in higher percentage such as 5%, it might be have some adhesive properties and bind to the teeth minerals.

Figure 1.15 and 1.6 show the chemical structures of NTG-GMA and DMPT respectively.

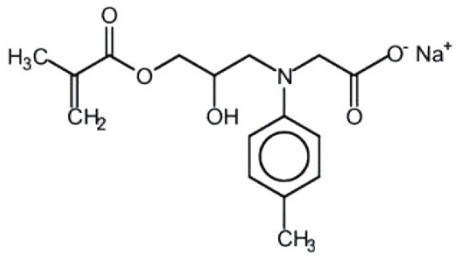

Figure 1.15: Chemical structure of NTG-GMA-Na.

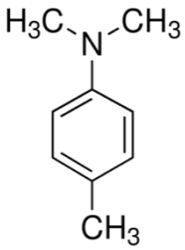

Figure 1.16: Chemical structure of DMPT.

Summary:

Dental caries is one of the most common chronic diseases affecting human beings. According to Adult Dental Survey in 2009, 40% of adults in the UK suffer from dental caries. Also, an estimation of millions of pounds is spent annually for the prevention and treatment of dental caries.

Consequently, dental caries destroy the dental tissues such as the enamel, dentine, dental pulp, and ultimately lead to tooth loss. In addition dental caries can negatively affect the overall well being of the individual. Children and young adults are significant sufferers as the necessity to have a better longevity of the restored teeth is more demanding. In addition, anxious children and adults can be barriers for dental treatment and eventually complicates any required treatment.

Concepts in restoring decayed teeth have changed lately. Partial caries removal and self-healing encouragement of the affected dental tissues are more approached. Therefore, revolutions of dental materials to restore affected teeth have been overwhelming recently.

Moreover, an attempt to regenerate dental hard tissue and promote the self-healing of the affected tissue is a new concept in dental management. Dental composites with superior properties have been approached lately. For example, Mehdawi et al. did a previous study at the Eastman Dental Institute in 2009. This study examined the re-mineralising effect and anti-bacterial potency of light curable methacrylate dental monomers containing calcium phosphate fillers and chlorhexidine. This study resulted in Brushite and hydroxyapatite crystals precipitated on the composite material surfaces in cell growth media. Moreover, this study indicated that this composite is cell compatible due to cell spreading on both crystals and exposed polymer composite surfaces. Finally it showed that these formulations could be anti-bacterial, re-mineralising, and biocompatible (Mehdawi et al., 2009).

So, this project aims also to develop Novel dental composites that are potentially able to promote the re-mineralising and anti-bacterial properties in order to improve the quality of dental management of caries. In this study adding calcium phosphate as a re-mineralising agent and polylysine as an anti-bacterial component was implemented. The addition of these components will eventually enhance the composites' properties and therefore address the new theory of restoring decayed teeth.

Hypothesis:

Several hypotheses were examined in this project using variable novel composite formulations and analytical techniques.

It was anticipated that MCPM and TCP would promote absorption of water into the composite and react with each other to form Brushite, which can convert into Hydroxyapatite. HA will be able to precipitate on the surface and eventually aid in the remineralisation of dentine and improve the tooth-restoration interface.

Adding higher calcium phosphate will result in more water sorption. This will eventually compensate for polymerisation shrinkage by encouraging more increase in mass and volume.

It was believed that the water sorption induced by the addition of calcium phosphate could speed the release of the antimicrobial agent (EPL).

Aim:

The aim of this project is to produce a dental composite that is capable of optimising re-mineralisation and provide anti-bacterial release to help inhibit bacterial micro-leakage.

Objectives:

8 different composite formulae were prepared with variable calcium phosphates and polylysine percentages. Re-mineralising agents as either MCPM or TCP were added in the powder composition of the novel composite. The individual and the combined effect of the added components were analysed. This project investigated the remineralisation characteristics, the expansion properties, and the potential anti-bacterial release of the polylysine by the novel composites in the following experiments:

1. Scanning Electron Microscopy (SEM), Energy-dispersive X-ray (EDX) determination of Ca/P ratios, and Raman spectroscopy to study the microstructure and the remineralisation properties of the novel composite.
2. Water sorption potential of the novel composite by quantifying the mass, density, and volume change during a 3 months (12 weeks) period of time in simulated body fluid and distilled water.
3. Calculating the water sorption and mass loss percentages (solubility) of different composite formulae.
4. Assessment of Polylysine (EPL) release into water was using Trypan Blue dye and visible absorbance spectroscopy during 3 months (12 weeks).

Generally, this research involves monitoring of the following issues:

- Microstructure
- Mass change and volume change
- Polylysine release profile

Chapter II

Materials and Methods

2.1 Materials:

Powder and liquid was fixed at 4:1 ratio to prepare the composite specimens. This is equivalent to 80% powder and 20% liquid. Different composite formulations containing variable percentages of the different powder components were produced. The powder phase contained glass particles, glass fibers, antimicrobial agents, and calcium phosphates. The liquid phase components of the experimental composite were similar in all the formulae and consisted of bulk (urethane dimethacrylate, UDMA) and diluent (polypropylene-glycol-dimethacrylate, PPGDMA) at a ratio of 3:1 respectively, photoinitator camphorquinone (CQ), hydrophilic monomer hydroxyethyl methacrylate (HEMA), and amine accelerator (N(p-tolyl)glycine-glycidyl methacrylate, NTG-GMA-Na).

2.1.1 Liquid phase components:

The liquid consisted of:

- 93% UDMA / PPGDMA monomer
- 5% 2-hydroxyethyl methacrylate (HEMA)
- 1% photoinitiator camphorquinone (CQ)
- 1% accelerator (*N*(*p*-tolyl)glycine-glycidyl methacrylate (NTG-GMA-Na))

With 3:1 bulk to diluent monomer overall this gives 69.75% bulk monomer to 23.25% diluent monomer.

CQ and NTG-GMA-Na are fully dissolved in the liquid phase. Due to the fact that UDMA is very viscous, when mixing the materials the CQ, and NTG-GMA-Na are added to the HEMA and diluent monomer until the powder is dissolved before UDMA addition.

Table 2.1 describes the abbreviations, chemical formula, and the supplier product code of the liquid phase components used in preparing the novel composites.

Function	Name	Abbreviation	Chemical Formula	Supplier and product code
Bulk Monomer	Urethane dimethacrylate	UDMA	$C_{23}H_{38}N_2O_8$	Esstech X-850-0000 & DMG 100112
Diluent Monomer	Poly(propylene glycol) (400) dimethacrylate	PPGDMA	$H_2C=(CH_3)CO(OC_3H_6)_n O_2CC(CH_3)=CH_2$	Polysciences 04380-250
Hydrophilic Monomer	2- hydroxyethyl methacrylate	HEMA	$CH_2=C(CH_3)COOCH_2CH_2OH$	Esstech X968-7044 & DMG 100220
Photo initiator	Camphorquinone	CQ	$C_{10}H_{14}O_2$	Sigma - Aldrich 124893 DMG 100134
Amine accelerator	N(p-tolyl)glycine-glycidyl methacrylate sodium salt	NTG-GMA-Na	$C_{16}H_{20}NO_5Na$	Esstech X863-0050

Table 2.1: Liquid phase components of the experimented composite.

2.1.2 Powder phase components:

Contributing 80% of the composite, the powder is made mainly of glass particles with an average size of 7 micron and glass fibers that measure 15x300 micron. Glass fibers toughen the material because when a force or pressure is applied in a material that has glass fibers, this pressure will travel along the fibres that have larger surface area so it takes longer time to crack. Glass fibre free materials will crack very easily and suddenly. Glass particles and fibres are both silanated thus they mix more easily and react chemically with the monomer).

Mono (MCP) and tri (TCP) calcium phosphate were added to the powder phase with equal mass ratios. They can react together and enhance remineralisation to fill the micro-leakage gap, which is the main reason for incorporating them.

Table 2.2 shows the composition of the powder phase used to prepare the novel composites. In this table the characteristics of the re-mineralising agents and the anti-bacterial component is listed.

Function	Name & Chemical Formula	Abbreviation	Particle Size	Supplier & Product
Bulk filler	Silane treated glass particles	GC	7 μm	DMG 020684
Re-mineralising agent	Beta-tricalcium phosphate	β-TCP	16.91 μm	Plasma Biotal P292 S
	Monocalcium phosphate monohydrate	MCPM	53 μm	Himed MCP-B26
Anti-microbial agent	ε-poly(L-lysine)	EPL	30 μm	Handary εpolyly®P

Table 2.2: Powder phase components of the experimented composite.

2.1.2.1 Re-mineralising agents:

The experimental composites contain calcium phosphates (CaP) as either β-tricalcium phosphate (β-TCP) and/or monocalcium phosphate anhydrous (MCPM) as a re-mineralising agent.

Table 2.3 shows the chemical name, formula, and abbreviation of the re-mineralising agent, mineral precipitate, and the mineral of dentine.

Function	Chemical name	Abbreviation/ mineral name	Chemical formula	Supplier
Re-mineralising agent	β-tricalcium phosphate	β-TCP	β-$Ca_3(PO4)_2$	Plasma Biotal P292 S
	Monocalcium phosphate monohydrate	MCPM	$Ca(H_2PO_4)_2 \cdot H_2O$	Himed MCP-B26
Mineral precipitate	Dicalcium phosphate dihydrate	DCPD/ Brushite	$CaHPO_4.2H_2O$	Made manually by mixing TCP with MCPM and 800mM citric acid solution
	Dicalcium phosphate anhydrous	DCPA/ Monetite	$CaHPO_4$	Sigma – Aldrich 016K0033
Mineral of dentine	Hydroxyapatite	HA	$2[Ca_5(PO_4)_3(OH)]$	Plasma Biotal Limited p309

Table 2.3: Re-mineralising agents used and the mineral precipitation name and chemical formula.

2.1.2.2 Anti- microbial agent:

The powder also contains 5 wt% Polylysine (ε-poly-L-lysine)(EPL). It was shown from previous work in this multidisciplinary project that when EPL was added to composites containing calcium phosphates surface mineral layer formation in artificial saliva could be enhanced (Walter, 2015). Therefore, EPL was used in the composites specimens prepared for the experiments in this study.

2.2 Methods:

2.2.1 Specimen manufacture:

In all formulations, powder and liquid components were weighed using a four-figure balance.

Powder	:	liquid
4	:	1

2.2.1.1 Liquid Phase preparation:

The liquid phase was prepared and stored for a minimum of 24 hours before use in order for the exclusion of air bubbles to occur. A maximum of one month was used as an expiry date. All components except the bulk monomer were combined in an amber (blue light-proof) bottle and mixed at a low speed for about 30 minutes. At a later stage the bulk monomer (UDMA) was added and the liquid phase was stirred again for another 30 minutes. In order for the powder components of the liquid phase (CQ and NTG-GMA) to fully dissolve the first mixing step was important, because they were unable to dissolve totally when the viscous UDMA was added from the beginning.

Again the liquid phase consisted of 3:1 bulk to diluent monomer and was constant in all the formulae used in the different experiments of this study.

UDMA	:	PPGDMA
3	:	1

5%	HEMA
1%	CQ
1%	NTG-GMA

Component	**Percentage by weight (%)**	
	Of the liquid phase	Of the total composite PLR 4:1
UDMA	69.75	13.9
PPGDMA	23.25	4.65
HEMA	5	1
CQ	1	0.2
NTG-GMA-Na	1	0.2
Powder phase	-	80

Table 2.4: Liquid phase components and percentages by weight.

2.2.1.2 Composite paste mixing and preparation:

8 different formulations with variable percentages of glass, MCPM, β-TCP, and EPL were prepared as described in table 2.5.

% Of the powder phase components				
Formula	**%Glass**	**% MCPM**	**% β-TCP**	**%EPL**
A- $M_0T_0P_0$	100%	0%	0%	0%
B- $M_0T_0P_5$	95%	0%	0%	5%
C- $M_{20}T_0P_0$	80%	20%	0%	0%
D- $M_{20}T_0P_5$	75%	20%	0%	5%
E- $M_0T_{20}P_0$	80%	0%	20%	0%
F- $M_0T_{20}P_5$	75%	0%	20%	5%
G- $M_{20}T_{20}P_0$	60%	20%	20%	0%
H- $M_{20}T_{20}P_5$	55%	20%	20%	5%

Table 2.5: Composite powder compositions used in the studies. M is MCPM, T is β-TCP, and P is EPL.

2.2.1.3 Manual Mixing:

Powder phase components were weighed on a rubber dental mixing pad, and then mixed together with the liquid using a metallic spatula. Composite paste mixture was then loaded in to 10 mm diameter and 1 mm height carbon spring steel O-rings. The specimens were inserted between two plastic sheets, pressed gently using glass blocks to remove any excess composite to get smooth better edges of samples. Specimens were then cured for 40 seconds on each side using a Demi Plus light emitting diode (LED) unit with output intensity from 1,100 mW/cm^2 to a peak of 1,330 mW/cm^2 (Kerr Dental, Orange, CA, USA), which radiates blue light with a wavelength of 450-470 nm. After sample removal from the rings they were stored at room temperature until usage. See figure 2.1.

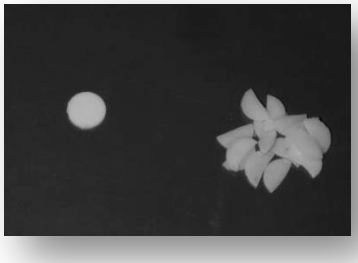

Figure 2.1: Example of sample preparation.

2.2.1.4 SpeedMixer™ Laboratory Mixer System:

In later parts of the study, formulae G ($M_{20}T_{20}P_0$) and H ($M_{20}T_{20}P_5$) were mixed and prepared using the speedMixer laboratory mixer system. SpeedMixer™ DAC 150.1 FV is a laboratory-sized instrument for the rapid mixing and grinding of materials that would require large amounts of time and effort to mix. It is designed by Hauschid engineering for research and development work. It has variable speed of 300 - 3500 rpm and works by spinning a high speed-mixing arm in one direction while the basket rotates in the opposite direction. The combination of forces in different planes enables fast mixing and eliminates air bubbles.

During the experiments in this study, some of the prepared samples were either examined dry or stored in 10 mL of deionized distilled water, artificial saliva, and simulated body fluids before examination. The composition of artificial saliva and simulated body fluids are summarised in table 2.6 and 2.7 respectively.

The composition of the artificial saliva.	
Component	**Grams per litre**
Methyl-p-hydroxybenzoate sodium salt	2.3 g
Sodium carboxymethyl cellulose	10.00 g
KCl	0.625 g
$MgCl_2.6H_2O$	0.059 g
$CaCl_2.2H_2O$	0.166 g
$K_2HPO_4.3H_2O$	1.05 g
KH_2PO_4	0.326
The pH of artificial saliva was adjusted to 6.75 with KOH	

Table 2.6: Artificial saliva components.

The artificial saliva used in the upcoming described studies was prepared according to Macknight-Hane and Whitford (1992) Formula (McKnight-Hanes and Whitford, 1992).

Simulated body fluid components		
Order	**Reagent**	**Amount in g for preparing 1 L**
1	NaCl	8.035
2	$NaHCO_3$	0.355
3	KCl	0.225
4	$K_2HPO_4.3H_2O$	0.231
5	$MgCl_2.6H_2O$	0.311
6	$_c$(HCl) = 1 mol/l	39
7	$CaCl_2.2H_2O$	0.387
8	Na_2SO_4	0.072
9	TRIS	6.118
10	$_c$(HCl) = 1 mol/l	0 to 5

Table 2.7: Simulated body fluid components.

During the preparation of the SBF the components were added by order from 1 to 10. The pH was adjusted to 7.40 at 36.5 ^oC using HCl. The SBF was prepared according to the ISO23317: 2012 protocol.

2.3 Microstructure analysis of the new mineral phases study:

In this study 6 formulations; A ($M_0T_0P_0$), B ($M_0T_0P_5$), C ($M_{20}T_0P_0$), E ($M_0T_{20}P_5$), G ($M_{20}T_{20}P_0$), and H ($M_{20}Y_{20}P_5$) -described earlier- were prepared and either examined dry or after storage in 10 mL of de-ionized distilled water, artificial saliva, and simulated body fluids for 7 days at 37˚C.

Each of the 24 samples was broken into 3 pieces using the Instron Model 4505 Universal Testing Machine, (High Wycombe, UK) so as to be able to study the core of the specimens. Next, each formulation was analysed both in the surface and in the core using Scanning Electron Microscopy (SEM), EDX Ca/P ratio identification and Raman microscopy to identify different Calcium phosphate (CaP's) phases.

2.3.1 Analytical Techniques used in this study:

The re-mineralising properties of the novel materials were characterized using several analytical instruments and techniques. These included Scanning Electron Microscopy, EDX, and Raman spectroscopy.

2.3.1.1 Scanning Electron Microscopy (SEM):

A focused beam of high-energy electrons in order to generate different signals at the surface of solid specimens is used in this analytical technique. These signals reveal information about the sample including the crystalline structure / orientation, chemical composition, external texture and morphology. A 2-dimensional image is created which displays differences in these properties. 1 cm to 5 microns in width areas can be imaged in a scanning mode using conventional SEM techniques. Selected point locations on the sample can also be analysed using SEM; this methodology is particularly useful in qualitatively or semi-quantitatively determining chemical compositions of the samples.

Specimens were left dry for 24 hours and coated with gold-palladium for imaging using a sputter coating machine (Polaron E5000, East Sussex, UK) for 90 second at 20 mA. The surface scanning was carried out using a scanning electron microscope (Phillip XL-30, Eindhoven, The Netherland) instrument operating with primary beam energy of 5 kV and a current of approximately 200 pA. Samples analysed in surface

and core at 5 different magnifications; 80, 250, 1000, and 2000 μm. In addition, at least 4 different areas in each the surface and the core of the samples were analysed using SEM.

2.3.1.2 Raman Microscopy:

Raman works by "scattering light". Simply it is a process where different photons interact with a specimen to form scattered radiation with variable wavelengths.

Raman spectroscopy is useful for chemical identification, characterisation of molecular structures and assessing effects of bonding, environment and stress on samples. It is considered a form of vibrational spectroscopy. Scattering occurs when there is change in the polarisability of the molecule.

Principles of the Raman effect:

When radiation impinges on a sample it may be reflected, absorbed or scattered. 2 types of scattering can be seen; Rayleigh (the incident radiation), and Stokes and Anti-Stokes Raman (the small amount of radiation that is scattered at some different wavelength). Variation in wavelength of the scattered photon provides the chemical and structural information of the sample (Andor.com).

Scattering without a change of frequency is called Rayleigh scattering, while that with a change in the frequency (wavelength) of the light is called Raman scattering. Depending upon the vibrational state of the molecule, Raman shifted photons of light can be either of higher or lower energy. These energies are principally in the ranges associated with rotational, vibrational and electronic level transitions in the molecules. The scattered radiation occurs over all directions and may also have observable changes in its polarization along with its wavelength (Andor.com).

In spectroscopy wavelength (λ) and wavenumber ($\bar{\nu}$) are related by

$$\tilde{\nu} = \frac{1}{\lambda}$$ Equation 1

Furthermore, the photon energy (ΔE) is given by

$$\Delta E = h\nu$$ Equation 2

$$\nu\lambda = c_n$$ Equation 3

Where:

$\bar{\nu}$ = the wavenumber

h = the Plank's constant

v = the frequency

λ = the wavelength

C_n = the speed of light in the medium

So when a laser beam hits a molecule, photons are absorbed and re-emitted. The majority of emitted radiation will be known as Rayleigh scattering (the same wavenumber / energy as the incident light). On the other hand, small fraction can be either at higher (anti-Stokes shift) or lower energy (Stokes shift). Due to interaction between the molecule and absorbed radiation, this leads to excitation of electrons from their ground to a virtual state the Raman scattering is formed as a result. While when the excited electrons decay back to the starting energy level the Rayleigh scattering occurs. The decay of the excited electrons to lower or higher energy level, however, will produce anti-stokes and stokes shifts respectively. The difference between incident and Raman scattering (Anti- stokes and Stokes shifts) is known as the Raman shift. Traditionally the Raman spectrum is generally plotted as intensity versus Raman shift in wavenumbers (cm^{-1}) (Andor.com).

Raman spectroscopy was used in the following thesis to qualify the formation of calcium phosphate layer. The samples were analysed in the surface and core in different areas using both area and point mapping techniques. The spectra were obtained using a Lab Ram spectrometer (Horiba, Jobin Yvon, France). The specimens were exited at 633.8 nm by a He-Ne laser though a microscope objective (50x). Raman spectra were obtained in the region 800-1700 cm^{-1} using a confocal hole of 300 μm, giving an approximate spatial resolution of 5 μm. To gain representative average spectra, several point and multiple area spectra were generated and their average was used for each sample.

Multiple areas and points were examined using the Raman spectroscopy. For example, at least 4 different points and 3 representative areas were mapped in each sample's core and surface.

Formulae A ($M_0T_0P_0$), B ($M_0T_0P_5$), C ($M_{20}T_0P_0$), E ($M_0T_{20}P_0$), G ($M_{20}T_{20}P_0$), and H ($M_{20}T_{20}P_5$) were included in the two experiments (SEM and Raman). The samples were analysed both in core and surface when kept dry, in de-ionised distilled water, artificial saliva, and simulated body fluid for 7 days at 37^{o}C.

2.3.1.3 EDX Method:

Samples containing 20%MCPM, 20% TCP, and/or 5%EPL immersed for 7 days in either AS or SBF were examined by EDX (i.e formulae G ($M_{20}T_{20}P_0$) and H ($M_{20}T_{20}P_5$).

In each formulae the surface and the core was analysed. Different points were investigated for apatite precipitations and identification of the Ca/P ratio. Several spectra points were analysed in the samples. At least 14 points were analysed to assess the Ca/P ratio in each sample's core or surface in both solutions.

2.4 Effect of calcium phosphate and ε-poly(L-lysine) on composite mass and volume changes:

In this experiment, the 8 formulae were all examined to study the individual and combined effect of CaP and EPL in water sorption potential of the experimental composite in both SBF and distilled water.

The quantity of water sorption was calculated by measuring the mass and density changes over 3 months (12 weeks) using a density kit (Mettler Toledo, Leicester, UK). Three specimens of each formulation were examined. The mass in air and under distilled water, after 0, 2, 4 and 6 hours and 1, 2, 3, and 7 days and 2, 3, 4 ,8, and 12 weeks storage in simulated body fluid or distilled water was recorded. Density was calculated using the following equation.

Density equation:

$\rho = (A/ A-B)(\rho_0 - \rho_L) + \rho_L$ Equation 4

Where ρ = specimen density, A = specimen mass in air, B = specimen mass under distilled water, ρ_0= density of distilled water and ρ_L= density of air (0.0012 g/cm3).

Mass and volume change percentage were calculated at each time point using the following equations 5, 6, and 7 respectively. The initial mass is the mass of the sample before immersion.

$$\Delta m\ (\%) = 100 \times \frac{m_t - m_0}{m_0}$$ Equation 5

$$\Delta v\ (\%) = 100 \times \frac{v_t - v_0}{v_0}$$ Equation 6

$$Volume = \frac{mass}{density}$$ Equation 7

Where

m_0 = the initial mass of the sample

m_t = is the sample mass at a time

v_0 = the initial volume of the sample

v_t = is the sample volume at a time

Averages and standard deviations of the three samples were calculated and plotted versus the square root (SQRT) of time.

2.5 Solubility and water content of the novel composite study:

All 8 different formulae were included in the study of solubility and water content. Three different samples from each formula were examined to determine the solubility and water content percentages in both simulated body fluid (SBF) and distilled water. The samples after 12 weeks in both solutions (SBF and distilled water) were vacuum dried using Heto PowerDry® LL1500 Freeze Dryer for 24 hours. The mass of these samples were measured and noted. Another cycle of drying was performed for duration of 24 hours to confirm that the samples were totally dry. Therefore, all the samples were dried for a total of 48 hours.

Solubility, water content, and the mass change per volume (mg/cc), were calculated using the following equations:

$$solubility\ (\%) = 100 \times \frac{m_{dt} - m_0}{m_0} \qquad \text{Equation 8}$$

$$\text{water content}\ (\%) = 100 \times \frac{m_{wt} - m_{dt}}{m_{wt}} \qquad \text{Equation 9}$$

$$\text{mass change/Vol}\ \left(\frac{\text{mg}}{\text{cc}}\right) = 100 \times \frac{m_{dt} - m_0}{v_0} \qquad \text{Equation 10}$$

Where:

m_{dt} *= the mass of the sample dried after 12 weeks immersion*

m_{wt} *= the mass of the sample wet after 12 weeks immersion*

m_0 *= the initial mass*

v_0 *= initial volume*

A standard deviation of the solubility and water content percentage was calculated and added to display any experimental error.

2.6 Anti-bacterial (polylysine) release study:

In this study, the polylysine release (EPL) was calculated. The absorbance of the distilled water storage solutions from mass loss studies was obtained using a Unicam Ultraviolet-visible (UV) 500 spectrometer (Thermo Spectrotonic, UK) for a period of up to 12 weeks.

Several methods can be used to assess the concentration of EPL released into solution. In the literature four methods were used to determine polylysine release; 2,4,6-trinitrobenzene sulfonate (TNBS) assay, Trypan blue (TB) assay, Orthophthalaldehyde (OPA) assay, and Bicinchoninic acid (BCA) assay. However, this study used a Trypan blue assay (TB assay), which is based on the polycationic character of EPL in acidic aqueous solutions.

In this method a non_covalent binding with the anionic dye TB leads to the precipitation of the dye. Consequently, a simultaneous decrease in the intensity of the blue colour of the solution occurs.

A modification to Grotzy and Manaka in 2010 method that compared four UV/Vis spectrophotometric methods was done (Grotzky et al., 2010). As a first step, the reagent solution (TB solution) was prepared. 0.080 g of TB was added in 10 ml distilled water to produce 8000-ppm TB solution. Adding 1 ml of this to 99 ml of distilled water diluted this solution to 80-ppm. This final prepared solution can then be used for up to 6 months.

To obtain a standard calibration curve a 10,000-ppm EPL was prepared by adding 0.1 g of EPL to 10 ml of distilled water. This was then diluted to give solutions of 20-ppm, 18-ppm, 14-ppm, 10-ppm, 8-ppm, 4-ppm, and 2-ppm. These and the sample storage solutions were then reacted with the TB solutions and analysed as described below.

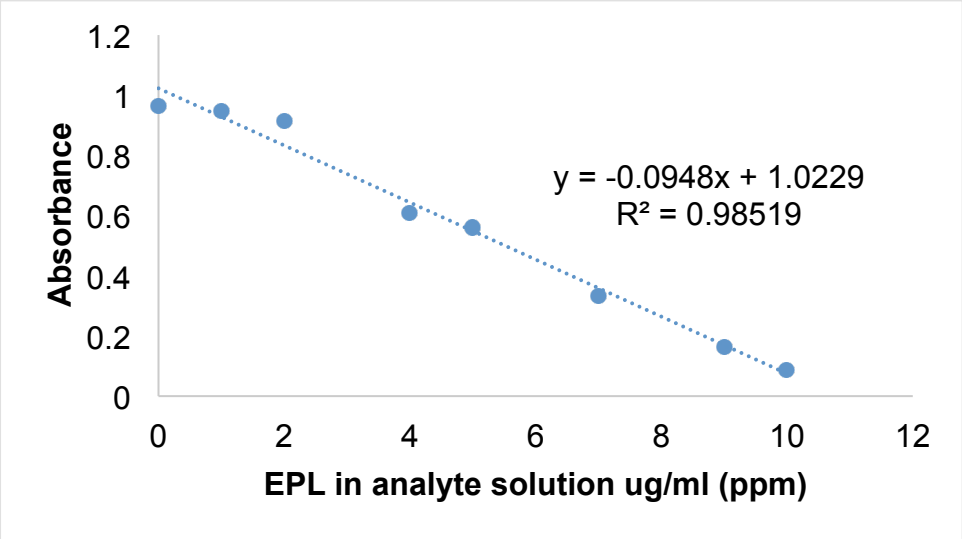

Figure 2.2: EPL calibration curve in distilled water.

For EPL analysis equal volumes of standard solution and TB solution were combined, incubated for 1 hour at 37 C, and then cooled down to room temperature for another hour. This mix was then centrifuged at 13,000 rpm for 20 minutes to sediment the precipitate as seen in figure 2.3. The supernatant was pipetted carefully into a disposable cuvette and then a Unicam UV 500 spectrometer was used to measure the absorption spectrum. This was recorded against distilled water as reference between 200 nm – 800 nm with the maximum absorbance of the TB dye being observed at 580 nm. The absorbance at 580 nm of 3 different samples from each formula was noted. The absorbance was then plotted against the known concentrations of polylysine (ppm) (See Figure 2.2).

The polylysine release from composites B ($M_0T_0P_5$), D ($M_{20}T_0P_5$), F ($M_0T_{20}P_5$), and H ($M_{20}T_{20}P_5$) into distilled water was assessed using the same method described above. Time points examined were 2 hours, 4 hours, 6 hours, 24 hours, 48 hours, 72 hours, 1 week, 2 weeks, 3 weeks, 4 weeks, 8 weeks, and 12 weeks. 3 different samples from each formula were used.

Figure 2.3: Centrifuge used in the EPL release experiment.

The amount of release was calculated using the following equation:

$$\% \text{ of EPL} = \frac{\left(C \times 10^{-6} \right) \times 2V}{M} \times 100$$

Equation 11

Where:

C = cumulative concentration of EPL (ppm)

V = volume of storage solution (10 ml)

M = total mass EPL in sample

The factor 2 accounts for dilution of the storage solution by the dye.

$$M = m_s \times \%m_{EPL} \times w_t(0.2g)$$

Equation 12

Where:

m_s = Mass of specimen

$\%m_{EPL}$ = % of mass EPL in specimen

$w_t(0.2)$ = weight fraction of liquid in the specimen (0.2)

2.7 Data analysis:

Factorial analysis:

This method allows investigating the impact of several variables at a similar time. Using this method, it is possible to reduce the number of the samples to measure the effect of several variables. So, a series of factorial design of samples formulation was prepared. The reason of having this design is to look at the individual and the combined effect of the added components. Table 2.8 shows the wt% of the variables in the powder phase components.

	Percentages of powder phase (wt%)							
β-TCP	0				20			
MCPM	0		20		0		20	
EPL	0	5	0	5	0	5	0	5

Table 2.8: Factorial design of the formulae showing the percentages of the powder phase components.

The factorial analysis can be defined as a mathematical analytical method to examine the effect of varying components in a formulation. Equation 13 demonstrates the factorial expression of the data where 8 samples are possible with 3 variables at 2 levels. [Variables are: MCPM, TCP, and EPL]

$$\ln P = <\ln P> + F_1 a_1 + F_2 a_2 + F_3 a_3 + F_1 F_2 a_{1,2} + F_1 F_3 a_{1,3} + F_2 F_3 a_{2,3} + F_1 F_2 F_3 a_{1,2,3} \quad \text{Equation 13}$$

<lnP> is the arithmetic mean of all 'ln P' values. F_i can be either +1 or -1. $2a_i$ is the average effect of changing the each variable "I" from low to high values and can be calculated using equation 13.

$$2a_i = <\ln P>_{F=+1} - <ln P>_{F=-1} \quad \text{Equation 14}$$

$\langle \ln P \rangle_{F=+1}$ and $\langle \ln P \rangle_{F=-1}$ are the arithmetic mean values of ln P for all four samples with F_i equal to +1 and -1 respectively. Interaction terms are calculated using:

$$2a_{ij} = \langle \ln P \rangle_{FiFj=+1} - \langle \ln P \rangle_{FiFj=-1} \quad \text{Equation 15}$$

$$2a_{ijk} = \langle \ln P \rangle_{FiFjFk=+1} - \langle \ln P \rangle_{FiFjFk=-1} \quad \text{Equation 16}$$

The effect of a variable was considered significant if its 95% confidence interval was less than the magnitude of a_i and if the interaction effects were small in comparison. If these error bars cross zero, the variable 'i' has no significant effect on the property.

The exponent of <lnP> equals the geometric mean of P. If the variables are significant, the "a" values can be converted into average percentage changes δ by using equation 17

$$\delta = 100(\exp(\pm 2a_i) - 1) \quad \text{Equation 17}$$

Error bar analysis:

95 % confidence interval error bars for 2a parameters were calculated according to equation 14.

$$\mathrm{CI} = \frac{1.96 \text{ X SD}}{\sqrt{\mathrm{n}}} \quad \text{Equation 18}$$

Where

SD standard deviation

n is the number of repetitions of the full set of the samples in the experiment design

Samples prepared were eight for the water sorption study (mass change, volume change, mass loss, and water content) and four for polylysine release study. Results were considered significantly different when the CI error bars did not overlap.

Regression analysis:

The linear regression analysis was performed using Linest function in Microsoft Excel for Mac 2011 version 14.4.8 software. In Linest the statistics calculated using the "least squares" to calculate a straight line that best fit the data in an experiment (gradient). The accuracy of this line depends on the degree of scatter in the data.

The equation for the line is:

$$y = mx + b$$ Equation 19

Where

y-values are a function of the independent x-values

m is the coefficients corresponding to x-values

b is a constant value

The Linest function syntax has the following argument:

$$LINEST(known\_y's, [known\_x's], [const], [stats])$$ Equation 20

Where

Known_y's are required and the set of y-values that already known in the relationship y = mx + b (mass change and volume change in this study)

Known_x's are optional and are the set of x_values known in the relationship y = mx + b (SQRT in this study)

Cons and stats are optional and either true or false.

So, using the Linest function the gradient and the standard error (SE) of the gradient was obtained. In addition the standard deviation (SD) and the confidence interval (CI) was calculated. See equations 15 and 17.

$$SD(\sigma) = SE * \sqrt{n}$$ Equation 21

Where

σ = standard deviation

SE = standard error of the gradient

n = number of samples

This analysis was used to calculate the initial gradient in mass increase, volume increase, and EPL release. Also, the gradient was plotted against CI to interpret any significant findings between the formulae.

Univariate Analysis of Variance:

Univariate analysis of variance separately studies the effects of different variables affecting a set of data. It looks at both the central tendency of the values and the range of values. In this study, three samples of each formula were analysed using a statistical programme (SPSS statistics version 21, IBM, USA) for the individual and combined effect of the additive components (MCPM, TCP, EPL, and the medium (SBF or water)) on the mass and volume change. The maximum change and the change after 12 weeks in volume and mass were analysed. Also, solubility and water content were analysed to assess the individual and the combined effect of the variables used in the study. This is to investigate any significant effect of these components at 0.05 level.

One way analysis of variance:

Mass change and volume change of formulae G ($M_{20}T_{20}P_0$) and H ($M_{20}T_{20}P_5$) after 1 week in SBF or water were analysed using a statistical programme (SPSS statistics version 21, IBM, USA).

One-way analysis of variance, (ANOVA) test was applied to compare results at p value of 0.05. Post hoc multiple comparison, Dunnett T3 and Bonferroni were applied to assess any differences in mean mass change and volume change respectively.

Figure 2.4 summarises all the experiments done on the novel composite studied in this thesis.

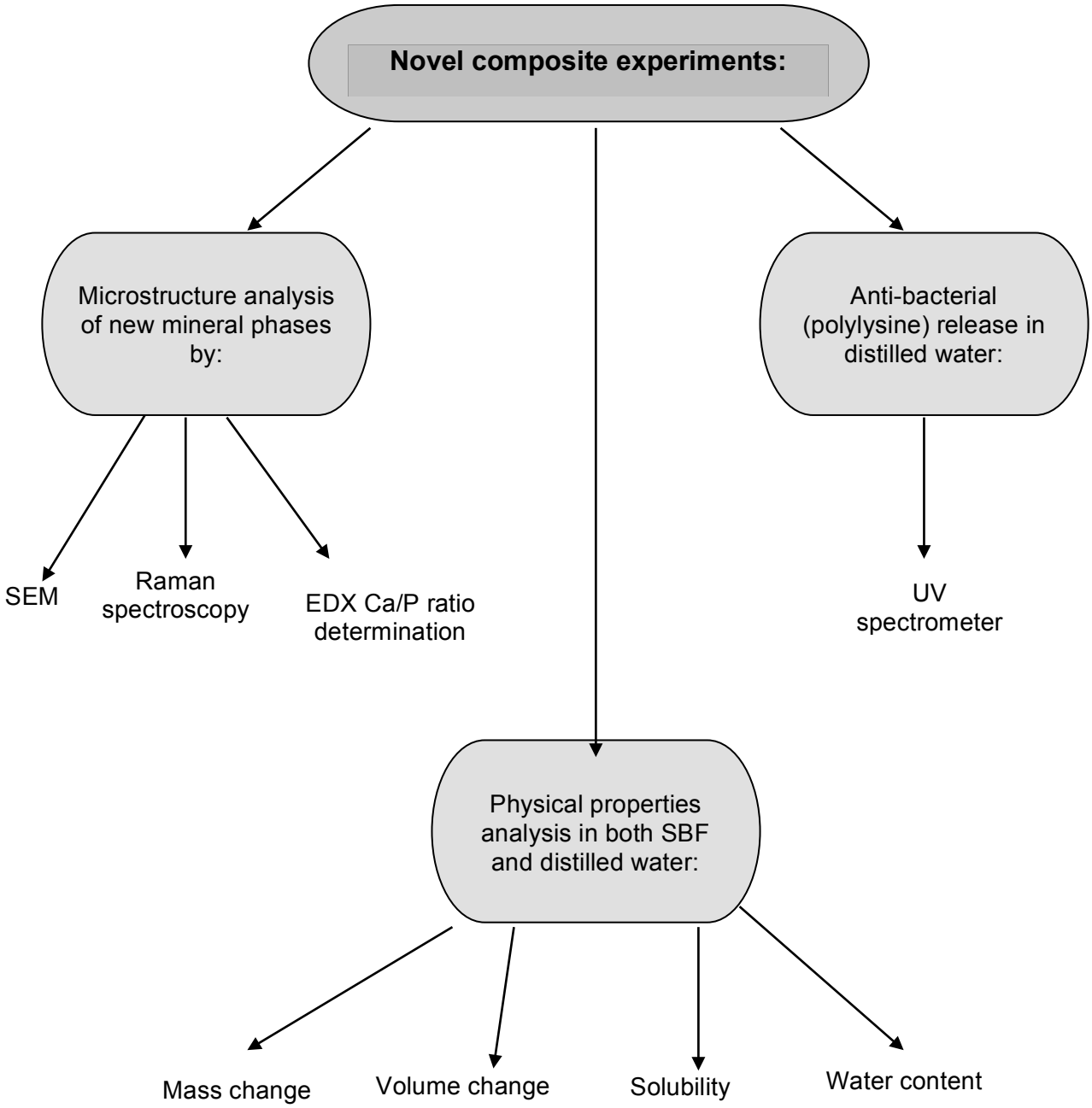

Figure 2.4: Flowchart of the studies done in the experimented composite.

Chapter III

Results

3.1 Identification of new mineral phases on the surfaces and in the bulk of the novel composites (Microstructure study analysis):

Figures 3.1, 3.2, 3.3, and 3.4 show the Raman spectra for the main components used in and/or obtained in the study. Figure 3.1 shows the peaks for the powder phase components. The glass has intense peaks at 1370 / 1400 cm^{-1}, MCPM at 913 cm^{-1}, and TCP at 968 / 943 cm^{-1}. These peaks in MCPM and TCP are due to the P-O bond stretch.

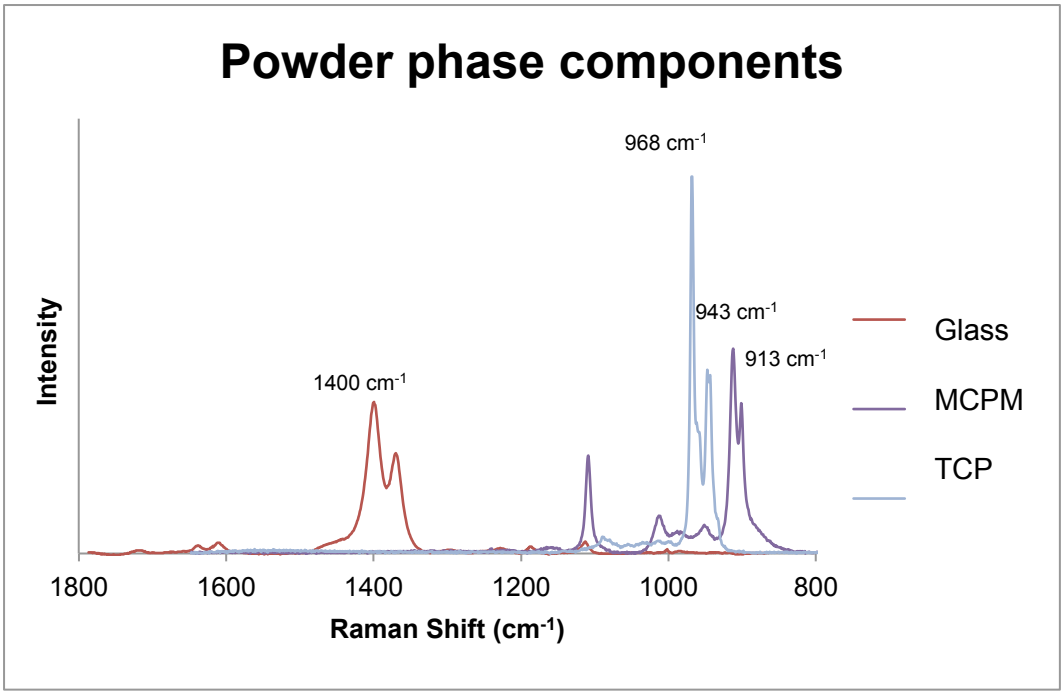

Figure 3.1: Raman spectra of powder phase components.

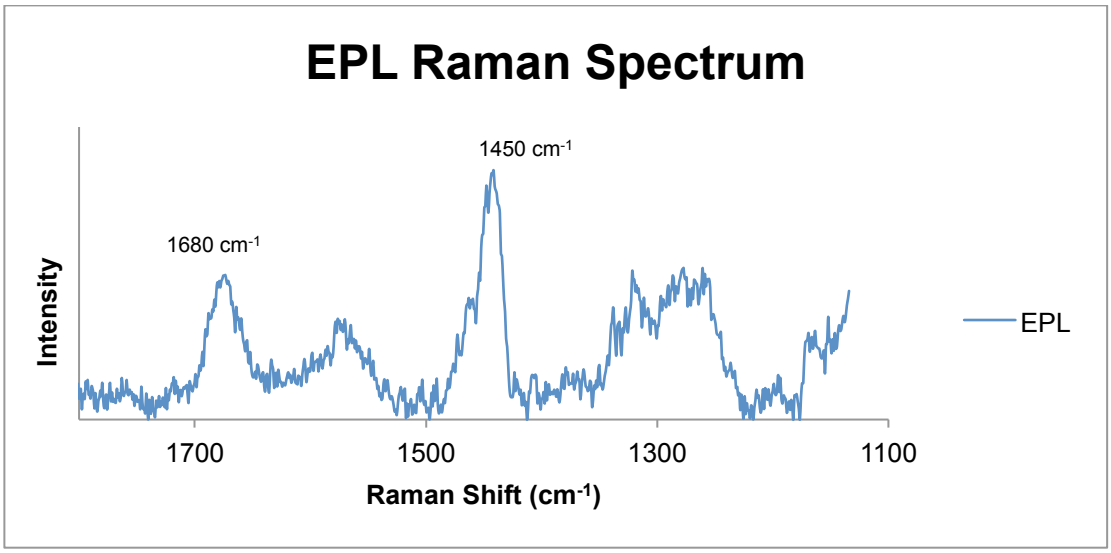

Figure 3.2: Raman spectra of polylysine (EPL).

The main peaks for polylysine are at 1450 cm^{-1} and 1680 cm^{-1} see (figure 3.2) The Raman spectrum of EPL is attributed to the amide (I) band at 1680 which is predominantly a C=O stretching vibration. While the amide (II) at 1570 cm^{-1} is due to C-N stretching coupled with N-H bond. The 1680 cm^{-1} peak is broad and weaker than that of the methylene-bending mode at 1450 cm^{-1}. The 1450 cm^{-1} peak is used as an internal intensity standard for proteins in Raman spectroscopy. In addition, the medium peak around 1300 cm^{-1} is due to the amide (III) vibration. This peak mainly involves N-H bending and C-N stretching motion (Carrier and Pézolet, 1984).

The Raman spectra of the liquid monomer phase are compared with the spectrum of UDMA in figure 3.3. Additionally the spectrum of the polymerised monomer is shown. The main Raman peaks are at 1400 cm^{-1} and 1450 cm^{-1} (C-H stretches) 1640 cm^{-1} (C=C stretch) and 1720 cm^{-1} (C=O stretch). Upon polymerisation the 1450 cm^{-1} is more intense relative to the other peaks.

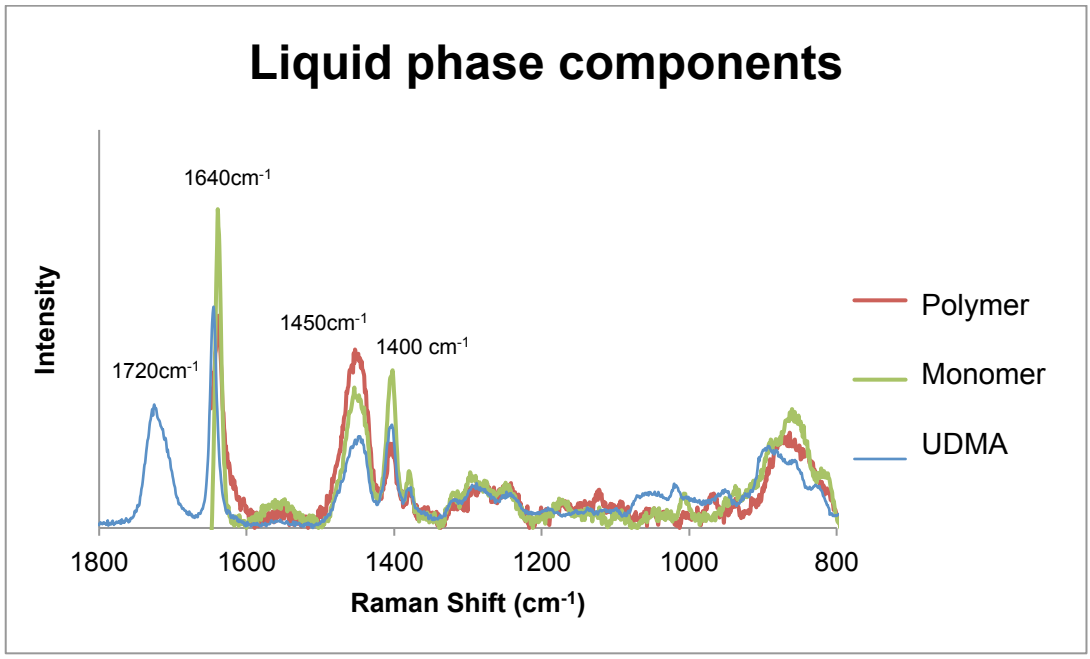

Figure 3.3: Raman spectra of monomer components before and after polymerisation and of UMDA monomer.

Figure 3.4 shows the Raman spectra of various calcium phosphates that may form in or on the materials with time. HA has a single intense P-O stretch peak at 960 cm^{-1}. Monetite and Brushite both peak at 989 cm^{-1}. However, in Monetite the peak is broader when comparing it to the Brushite peak.

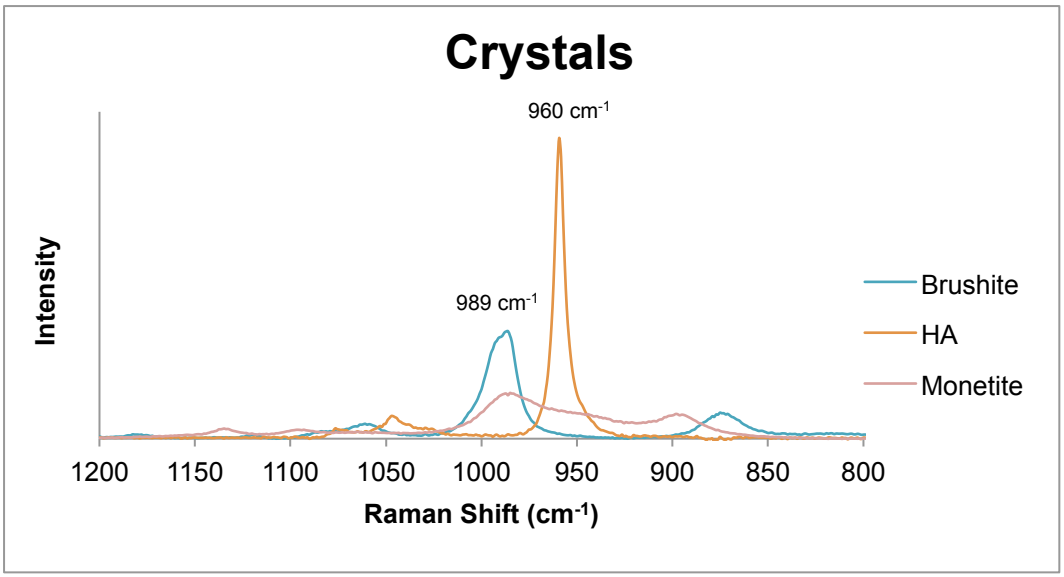

Figure 3.4: Raman spectra for various calcium phosphates.

Figure 3.5 shows the Raman shift of the different components of artificial saliva. The Raman shift ranges between 400 cm^{-1} and 1800 cm^{-1}.

The components of artificial saliva showed the following main peaks:

- Methyl-p-hydroxybenzoate sodium salt has main high peaks above 600 and 800, between 1100 – 1200 cm^{-1}, and around 1600 - 1700 cm^{-1} (Sigmaaldrich.com).
- Sodium carboxymethyl cellulose main Raman peaks between 1200, 1400 and 1600 cm^{-1} (Ambjörnsson et al., 2013).
- KCl main peak is bellow 400 cm^{-1} and ranges between 100 and 150 cm^{-1} (Marculescu, 1974).
- $MgCl_2.6H_2O$ main peaks are above 1800 cm^{-1} and range between 3300 – 3500 cm^{-1} (Garcia et al., 2006).
- $CaCl_2.2H_2O$ has a high peak below 200 cm^{-1} (Uriarte et al., 2015).
- $K_2HPO_4.3H_2O$ high peak around 4000 cm^{-1} (Jurado et al., 2012).
- KH_2PO_4 has a band at approximately 915 cm^{-1} (Jurado et al., 2012).
- Also KOH was used as a buffer and its Raman main peak is around 660 cm^{-1} (Arsov et al., 1991).

Due to the fact that KCl, $MgCl_2.6H_2O$, $CaCl_2.2H_2O$, $K_2HPO_4.3H_2O$, and KH_2PO_4 were added in very low amounts, Methyl-p-hydroxybenzoate sodium salt and Sodium carboxymethyl cellulose main peaks dominated the Raman of the artificial saliva components.

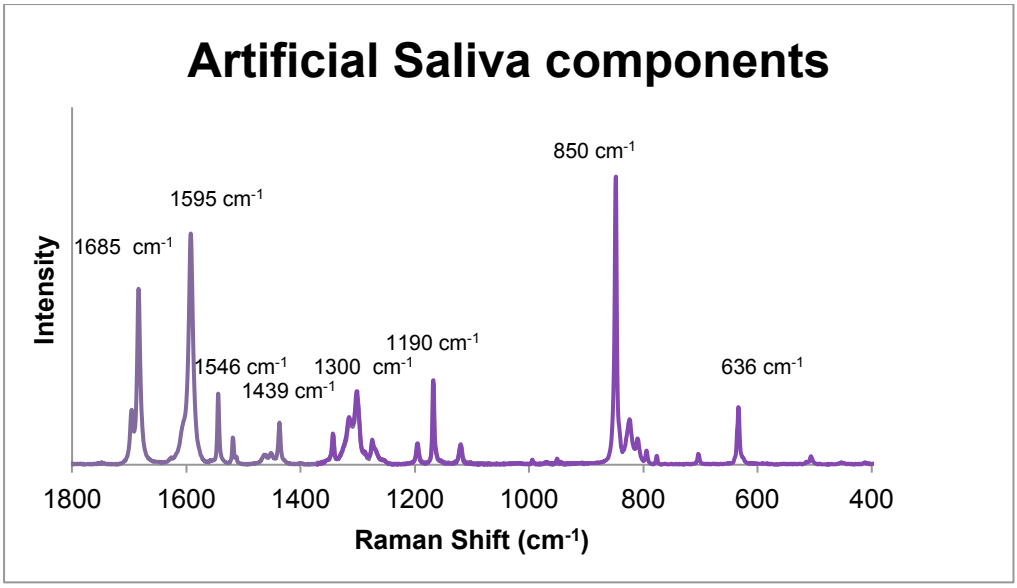

Figure 3.5: Raman spectra of artificial saliva components.

3.1.1 Effects of individual and combined calcium phosphates and polylysine on bulk and surface precipitations after storage in different fluids (SEM and Raman spectroscopy analysis):

The following section provides selected SEM and Raman of specimens, which demonstrate surface calcium phosphate precipitation, which could indicate material dentine remineralisation potential. Also shown are images and Raman confirming chemical changes in the bulk of the materials, which could provide a second setting reaction and / or self-heal mechanism. In the first part control samples are shown. A comparison between the combined and individual effects of adding calcium phosphate and anti-bacterial polylysine in the powder phase is then provided for samples stored in 3 different solutions; distilled water, artificial saliva, and simulated body fluid. EDX analysis of selected formulations was also done.

Both the bulk and the surface of all the formulae in the different solutions were examined, however, only selected and most significant findings are illustrated and explained in the following sections. A summary of all the results is provided in tables 3.1 and 3.2.

Formula A ($M_0T_0P_0$):

Formula A ($M_0T_0P_0$) is a control formulation. SEM images of the surface and the core showed flat clear surfaces and protruding particles respectively when kept dry or left for 7 days in the 3 solutions; distilled water, artificial saliva, or simulated body fluid (see for example Figure 3.6 a and b). No crystal precipitation was found as expected because this formula only contains Glass in the filler phase. Raman showed a high peak at 1400 cm^{-1} due to glass but no phosphate peaks (see Figure 3.6 c).

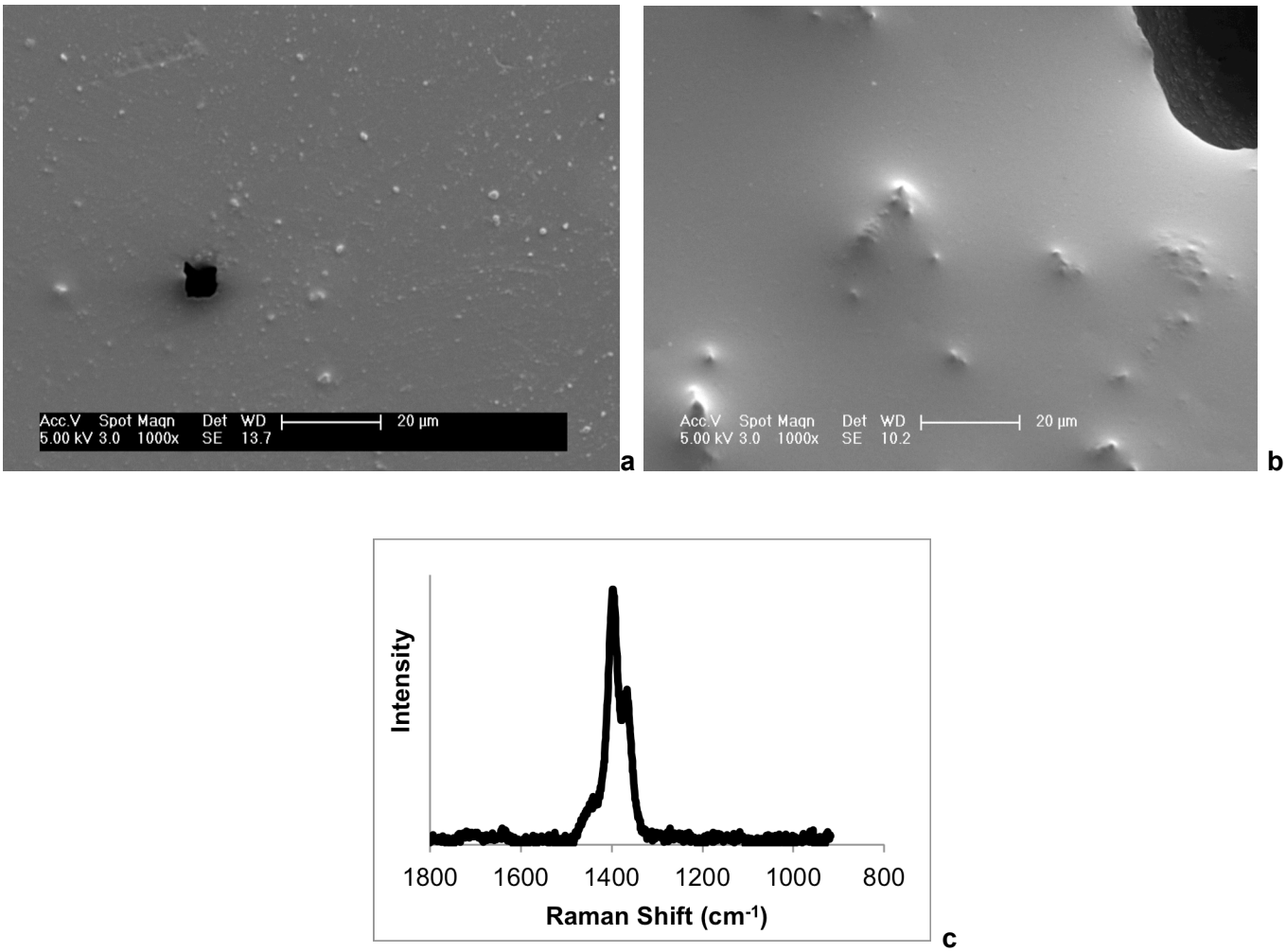

Figure 3.6: Formula A a) SEM of dry sample's surface b) SEM of core after 7 days in SBF showing no precipitation and c) Example Raman spectrum of the core showing glass peaks around 1400 cm^{-1}.

Formula B ($M_0T_0P_5$):

Formula B ($M_0T_0P_5$) containing only 5% EPL in the glass filler phase, had similar SEM and Raman to the first control formula apart from the observation of polylysine particles in core by SEM. Raman spectra were dominated by the glass peak at 1400cm^{-1} as seen in figure 3.7.

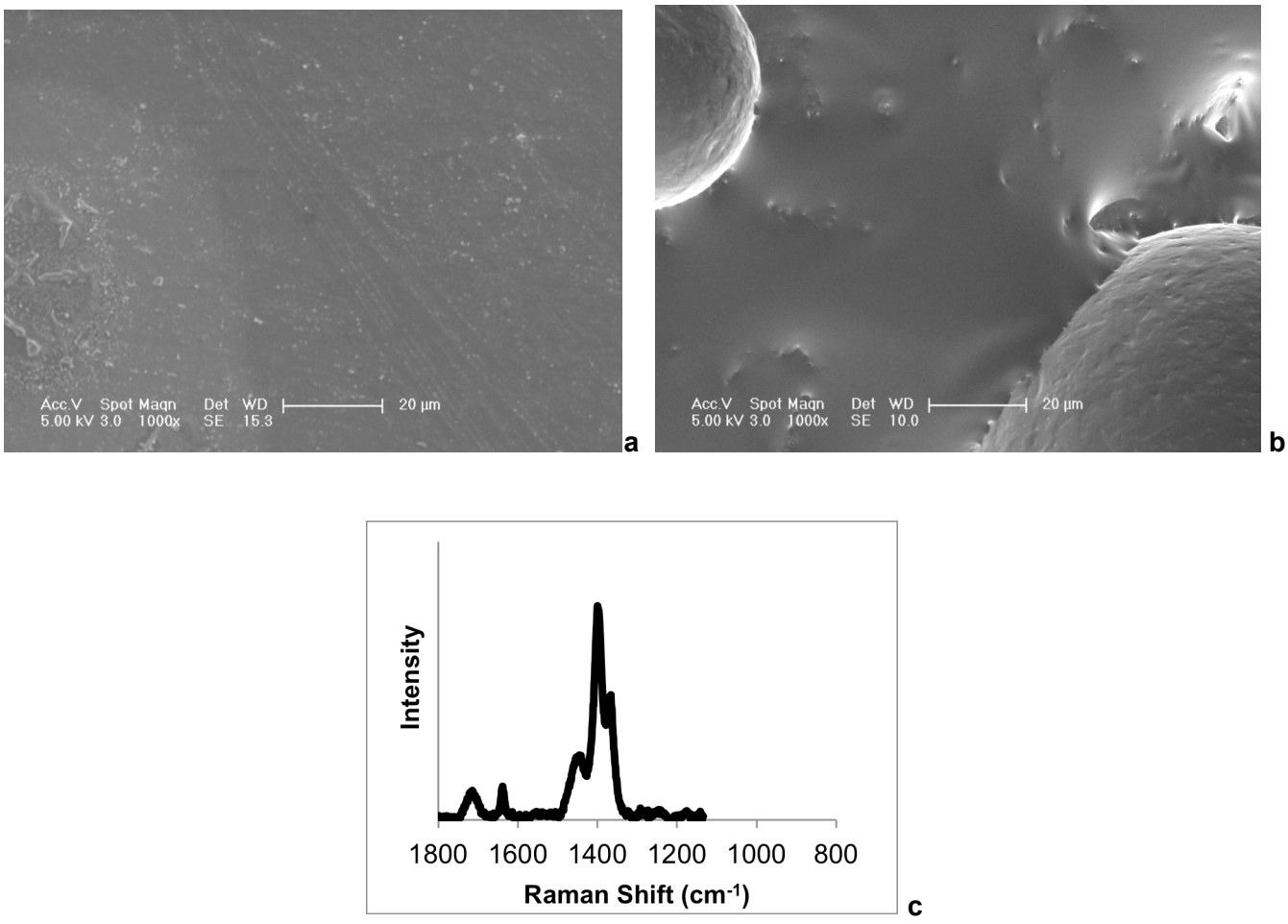

Figure 3.7: Formula B a) SEM of the surface after 7 days in AS b) SEM of core after 7 days in AS with no precipitation but some un-dissolved EPL. c) Raman spectra of the core showing a high peak at 1400 cm^{-1} due to glass in addition to monomer / polymer peaks at higher wavenumbers.

No precipitation was noted on this formula when kept in SBF for 7 days. Raman showed a high peak at 1400 cm^{-1} and other high peaks due to organic compounds, which might include the polymer, EPL and / or SBF components. See figure 3.8.

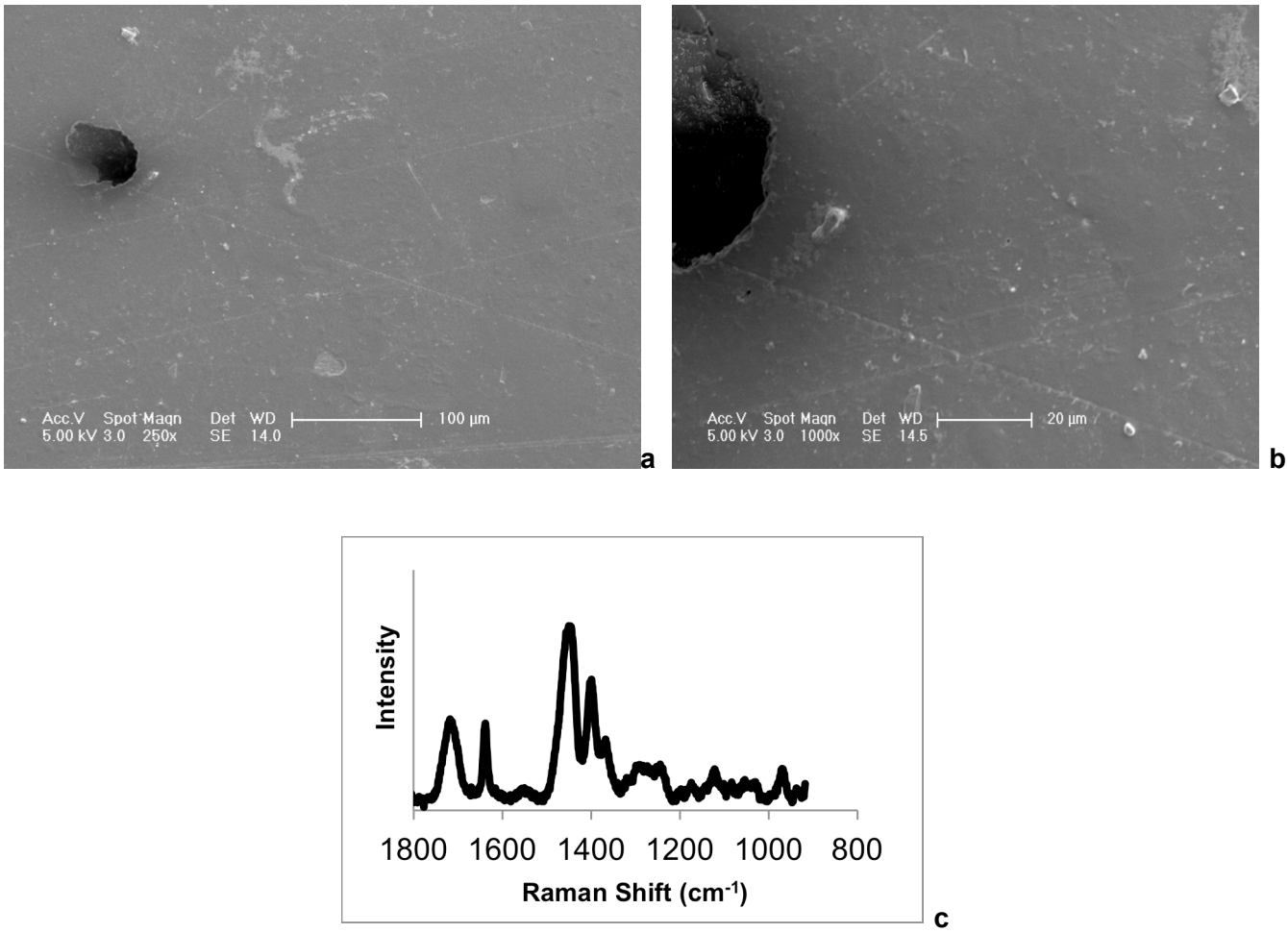

Figure 3.8: Surface of formula B at a) 250X, b) at 1000X after 7 days in SBF indicating no precipitation.
c) Raman spectrum of the surface of formula B after 7 days in SBF.

Formula C ($M_{20}T_0P_0$):

($M_{20}T_0P_0$) contains 20% MCPM in the powder phase. The most significant changes with this formula were noted when it was kept in artificial saliva and simulated body fluid (Figure 3.9 and 3.10) for 7 days. SEM images of the surface for the formula when kept in artificial saliva showed no precipitation (figure 3.9 a) but, the core (figure 3.9 b) showed "layered sheet like" roughly rectangular structures that were ~ 1x 5 x 10 micron in size. The crystals in the core of this sample were analysed by Raman and a Monetite peak was noted as seen in figure 3.9 c.

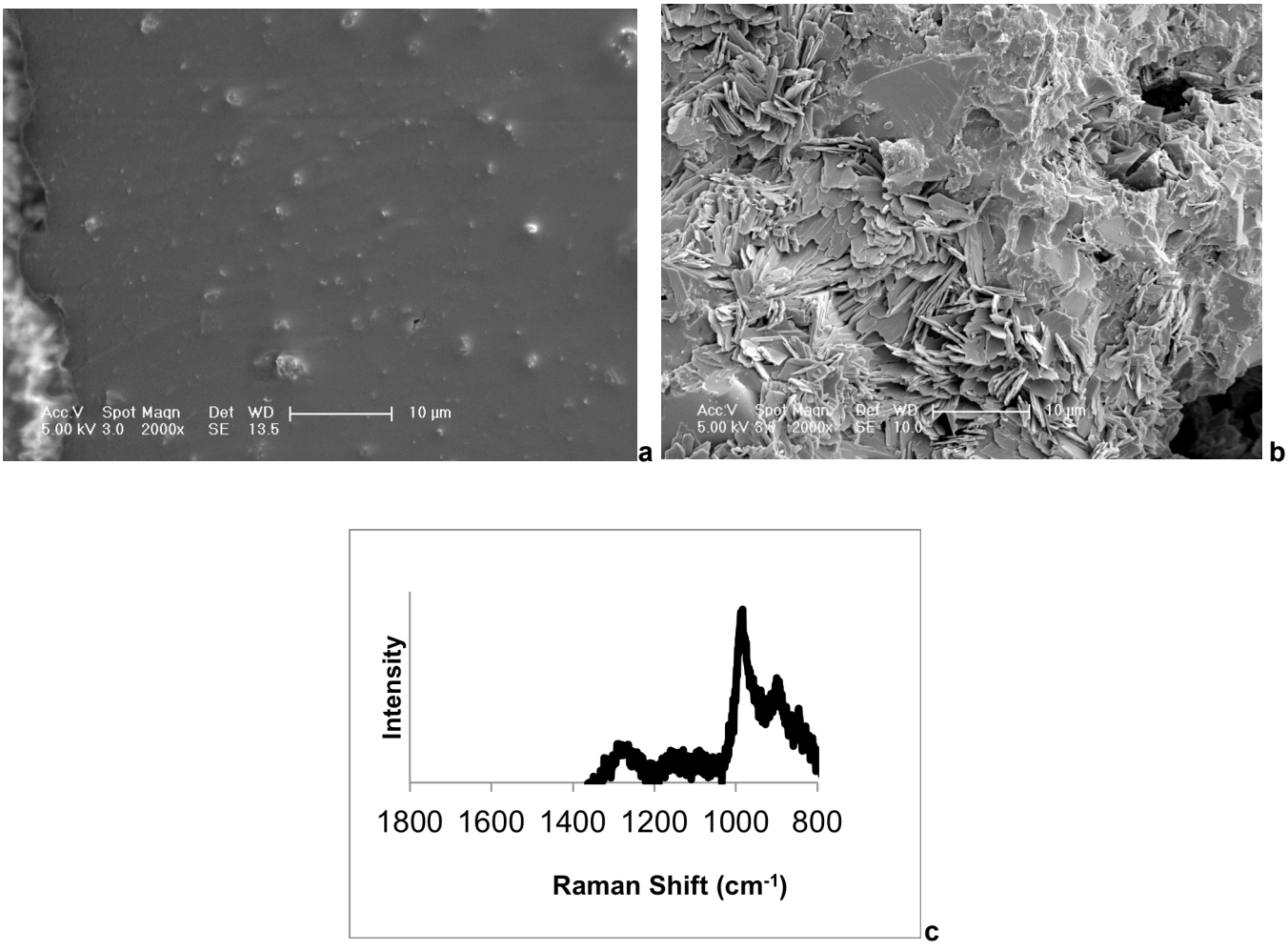

Figure 3.9: a) SEM of the surface of sample C after 7 days in AS with no precipitation, b) SEM of core after 7 days in AS showing crystal precipitation and c) Raman of crystals in core showing Monetite peaks.

More significant effects were noted in this formula when kept in simulated body fluid (figure 3.10). A few crystal precipitations were seen on the surface of the specimens (figure 3.10 a) but many more in the core (figure 3.10 b). Flat rectangular or triangular crystals were seen in both figure 3.10 a and b. Raman analysis of the core and the surface showed a Raman peak consistent with Brushite (figure 3.10 c).

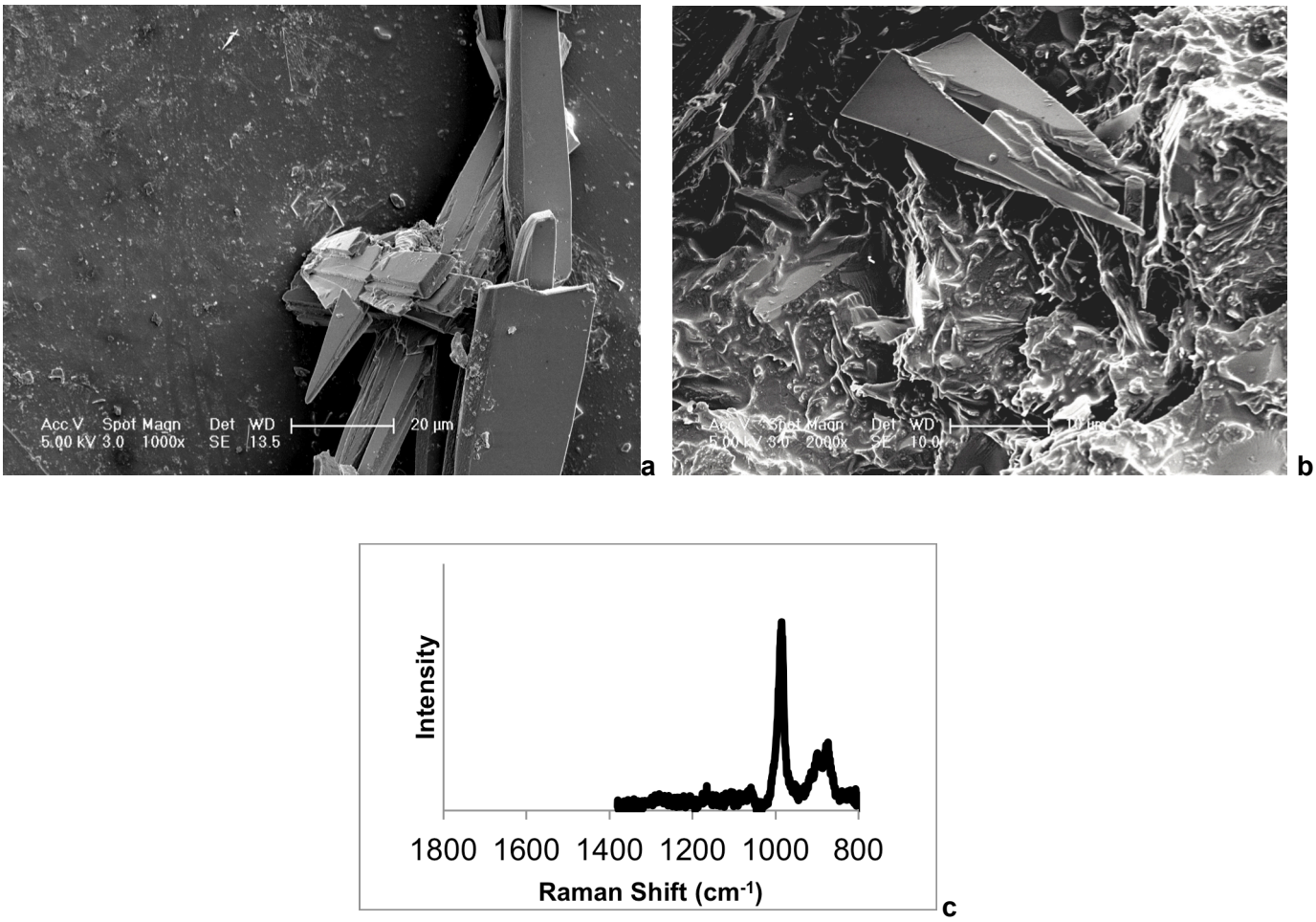

Figure 3.10: Sample C a) surface after 7 days in SBF.
b) The core after 7 days in SBF with crystal precipitation.
c) Raman spectrum of the core shows high Brushite peak at 989 cm^{-1}.

Formula E ($M_0T_{20}P_0$):

In formula E ($M_0T_{20}P_0$), 20% β-TCP was added. No crystal formation was seen in this formula's core or surface with any of the storage solutions (figure 3.11). The surface (figure 3.11 a) and core (figure 3.11 b) SEM images showed clear surfaces. Raman spectrum of core and surface gave dominant β-TCP peaks at 943 cm^{-1} and 968 cm^{-1} as illustrated in figure 3.11 c.

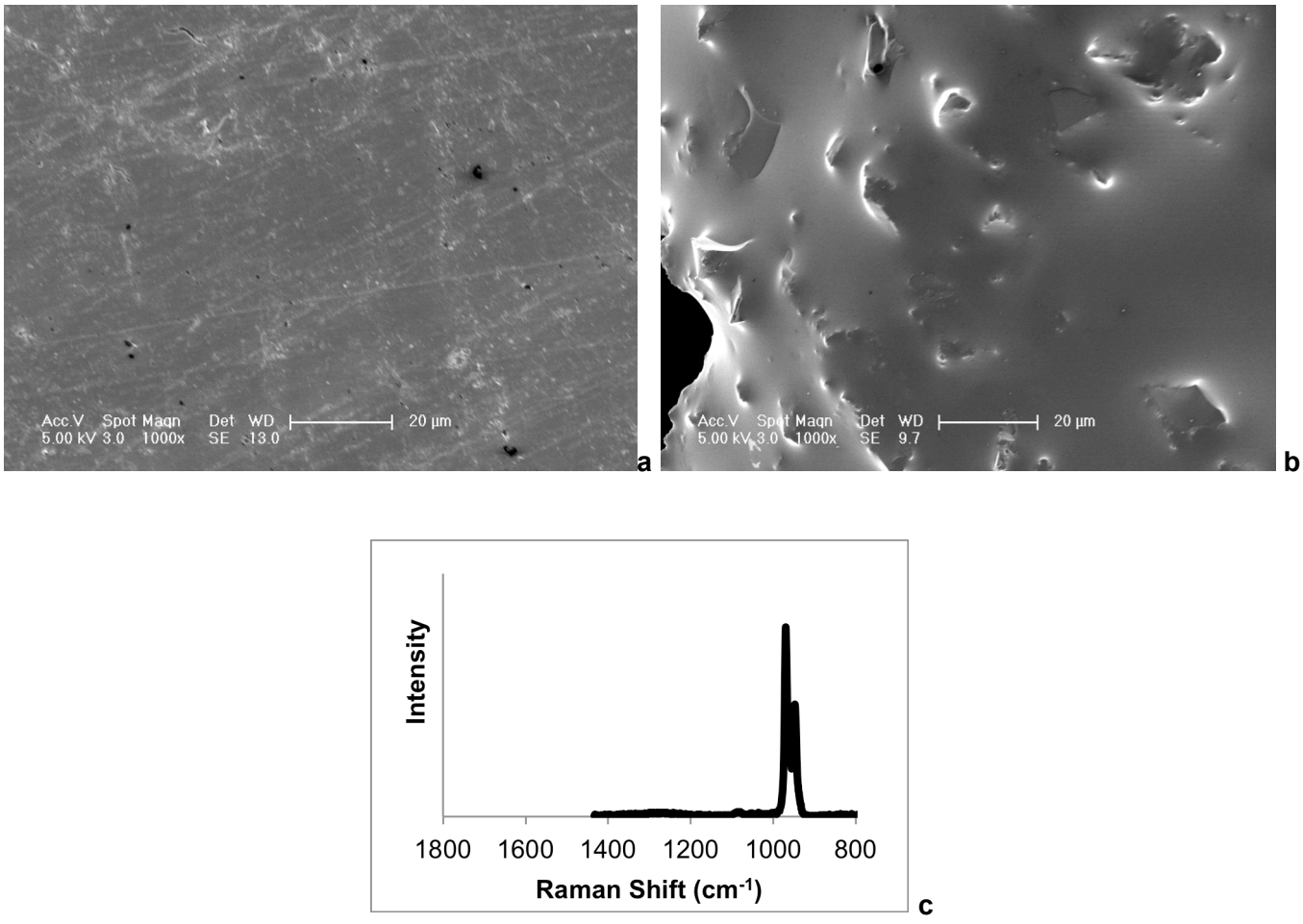

Figure 3.11: a) The surface of formula E in SBF
b) The core of formula E in SBF with no precipitation, c) Example of β-TCP's dominant peaks at 943 cm^{-1} and 968 cm^{-1} seen in surface and core.

Formula G ($M_{20}T_{20}P_0$):

Surface precipitation:

This formula contains both 20%MCPM and 20%β-TCP. In figure 3.12, the surface of formula G when analysed by SEM after 7 days in SBF showed flat crystals with a thickness of around 1 micron. Raman of these crystals showed a Brushite peak at 989 cm^{-1}.

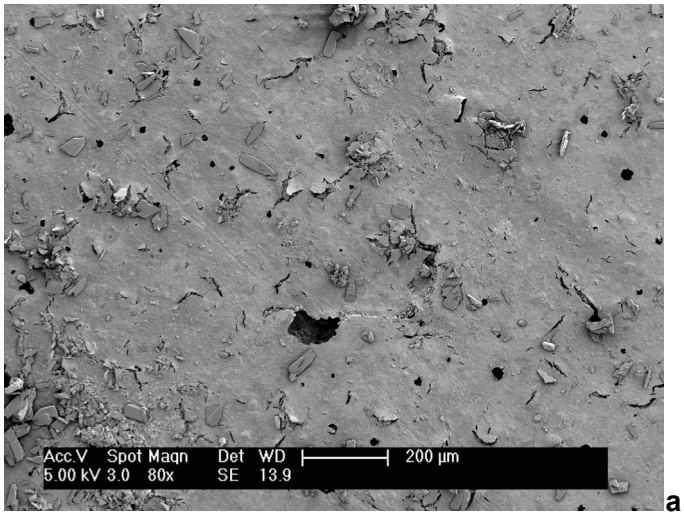

a

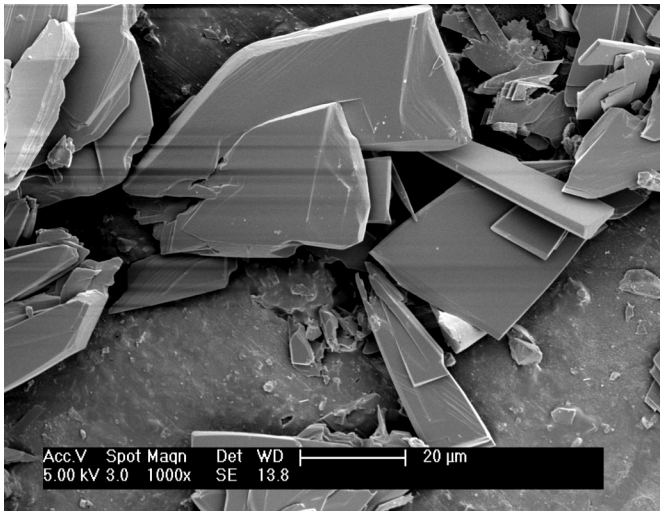

b

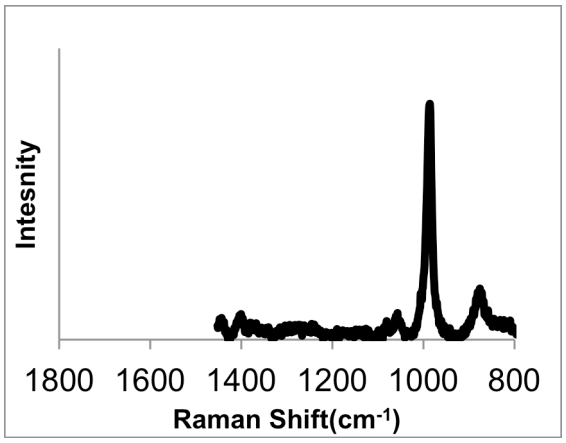

c

Figure 3.12: a) The surface of formula G ($M_{20}T_{20}P_0$), after 7 days in SBF at 80X magnification. B) at 1000X showing calcium phosphate precipitations
c) Raman shift of the formula's surface after 7 days in SBF with a high peak at 989 cm^{-1}.

Core precipitation:

The core of this formula when kept dry showed no crystal precipitation (figure 3.13). However, in figure 3.14 the SEM images of the core of this formula showed calcium phosphate precipitation in all solutions.

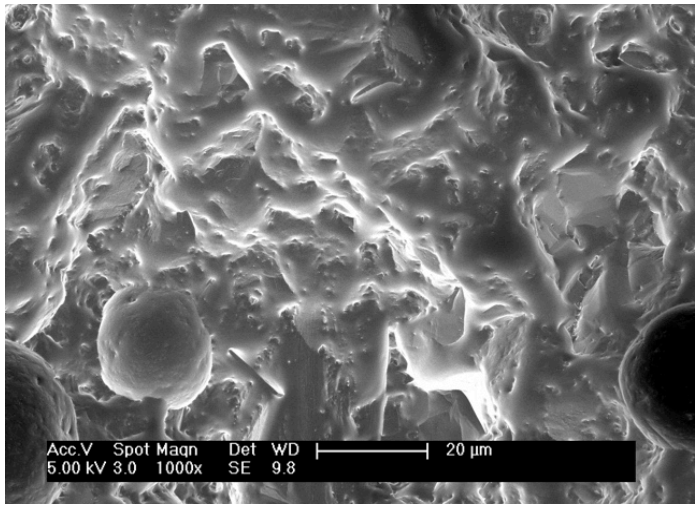

Figure 3.13: SEM of formula G ($M_{20}T_{20}P_0$) core when kept dry showing no crystal precipitation.

Comparing the SEM images in figures 3.13 and 3.14 (a, c, and e), there are significant differences.

Raman shifts of the core of this sample showed Monetite peaks in both artificial saliva and distilled water (figure 3.14, b and d). However, Raman shift of the core in simulated body fluid showed a mixture of Monetite and Brushite. However, Brushite was seen as the dominant phase (see figure 3.14 f).

A combined range of crystals precipitation was seen in the core of the formula when kept in distilled water, artificial saliva, and simulated body fluid as seen in figure 3.14 a, c and e.

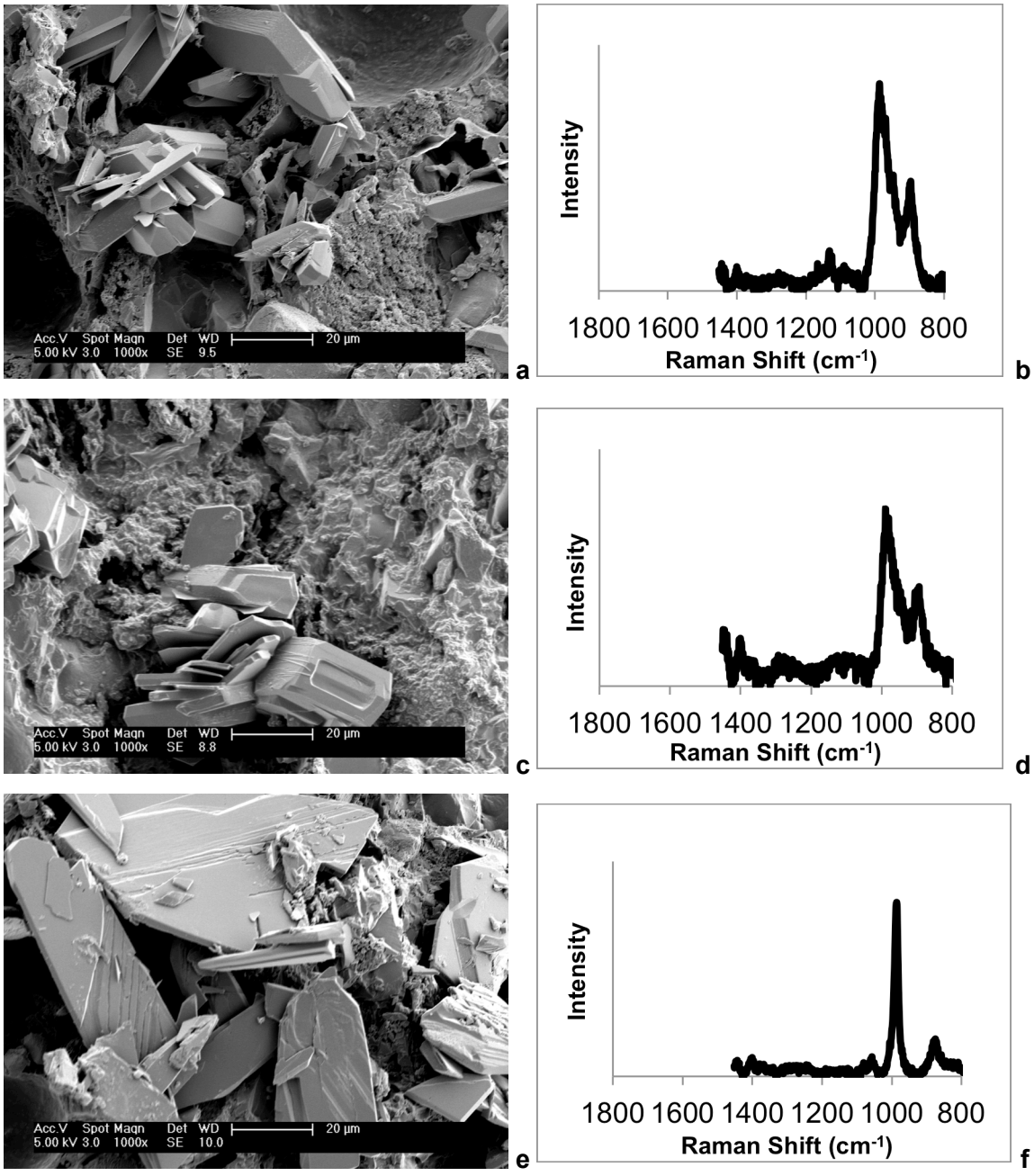

Figure 3.14: SEM of formula G ($M_{20}T_{20}P_0$), core a) in distilled water, c) in AS, e) in SBF with different crystals precipitations and Raman spectra of formula G ($M_{20}T_{20}P_0$) core showing b) Monetite in distilled water, d) Monetite in AS, f) Brushite in SBF.

Formula H ($M_{20}T_{20}P_5$):

Surface precipitation:

Formula H showed the most interesting results. It contains MCPM, TCP, and EPL at 20%, 20% and 5% respectively. SEM images of the surface after 7 days in simulated body fluids showed crystals typical of Brushite / Monetite but in addition other crystal formation (see figure 3.15 a and b). Raman mapping and comparison with work of others confirmed the new crystal structures were most likely to be a form of apatite (hydroxyapatite). These gave a single dominant high Raman peak at 960 cm^{-1} (figure 3.15 c). In figure 3.15 a and b, the fine crystals are most probably Brushite but the flat plates are perhaps Monetite.

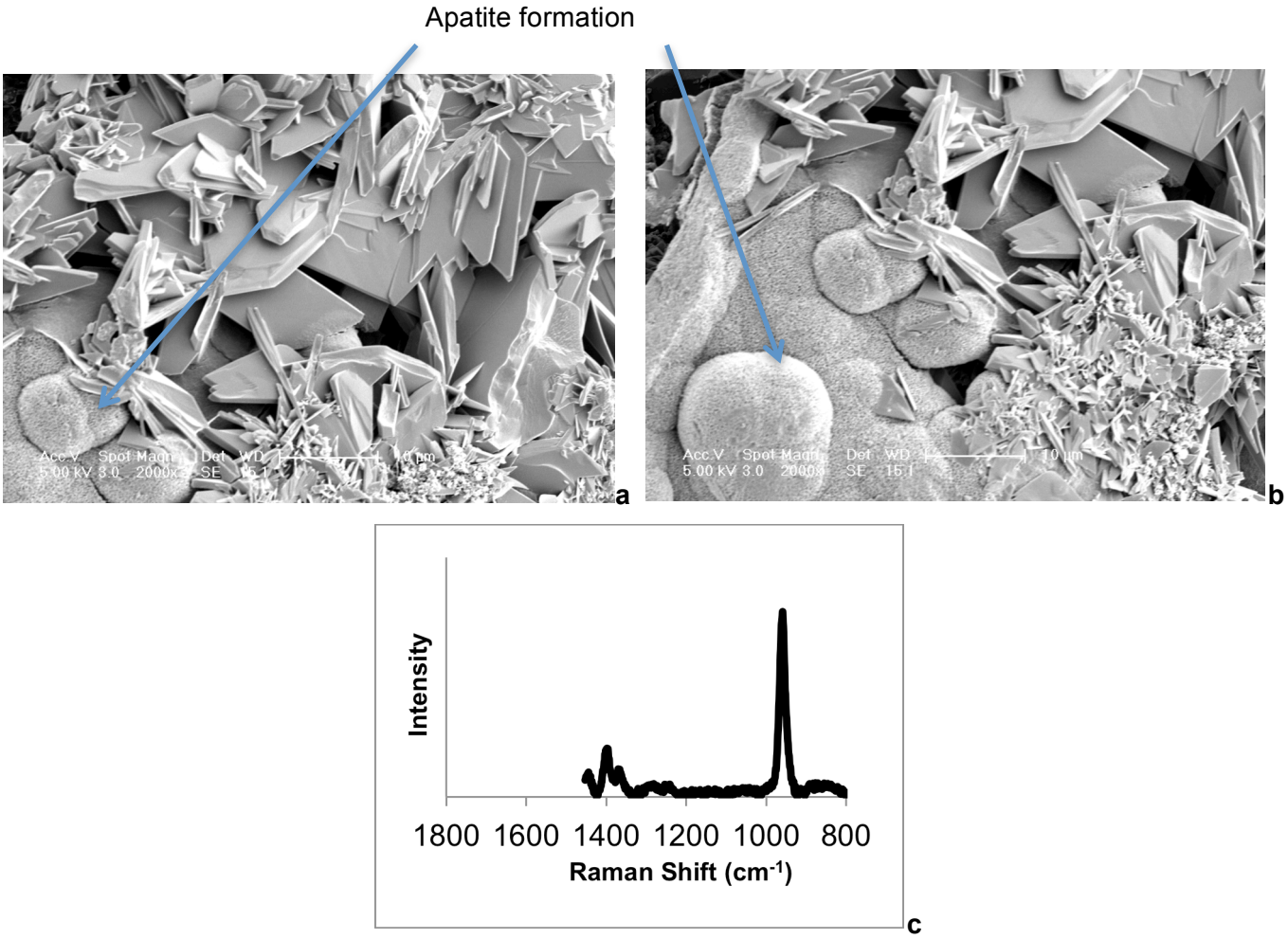

Figure 3.15: a and b) Surface of formula H ($M_{20}T_{20}P_5$) at 2000X.
Both images are for the sample after 7 days in SBF showing crystal precipitations.
c) Raman mapping of the surface of the sample after 7 days in SBF showing one HA single peak at 960 cm^{-1}.

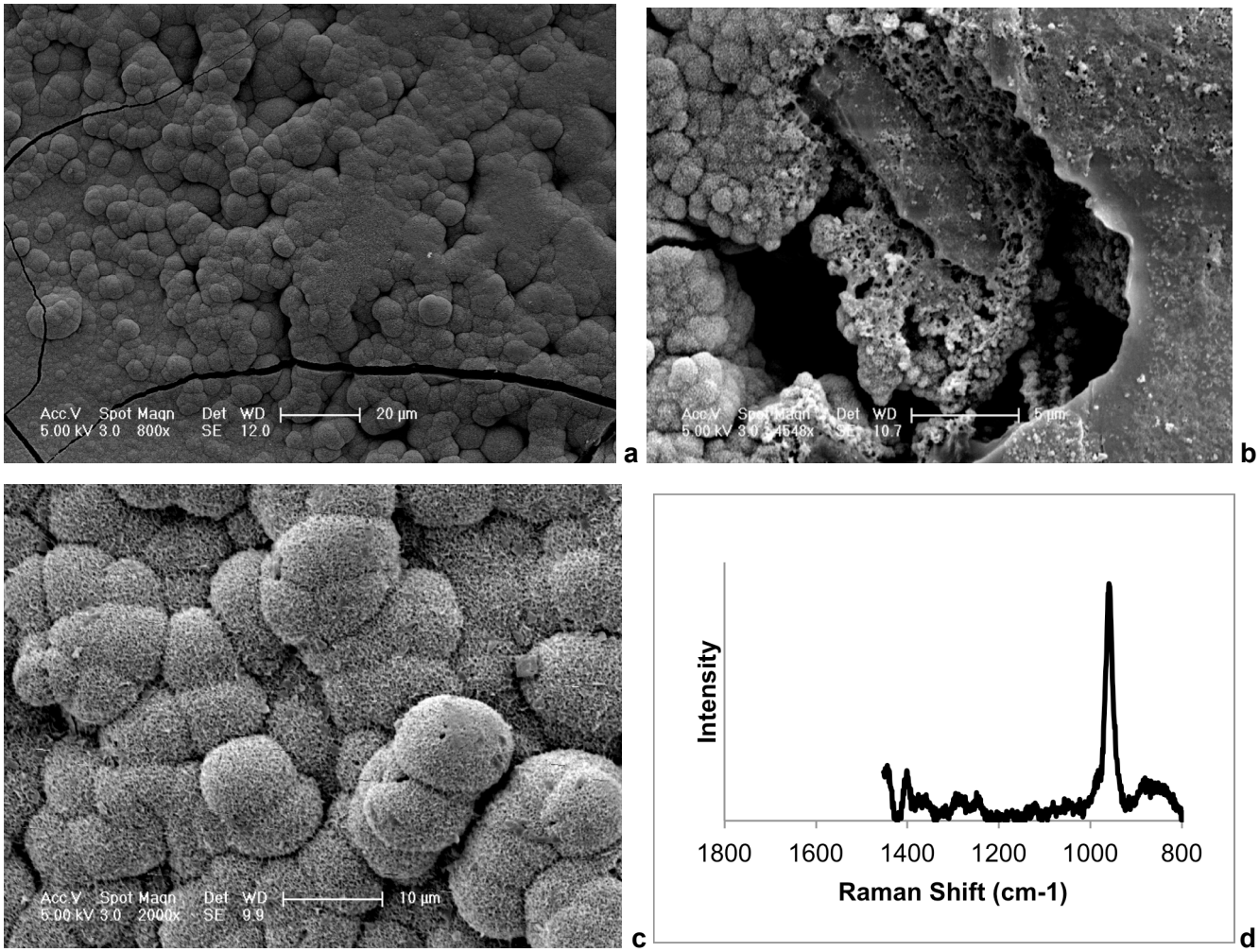

Figure 3.16: The surface of sample H ($M_{20}T_{20}P_5$) upon immersion in SBF for 4 weeks showing calcium phosphate precipitation layer formation, a) at 800X b) at 4548X c) at 2000X. d) Raman mapping of the surface of the sample after 1 month in SBF showing one HA single peak at 960 cm^{-1}.

Referring to figure 3.16 a, b and c, calcium phosphate precipitations can be seen on the surface of formula H ($M_{20}T_{20}P_5$) after 4 weeks immersion in SBF. These precipitations look different compared to precipitations on the surfaces of other samples. As stated earlier these crystals can be apatite (HA) crystals. Also, comparing images 3.16 to 3.15, the calcium phosphate precipitations are more mature in images of figure 3.16 upon 4 weeks immersion. The honeycomb appearance of these crystals suggests it is possibly HA.

Core precipitation:

The core of this formula showed also crystals formation after 7 days in simulated body fluid (see for example figure 3.17 a and b). A mixture of apatite and Brushite crystals was seen. However, Raman mapping of the core showed a dominant Brushite peak as seen in figure 3.17 c.

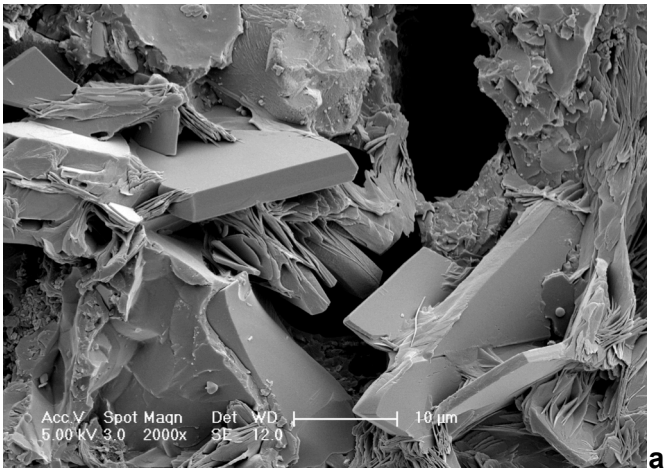

a

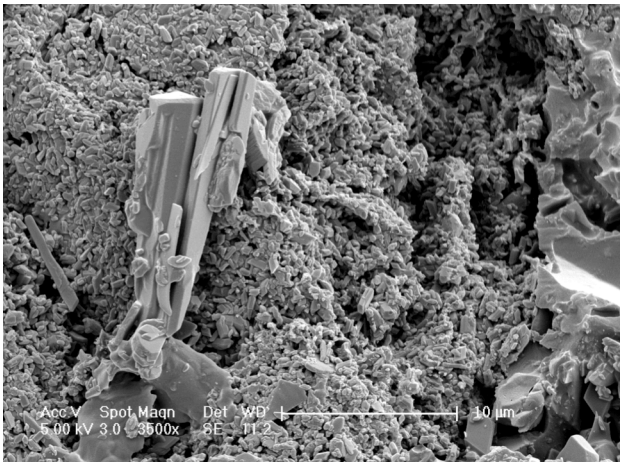

b

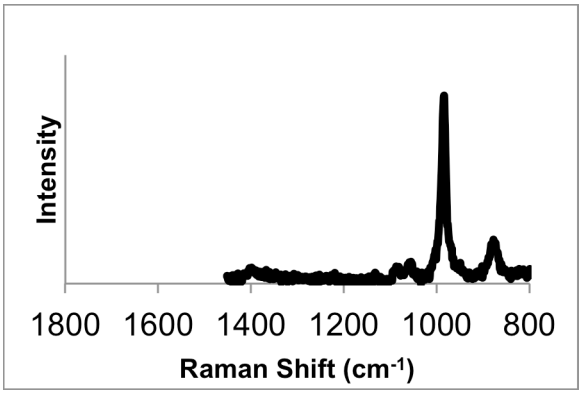

c

Figure 3.17: a and b) SEM image of the core of formula H ($M_{20}T_{20}P_5$) after 7 days in SBF at 2000X and 3500X respectively with crystal precipitations.
c) Raman shift of the surface showing a Brushite high peak at 989 cm^{-1}.

To summarise, tables 3.1 and 3.2 show the dominant components other than the polymer identified by Raman and/or SEM on the surfaces and cores of the experimental composites when stored under different conditions.

Formula	Dry	Water	AS	SBF
A-$M_0T_0P_0$	Glass			
B-$M_0T_0P_5$	Glass + EPL			
C-$M_{20}T_0P_0$	Glass +MCPM		Monetite	Brushite
E-$M_0T_{20}P_0$	Glass + TCP			
G-$M_{20}T_{20}P_0$	Glass + MCPM + TCP	Monetite		Brushite + Monetite
H-$M_{20}T_{20}P_5$	Glass + MCPM + TCP + EPL	Monetite		Brushite

Table 3.1: Dominant components other than the polymer identified by Raman and/or SEM in the core of composites stored under different conditions.

Formula	Dry	Water	AS	SBF
A-$M_0T_0P_5$	Glass			
B-$M_0T_0P_5$	Glass + EPL	Glass		
C-$M_{20}T_0P_0$	Glass + MCPM	Glass		Brushite
E-$M_0T_{20}P_0$	Glass + TCP			
G-$M_{20}T_{20}P_0$	Glass + TCP + MCPM	Glass + TCP	Brushite	
H-$M_{20}T_{20}P_5$	Glass + TCP + MCPM	Glass + TCP	Brushite	HA + Brushite

Table 3.2: Dominant components other than the polymer identified by Raman and/or SEM on the surfaces of composites stored under different conditions.

Calcium phosphate resultant precipitant in the 6 different formulae when immersed in AS and SBF in the core and surface is summarised in table 3.3 and 3.4.

Mainly the precipitation occurred when samples were immersed in AS and SBF. Also, only sample C ($M_{20}T_0P_0$), G ($M_{20}T_{20}P_0$), and H ($M_{20}T_{20}P_5$) showed the potential of crystal precipitation.

Formula	AS	SBF
A-$M_0T_0P_5$	-	-
B-$M_0T_0P_5$	-	-
C-$M_{20}T_0P_0$	Monetite	Brushite
E-$M_0T_{20}P_0$	-	-
G-$M_{20}T_{20}P_0$	Monetite	Brushite and Monetite
H-$M_{20}T_{20}P_5$	Monetite	Brushite

Table 3.3: Calcium phosphate resultant precipitant in the core of the composites when stored in AS and SBF.

In AS, the core of formulae C ($M_{20}T_0P_0$), G ($M_{20}T_{20}P_0$), and H ($M_{20}T_{20}P_5$) showed Monetite (Raman peak and/or SEM findings). In SBF these formulae showed Brushite and or Monetite precipitation.

Formula	AS	SBF
A-$M_0T_0P_5$	-	-
B-$M_0T_0P_5$	-	-
C-$M_{20}T_0P_0$	-	Brushite
E-$M_0T_{20}P_0$	-	-
G-$M_{20}T_{20}P_0$	Brushite	Brushite
H-$M_{20}T_{20}P_5$	Brushite	Brushite and HA

Table 3.4: Calcium phosphate resultant precipitant on the surfaces of the composites when stored in AS and SBF.

The surface of the samples in AS of formulae G ($M_{20}T_{20}P_0$), and H ($M_{20}T_{20}P_5$) showed Brushite Raman peak and/or SEM findings. In SBF formulae C ($M_{20}T_0P_0$), G ($M_{20}T_{20}P_0$), and H ($M_{20}T_{20}P_5$) showed Brushite precipitation. More significantly the surface of formula H ($M_{20}T_{20}P_5$) showed the potential of HA crystals (apatite) precipitation when immersed in SBF (by Raman and SEM images).

Manual vs. SpeedMixer™ mixing:

Comparison between manual and laboratory mixing was done. SEM images of G and H mixed manually showed some surface porosity of the specimens that might lead to material failure and weakness. So, samples G ($M_{20}T_{20}P_0$) and H ($M_{20}T_{20}P_5$) were mixed using SpeedMixer™ Laboratory Mixer System in an attempt to reduce the heterogeneities like surface porosities or air bubbles in the dental composite. No detectable difference in crystals precipitations was seen with both types of mixing. So the speed mixer did not noticeably reduce the porosities.

3.1.2 EDX determination of calcium / phosphate ratios:

In this part of the study, analysis of the calcium to phosphate ratio using the EDX was undertaken for further confirmation of any new precipitate identification.

Only 2 formulae were included in this study, formula G ($M_{20}T_{20}P_0$) and H ($M_{20}T_{20}P_5$) when immersed in either artificial saliva or simulated body fluid.

Samples after 7 days immersion in artificial saliva:

Formula G ($M_{20}T_{20}P_0$):

Figure 3.18 a and b show SEM images of areas with different Ca/P ratios in the surface and core of the sample G respectively.

Surface:

The Ca/P ratio on the surface of sample G ($M_{20}T_{20}P_0$) in several points showed a ratio ranging from 0.68 to 1.47 Ca/P (see table 3.5). Most of the points gave a ratio consistent with OCP or DCPA/DCPD Ca/P.

Core:

The core of this sample also showed different ranges of Ca/P ratio. For example, the range was between 0.14 to 1.21. In most of the points the DCPA/DCPD Ca/P ratio of 1.0 was seen (see table 3.5).

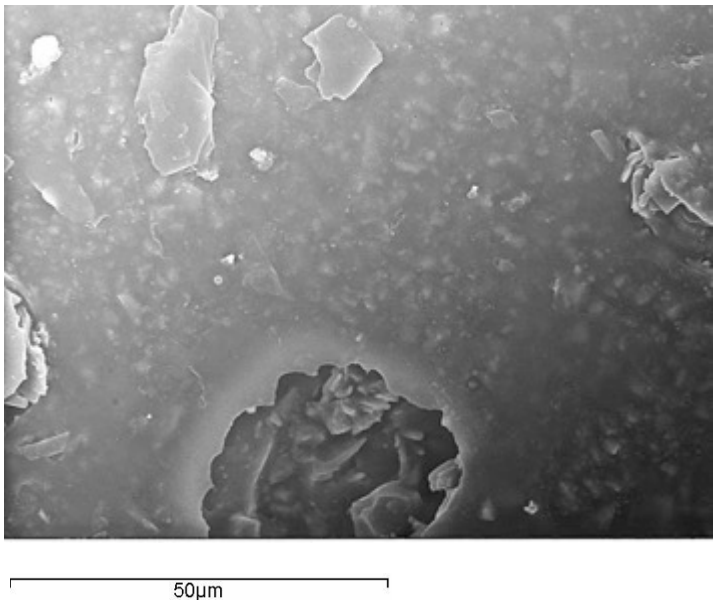

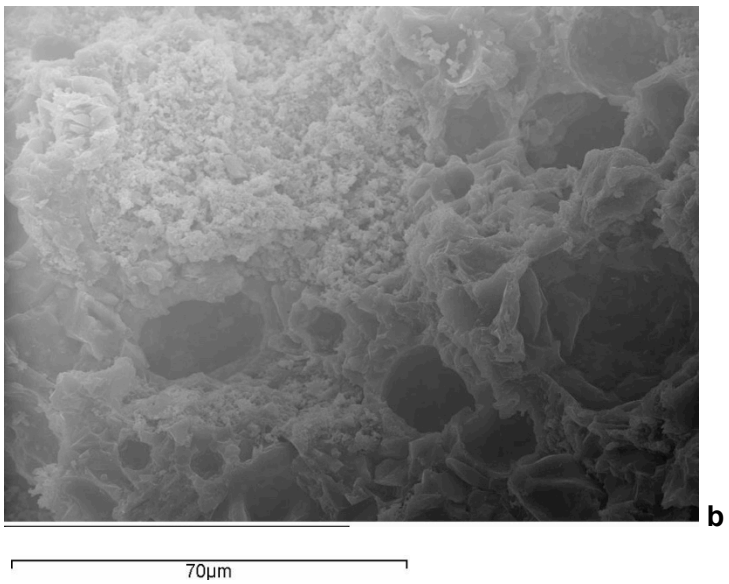

Figure 3.18: Sample G ($M_{20}T_{20}P_0$) a) surface and b) core after 7 days in artificial saliva.

Table 3.5 summarises the range of spectra seen on the surface and core of formula G ($M_{20}T_{20}P_0$) after 7 days in artificial saliva. According to the table, most of the ratios were consistent with MCPM, TCP, OCP, and DCPA/DCPD.

Surface of G ($M_{20}T_{20}P_0$)		
Spectrum	**Ca/P**	**Apatite Identification**
Spectrum 1	0.99	DCPA/DCPD
Spectrum 2	0.88	
Spectrum 3	0.68	
Spectrum 4	1.47	OCP - TCP
Spectrum 5	1.43	
Spectrum 6	1.08	DCPA/DCPD
Spectrum 7	1.02	
Spectrum 8	1.16	DCPA/DCPD - OCP
Core of G ($M_{20}T_{20}P_0$)		
Spectrum	**Ca/P**	**Apatite Identification**
Spectrum 1	1.05	DCPA/DCPD
Spectrum 2	0.99	
Spectrum 3	0.90	MCPM - DCPA/DCPD
Spectrum 4	0.81	
Spectrum 5	0.67	
Spectrum 6	0.87	
Spectrum 7	0.78	
Spectrum 8	0.47	MCPM
Spectrum 9	0.53	
Spectrum 10	0.57	
Spectrum 11	0.14	Polymer
Spectrum 12	1.10	DCPA/DCPD - OCP
Spectrum 13	1.21	

Table 3.5: Ca/P ratio in the surface and core of samples G ($M_{20}T_{20}P_0$) after immersion in artificial saliva at multiple different points and identification of the probable component.

Formula H ($M_{20}T_{20}P_5$):

On the other hand, surface of formula H ($M_{20}T_{20}P_5$) in artificial saliva showed the following:

Surface:

The Ca/P ratio of several points on the surface shows the DCPA/DCPD ratios as seen in figure 3.19 a. Ca/P ratios was between 0.97 to 1.36.

Core:

The core of this sample also showed DCPA/DCPD Ca/P ratios and the range was between 0.13 to 1.58. (See table 3.6)

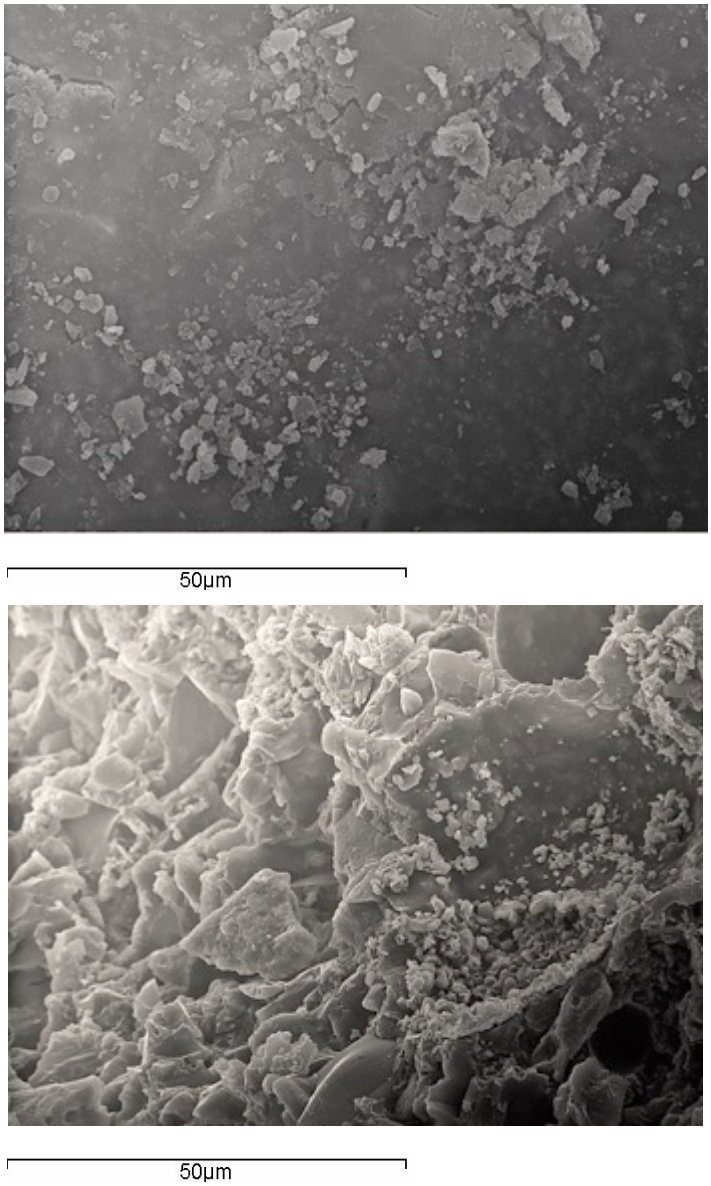

Figure 3.19: Sample H ($M_{20}T_{20}P_5$) a) surface and b) core after 7 days in artificial saliva.

Surface of H ($M_{20}T_{20}P_5$)		
Spectrum	**Ca/P**	**Apatite identification**
Spectrum 1	1.36	OCP
Spectrum 2	1.17	DCPA/DCPD - OCP
Spectrum 3	1.29	
Spectrum 4	1.23	
Spectrum 5	1.10	
Spectrum 6	1.00	DCPA/DCPD
Spectrum 7	0.97	
Core of H ($M_{20}T_{20}P_5$)		
Spectrum	**Ca/P**	**Apatite identification**
Spectrum 1	1.05	DCPA/DCPD
Spectrum 2	1.09	
Spectrum 3	0.93	
Spectrum 4	1.14	DCPA/DCPD - OCP
Spectrum 5	1.18	
Spectrum 6	1.24	
Spectrum 7	1.58	TCP
Spectrum 8	0.13	Polymer

Table 3.6: Ca/P ratio in the surface and core of samples H ($M_{20}T_{20}P_5$) after immersion in artificial saliva showing several spectrums in both surface and core.

Samples after 7 days in simulated body fluid:

Formula G ($M_{20}T_{20}P_0$):

Figure 3.20 a and b show example SEM of the different apatite formations and Ca/P ratios in the surface and core of sample G respectively.

Surface:

The Ca/P ratio on the surface of sample G ($M_{20}T_{20}P_0$) in several points showed a ratio ranging from 0.74 to 1.38 Ca/P as seen in table 3.7. However, most of the points showed OCP or DCPA/DCPD Ca/P.

Core:

The core of this sample also showed different ranges of Ca/P ratio. For example, the range was between 0.84 to 1.54. Also, in most of the points DCPA/DCPD Ca/P ratio was seen.

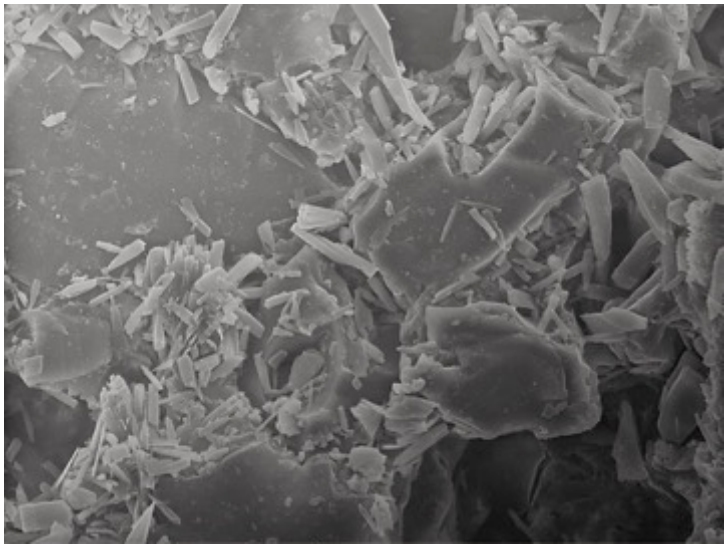

a

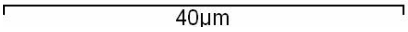

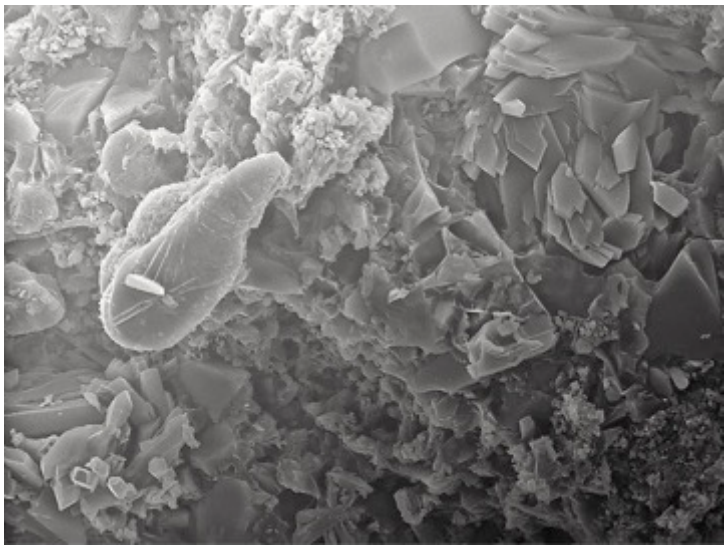

b

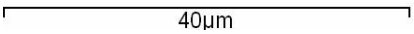

Figure 3.20: Sample G ($M_{20}T_{20}P_0$) a) surface and b) core after 7 days in simulated body fluid.

Surface of G ($M_{20}T_{20}P_0$)		
Spectrum	**Ca/P**	**Apatite identification**
Spectrum 1	1.38	OCP - TCP
Spectrum 2	1.25	DCPA/DCPD - OCP
Spectrum 3	1.16	
Spectrum 4	1.12	
Spectrum 5	1.08	DCPA/DCPD
Spectrum 6	0.98	
Spectrum 7	0.74	
Core of G ($M_{20}T_{20}P_0$)		
Spectrum	**Ca/P**	**Apatite identification**
Spectrum 1	0.98	DCPA/DCPD
Spectrum 2	0.84	MCPM - DCPA/DCPD
Spectrum 3	0.87	
Spectrum 4	1.54	TCP
Spectrum 5	1.22	DCPA/DCPD - OCP

Table 3.7: Ca/P ratio in the surface and core of samples G after immersion in SBF from several points in both surface and core.

Formula H ($M_{20}T_{20}P_5$):

Surface:

In simulated body fluid, it showed Ca/P ratios between 0.86 to 1.78. The Ca/P ratio of several points shows the expected ratio for HA as seen in figure 3.21 a. In this formula several points showed Ca/P ratio of HA ≈1.67.

Core:

The core of this sample also showed DCPA/DCPD Ca/P ratios and the range is between 0.49 to 1.51 as seen in table 3.8. Figure (3.21 b) shows the core of this formula after 7 days immersion in simulated body fluids.

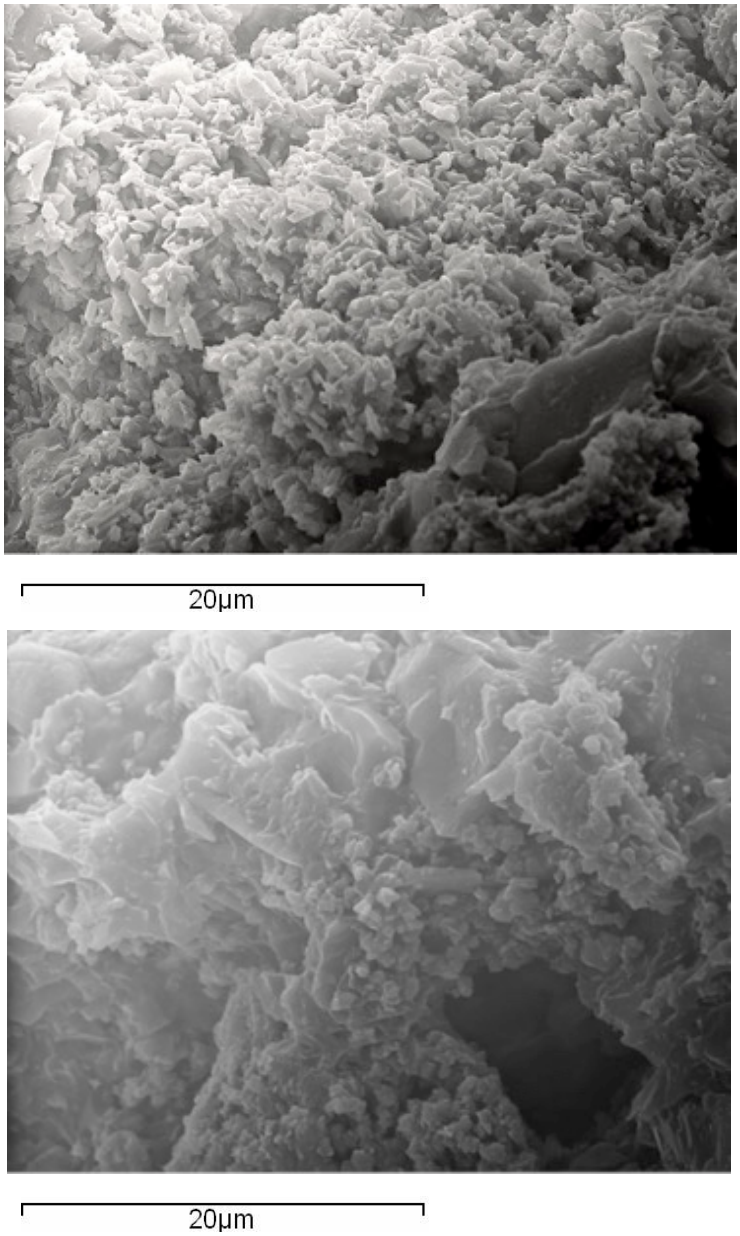

Figure 3.21: Sample H ($M_{20}T_{20}P_5$) a) surface and b) core after 7 days in simulated body fluid.

Surface of H ($M_{20}T_{20}P_5$)		
Spectrum	**Ca/P**	**Apatite identification**
Spectrum 1	0.86	DCPA/DCPD
Spectrum 2	1.09	
Spectrum 3	1.25	DCPA/DCPD - OCP
Spectrum 4	1.31	OCP
Spectrum 5	1.45	TCP
Spectrum 6	1.69	≈ HA
Spectrum 7	1.75	
Spectrum 8	1.78	
Core of H ($M_{20}T_{20}P_5$)		
Spectrum	**Ca/P**	**Apatite identification**
Spectrum 1	0.49	MCPM
Spectrum 2	0.98	DCPA/DCPD
Spectrum 3	1.19	DCPA/DCPD - OCP
Spectrum 4	1.51	TCP
Spectrum 5	1.55	

Table 3.8: Ca/P ratio in the surface and core of samples H ($M_{20}T_{20}P_5$) after immersion in SBF showing several spectrums in both surface and core.

3.2 Effect of calcium phosphate and ε-poly (L-lysine) on composite mass and volume changes:

Measuring the mass change and volume of the samples is important. In fact an increase in mass and volume indicates the potential of the material to absorb water, compensate for polymerisation shrinkage and induce components reaction and/or release.

Mass Change increase after 12 weeks in simulated body fluid (SBF):

Figures 3.22 a and b show the mass change percentage of all the formulations without and with EPL respectively when plotted against square root of time. These formulations where kept in simulated body fluid at 37°C during the experiment.

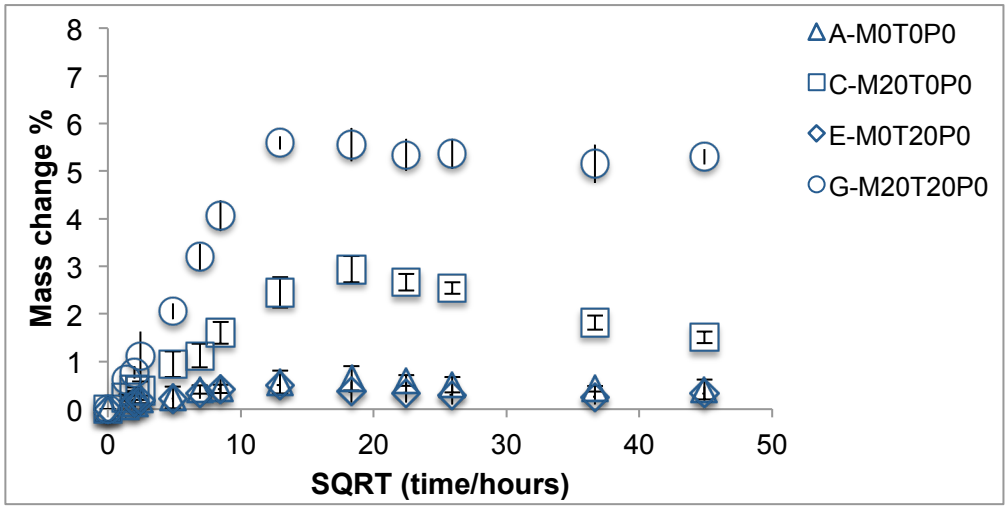

Graph a

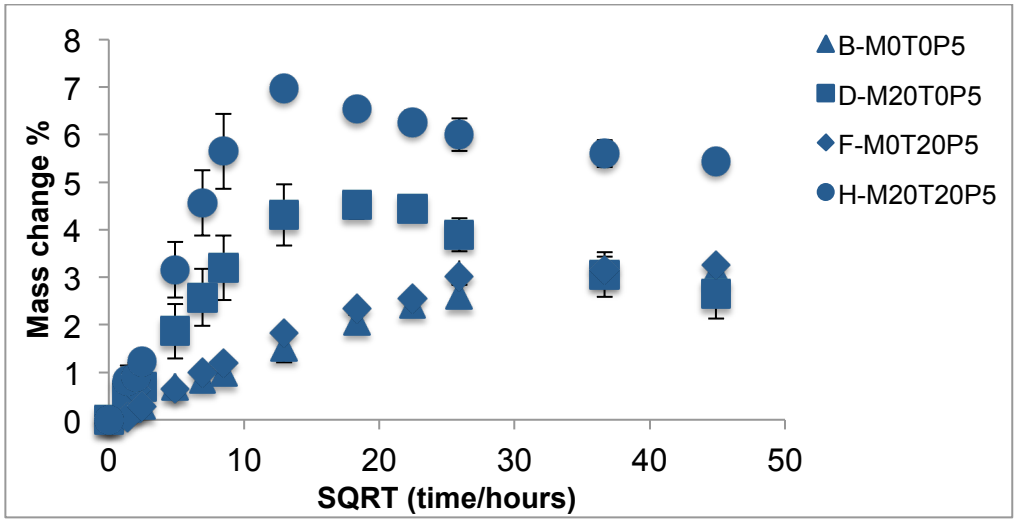

Graph b

Figure 3.22: Mass changes against SQRT (time/hours) of each formulation in SBF in different time periods at 37°C: a) formulations with 0% EPL and. b) with 5 wt% EPL during 12 weeks. Errors bars are 95% confidence interval, n=3.

Generally, in all the formulae, the increase in mass change was higher at the early stages and started to level off during the late stages.

Novel composite with 0% EPL:

The control formula, which is lacking both CaPs and EPL (formula A ($M_0T_0P_0$)) showed the least increase in mass change during the 12 weeks in SBF. Looking at graph a (samples with 0% EPL), adding β-TCP alone did not significantly cause an increase in mass change (formula E ($M_0T_{20}P_0$)). Composites containing 20% MCPM and lacking β-TCP and EPL (formula C ($M_{20}T_0P_0$)) however, showed a much higher increase in mass than formula A ($M_0T_0P_0$) or formula E ($M_0T_{20}P_0$). In 0% EPL group, formula G ($M_{20}T_{20}P_0$) containing 40% CaP (20% MCPM and 20% β-TCP) showed the highest increase in mass. This reached 5.6 % at 1 week (figure 3.22 a).

Novel composite with 5% EPL:

When EPL was incorporated at 5 wt%, a similar pattern in mass increase during the 12 weeks was seen. However, for each given CaP content, 5% EPL addition caused further increase in mass change (figure 3.22 b). Formula H ($M_{20}T_{20}P_5$) with both CaP (20% MCPM and 20% β-TCP) and 5% EPL showed the highest increase in mass of all the formulae. In this formula, a maximum increase of 7.0% in mass was seen after 1 week.

Throughout the first 2 weeks of the study, there was a linear increase in percentage mass change versus square root of time (SQRT). This is more clearly seen in table 3.9.

Formula	Gradient of increase in mass versus SQRT time) ($wt\%/hr^{0.5}$) ± SD	Square of the correlation coefficient (R^2)	Maximum increase in mass (%)	95 % Confidence Interval (CI) of maximum increase in mass	Gradient of late increase in mass versus SQRT time ($wt\%/hr^{0.5}$)	Mass increase after 12 weeks (%)
A ($M_0T_0P_0$)	0.04 ± 0.01	0.93	0.7	0.01	- 0.01	0.4
B ($M_0T_0P_5$)	0.11 ± 0.09	0.99	2.1	0.21	0.03	3.1
C ($M_{20}T_0P_0$)	0.17 ± 0.01	0.99	2.9	0.02	- 0.05	1.5
D ($M_{20}T_0P_5$)	0.27 ± 0.05	0.93	4.5	0.05	- 0.08	2.7
E ($M_0T_{20}P_0$)	0.04 ± 0.02	0.80	0.5	0.02	- 0.01	0.3
F ($M_0T_{20}P_5$)	0.13 ± 0.02	0.97	2.3	0.02	0.03	3.3
G ($M_{20}T_{20}P_0$)	0.45 ± 0.02	0.99	5.6	0.03	- 0.00	5.3
H ($M_{20}T_{20}P_5$)	0.58 ± 0.07	0.97	7.0	0.08	- 0.04	5.4

Table 3.9: The novel composite maximum increase in mass and gradient during early (2 weeks) and late time (10 weeks) when immersed in SBF. Errors SD (n=3).

Table 3.9 demonstrates that the increase in mass change during the early time (first 1 - 2 weeks) was higher compared to the late time (last 10 weeks). So according to the gradient of the increase in mass change, the initial gradient in all the samples was higher compared to gradient in the late time. However, most of the samples showed negative gradient during the last 10 weeks of the experiment.

Also, samples containing MCPM and EPL showed higher gradient in the early time of increase in mass change. Formula H ($M_{20}T_{20}P_5$) showed the highest gradient in the first 1 – 2 weeks of 0.58 $wt\%/hr^{0.5}$. On the other hand, formula A ($M_0T_0P_0$) and E showed the lowest gradient for early increase in mass change of 0.04 $wt\%/hr^{0.5}$.

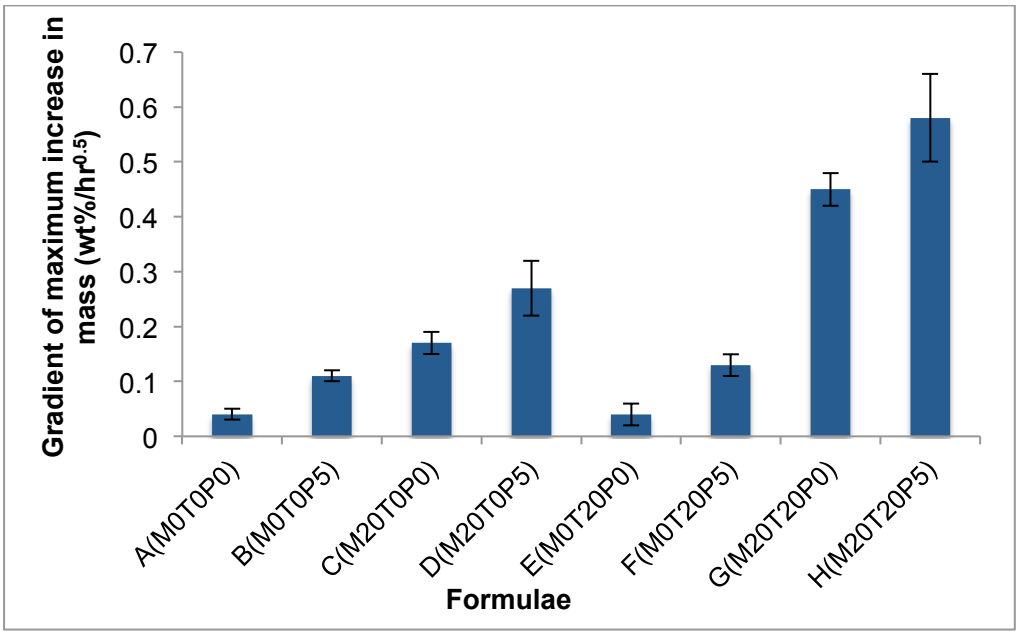

Figure 3.23: Gradient of early increase in mass (2 weeks) for the 8 formulae when immersed in SBF with 95% confidence interval error bars (n=3).

Statistically, all the variables showed significant effect on the increase in maximum mass (after 2 weeks) in SBF ($P<0.05$) (Appendix II (table 2)). Figure 3.23 shows the gradient of early increase in mass in each formula. The error bars in this graph are the 95% confidence interval of the standard deviation of the gradient. For each given CaP content, 5% EPL addition showed higher gradient of the early increase in mass change. So, formulae B ($M_0T_0P_5$), D ($M_{20}T_0P_5$), F ($M_0T_{20}P_5$), and H ($M_{20}T_{20}P_5$) showed higher gradient in the early increase in mass change than formulae A ($M_0T_0P_0$), C ($M_{20}T_0P_0$), E ($M_0T_{20}P_0$), and G ($M_{20}T_{20}P_0$) respectively. Also, formulae with MCPM showed higher gradient than formulae with 0%MCPM and/or with 20% TCP.

Mass Change increase after 12 weeks in distilled water:

Graphs a and b in figure 3.24 show the mass change percentage of the experimental composite when plotted against square root of time. These formulations where kept in distilled water at 37°C during the experiment for 3 months (12 weeks).

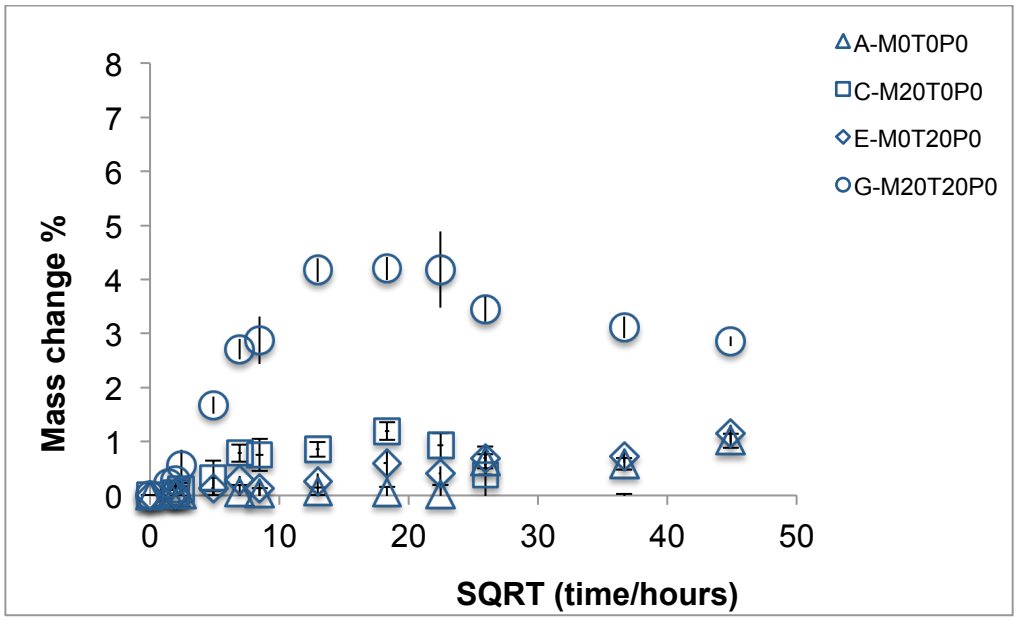

Graph a

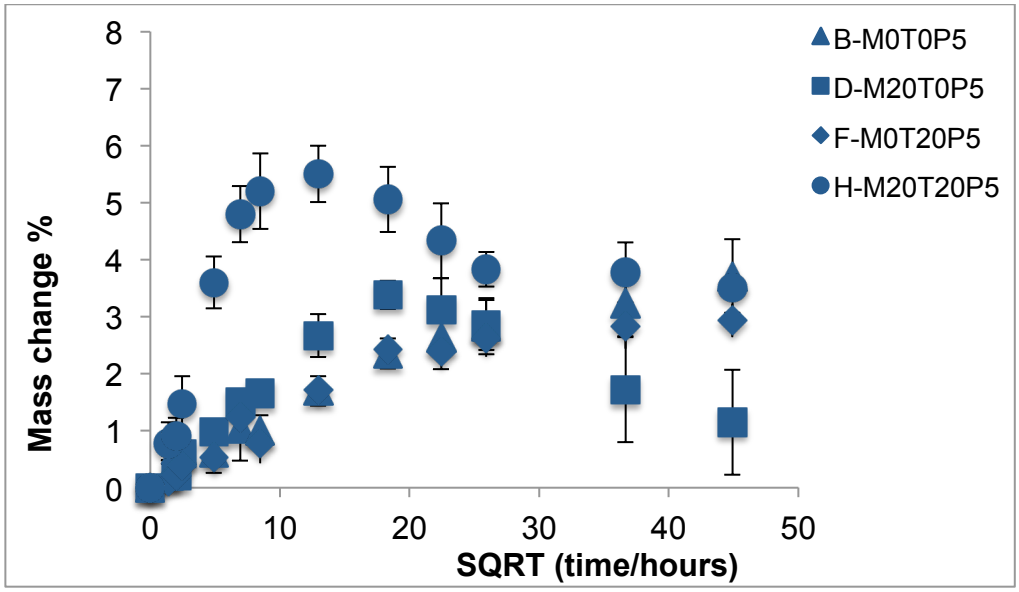

Graph b

Figure 3.24: Mass changes against SQRT (time/hours) of each formulation upon immersion in water at different time periods at 37°C: a) formulations with 0% EPL and b) with 5 wt% EPL. Errors bars are 95% confidence interval, n=3.

Within 12 weeks, the mass increase was high during the early time but generally in most of the formulae after 2 to 3 weeks it started to level off.

Novel composite with 0% EPL:

When comparing formulae with 0% and 5% EPL, composites lacking both CaPs and EPL (formula A ($M_0T_0P_0$)) showed the least increase in mass during the 12 weeks in water. Composites containing 20 wt% β-TCP but 0%MCPM and 0% EPL (formula E ($M_0T_{20}P_0$)) showed slightly more increase in mass change when compared to the control formula. However, composites containing 20% MCPM and lacking β-TCP and EPL (formula C ($M_{20}T_0P_0$)), this formula showed more increase in mass change. On the other hand, composites containing 40% CaP (20% MCPM and 20% β-TCP) but lacking EPL (formula G ($M_{20}T_{20}P_0$)) showed the highest increase in mass between the formulae containing 0% EPL. It reached the maximum increase in the second week to approximately 4.2% (Graph a). So, mass change was higher when both MCPM and β-TCP were added to the powder phase.

Novel composite with 5% EPL:

When EPL was added at 5 wt% to all the formulae, the mass increase was higher in generally all the formulae (Graph b). So, formula with 0% CaP but with 5% EPL (formula B ($M_0T_0P_5$)), showed the least increase in mass change. Also, when 5% EPL was combined with 20% β-TCP (formula F ($M_0T_{20}P_5$)) the increase was low. But, when EPL was included with 20% MCPM (formula D ($M_{20}T_0P_5$)), the increase in mass was higher. When EPL was incorporated with both CaP (20% MCPM and 20% β-TCP) (formula H ($M_{20}T_{20}P_5$)), this formula showed the highest increase in mass change and reached the maximum in the first week to approximately 5.5% increase in mass as shown in figure 3.24 (Graph b). Accordingly, in all the formulae when 5% EPL was added, the mass increase was higher comparing it to formulae with 0% EPL.

Throughout the first 2 weeks of the study, figure 3.24 showed that there was a linear relation between the percentage of mass change and SQRT time in hours (early time) when samples were kept in distilled water at 37°C.

Formula	Gradient of increase in mass versus SQRT time (wt%/hr$^{0.5}$) ± SD	Square of the correlation coefficient (R^2)	Maximum increase in mass (%)	95 % Confidence Interval (CI) of maximum increase in mass	Gradient of late increase in mass versus SQRT time (wt%/hr$^{0.5}$)	Mass increase after 12 weeks (%)
A ($M_0T_0P_0$)	0.00 ± 0.004	0.73	0.1	0.00	0.03	1.0
B ($M_0T_0P_5$)	0.12 ± 0.02	0.95	2.4	0.02	0.05	3.7
C ($M_{20}T_0P_0$)	0.07 ± 0.02	0.91	1.2	0.02	- 0.09	- 1.2
D ($M_{20}T_0P_5$)	0.20 ± 0.02	0.98	3.4	0.02	- 0.09	1.2
E ($M_0T_{20}P_0$)	0.04 ± 0.01	0.79	0.6	0.01	0.02	0.7
F ($M_0T_{20}P_5$)	0.13 ± 0.02	0.95	2.4	0.02	0.02	2.9
G ($M_{20}T_{20}P_0$)	0.27 ± 0.06	0.91	4.2	0.06	- 0.05	2.9
H ($M_{20}T_{20}P_5$)	0.48 ± 0.12	0.88	5.5	0.14	- 0.03	3.5

Table 3.10: The novel composite maximum increase in mass and gradient (wt%/hr$^{0.5}$) during early (2 weeks) and late time (10 weeks) when immersed in water. Errors SD (n=3).

Table 3.10 shows that the initial gradient in all the samples was higher compared to the late time gradient. Furthermore, most of the samples showed negative gradient during the last 10 weeks of the experiment.

Also, samples containing MCPM and EPL showed higher gradient in the early time of the increase in mass change. For example formula H ($M_{20}T_{20}P_5$) showed the highest gradient in the first 1 – 2 weeks of 0.48 wt%/hr$^{0.5}$. On the other hand, formula A ($M_0T_0P_0$) showed very low gradient of early increase in mass versus SQRT time change (<0.01 wt%/hr$^{0.5}$). Thus, there is comparable difference between the gradient of these 2 formulae in the early increase in mass change when samples immersed in water.

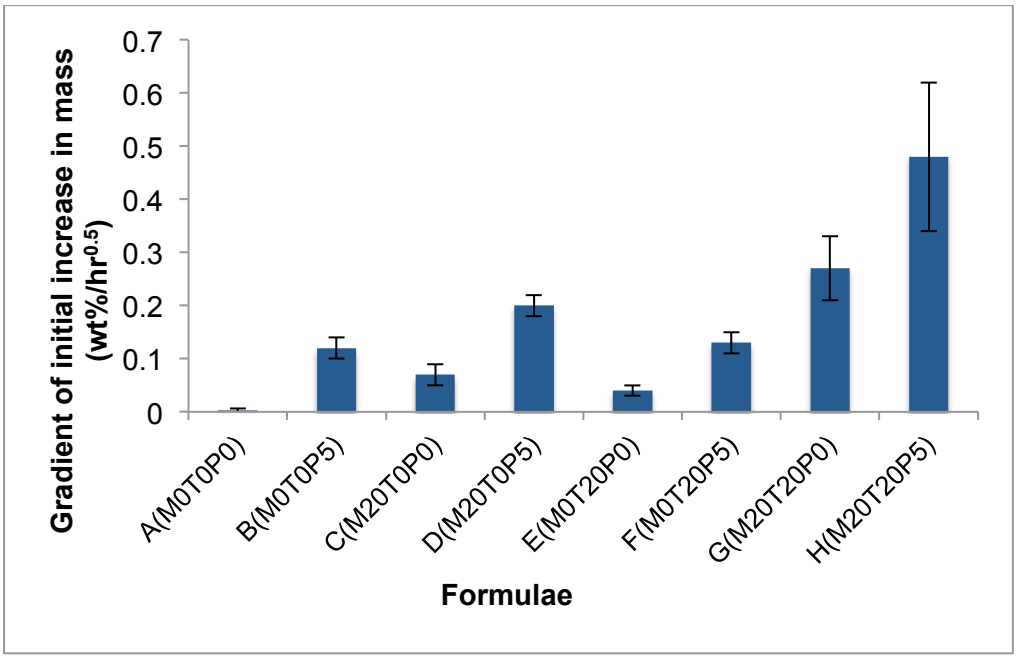

Figure 3.25: The initial gradient of early increase in mass (2 weeks) for the 8 formulas when immersed in water with 95% confidence interval error bars (n=3).

Statistically, all the variables showed significant effect on the maximum increase in mass in water ($p<0.05$) (Appendix II (table 3)). Figure 3.25 shows the gradient in the early increase in mass change. The error bars in this graph are the 95% confidence interval of the standard deviation of the gradient. For each given CaP content, 5% EPL addition showed higher gradient of the early increase in mass change. So, formulae B ($M_0T_0P_5$), D ($M_{20}T_0P_5$), F ($M_0T_{20}P_5$), and H ($M_{20}T_{20}P_5$) showed higher gradient in the early increase in mass change than formulae A ($M_0T_0P_0$), C ($M_{20}T_0P_0$), E ($M_0T_{20}P_0$), and G ($M_{20}T_{20}P_0$) respectively. Also, formulae with MCPM showed higher gradient than formulae with 0%MCPM and/or with 20% TCP.

Factorial analysis for mass change in SBF and water:

According to figure 3.26, this graph shows the individual and combined effect of the additive variables on the increase in mass for the samples when immersed in SBF and water using the factorial analysis.

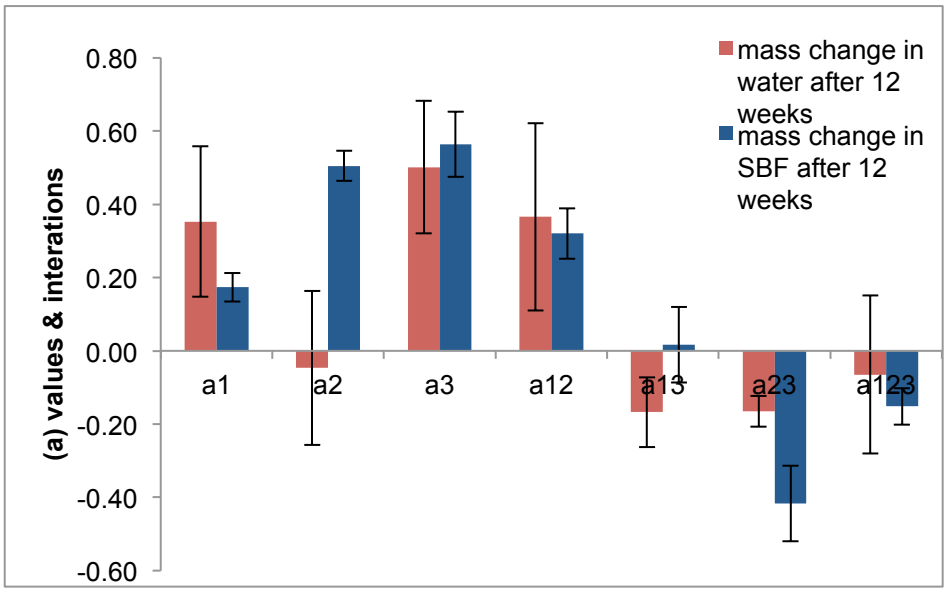

Figure 3.26: The factorial analysis of the effect of TCP, MCPM, and EPL on the increase in mass after 12 weeks for the samples when immersed in SBF and water, where: a_1, a_2, a_3 are the level of effects of TCP, MCPM, and EPL respectively. Errors SD (n=3).

In SBF:

The mass increase in SBF was highly affected by TCP, MCPM and EPL as a_1, a_2 and a_3 (See equation (17) in the factorial analysis section) were all larger than their error bars but there were in addition complex interaction effects.

The mass change in SBF, increased 29% when adding 20% TCP. Adding 20% MCPM increased the mass 64% and adding 5% EPL increased it up to 68%. (Appendix VIII (figure 3))

In water:

The mass increase in water is affected by all variables but there are strong interaction effects between variable 2 (MCPM) and the other 2 variables. The large interaction affects of terms a_{12}, and a_{23} plus means, however, that the average effect of MCPM is negligible. On average, mass change in water increased 48% when 20% TCP added. Adding 5% EPL increased the mass 61%. (Appendix VIII (figure 4))

Factorial analysis for mass change with and without MCPM:

Due to the strong interaction effects with MCPM further analysis was done to look at the effect on mass increase after 12 weeks with and without MCPM.

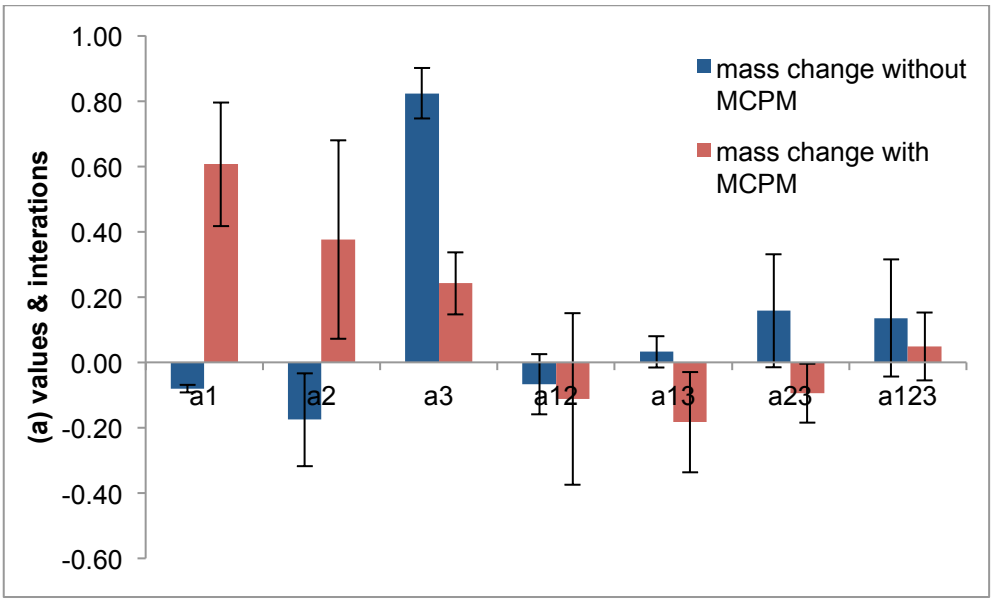

Figure 3.27: The factorial analysis of the effect of TCP, medium, and EPL on the increase in mass after 12 weeks for the samples when immersed in SBF and water, where: $a_1$is the effect of TCP, a_2 is the effect of the medium (SBF or water), and a_3 is the effect of EPL. Errors SD (n=3).

According to figure 3.27, mass change without MCPM was highly affected by EPL (a_3). However, when MCPM was added, all other factors (TCP, medium and EPL) demonstrated positive effects on the increase in mass (a_1, a_2, and a_3 in Figure 3.27 are all larger than their error bars and interaction terms).

According to equation (17), with 0% MCPM, EPL causes on average 81% increase in mass change after 12 weeks. On the other hand, with 20% MCPM adding EPL caused only 38.4% increase in mass after 12 weeks. (Appendix VIII (figures 1 and 2)

Also, with 0% MCPM, TCP caused on average mass loss by 17%, on the other hand with 20% MCPM, TCP caused 70% increase in average mass. (Appendix VIII (figures 1 and 2)

Mass change difference between the two solutions:

After 12 weeks:

In this section the effect of the 3 variables (TCP, medium, and, EPL) on the increase in mass after 12 weeks in SBF and water is analysed. The interaction effects were negligible, so the average effects of each variable were calculated. Figure 3.28 shows the effect of the increase in mass change in samples with and without MCPM. The average effect of each variable was assessed using factorial analysis.

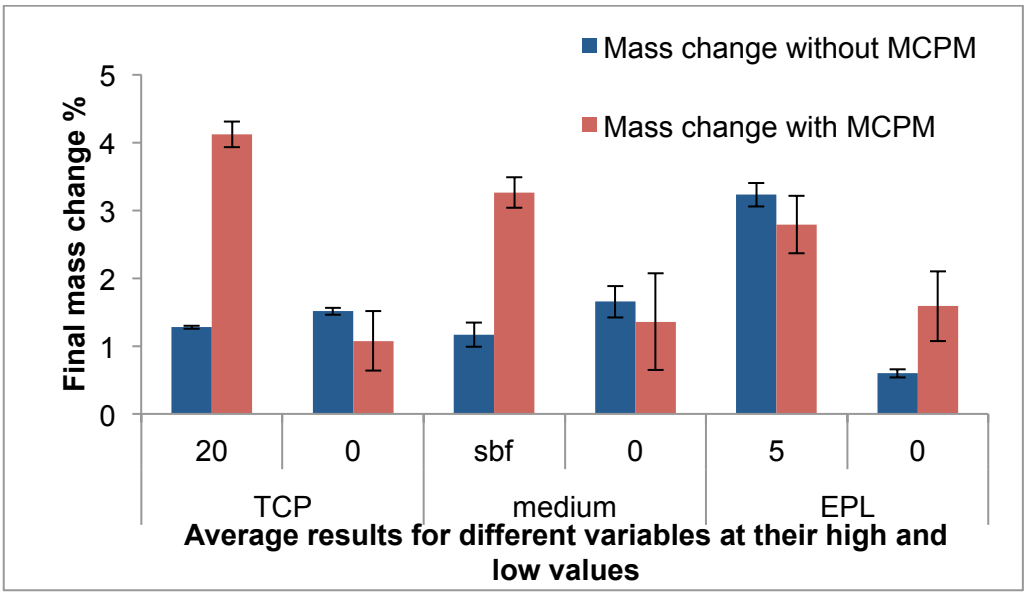

Figure 3.28: Average effects of TCP, medium and EPL on final mass change. Errors bars are 95% confidence interval, n=3.

The maximum mass change and the mass change after 12 weeks were all significantly affected by MCPM, TCP, EPL, and the storage medium (SBF or water). (Appendix II (table 1) and appendix IV (table 1))

According to figure 3.28, on average, formulae with 0% MCPM, the final mass changed from 1.5% to1.28% with 20% TCP. When the samples were kept in SBF, the final mass changed from 1.7% to 1.2%. However, with 5% EPL the final mass changed from 0.6% to 3.2%.

Formulae with MCPM, 20% TCP caused, on average, increase in mass from 1.1% to 4.1% in final mass. Immersing the samples in SBF increased the final mass from 1.4% to 3.3%. Adding 5% EPL increased the final mass from 1.6% to 2.8%.

The difference in mass change after 1 week:

In this section the significant difference between the increase in mass in SBF and water is investigated. The microstructure study (section 3.1), showed calcium phosphate precipitation after 7 days in SBF (tables 3.3 and 3.4) for formulae C ($M_{20}T_0P_0$), G ($M_{20}T_{20}P_0$), and H ($M_{20}T_{20}P_5$). The difference in the increase in mass change between these formulae in SBF and water is therefore plotted against time in hours in figure 3.29. Formula A ($M_0T_0P_0$) is provided for comparison.

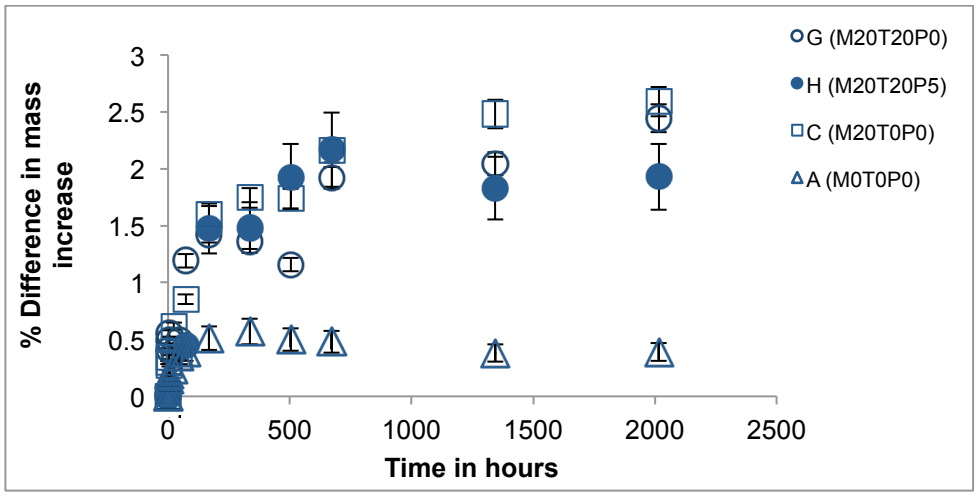

Figure 3.29: The % difference in mass increase in SBF vs. water during 12 weeks (Difference%= %mass in SBF - %mass in water).

The difference in mass change in SBF versus water after 7 days in formulae A ($M_0T_0P_0$) is 0.5%. On the other hand it is approximately around 1.6%, 1.4%, and 1.5% in formulae C ($M_{20}T_0P_0$), G ($M_{20}T_{20}P_0$), and H ($M_{20}T_{20}P_5$) respectively. Table 3.11 shows the increase in mass in SBF vs. water after 1-week (168 hours) immersion. The difference in the increase in mass in the 2 solutions was significant for formulae H ($M_{20}T_{20}P_5$) and G ($M_{20}T_{20}P_0$) and C ($M_{20}T_0P_0$). However, it was insignificant in A ($M_0T_0P_0$).

Mass increase after 1 week				
	H ($M_{20}T_{20}P_5$)	**G ($M_{20}T_{20}P_0$)**	**C ($M_{20}T_0P_0$)**	**A ($M_0T_0P_0$)**
In water	5.5%± 0.66(a)	4.2% ± 0.21	0.9% ± 0.13 (b)	0.1% ± 0.07(b)
In SBF	7.0% ± 0.05	5.6% ± 0.14(a)	2.5% ± 0.31	0.6% ± 0.3(b)

Table 3.11: The % mass increase of formulae A ($M_0T_0P_0$), C ($M_{20}T_0P_0$), G ($M_{20}T_{20}P_0$) and H ($M_{20}T_{20}P_5$) after 1 week in SBF or water. Same letters indicate no significant differences at p = 0.05. Errors are SD (n=3). (Appendix I (tables 1 and 2)).

Volume Change increase after 12 weeks in simulated body fluid (SBF):

Graphs a and b in figure 3.30 show the percentage change in volume of all the formulations plotted against square root of time. These formulations where kept in simulated body fluid at 37°C during the experiment.

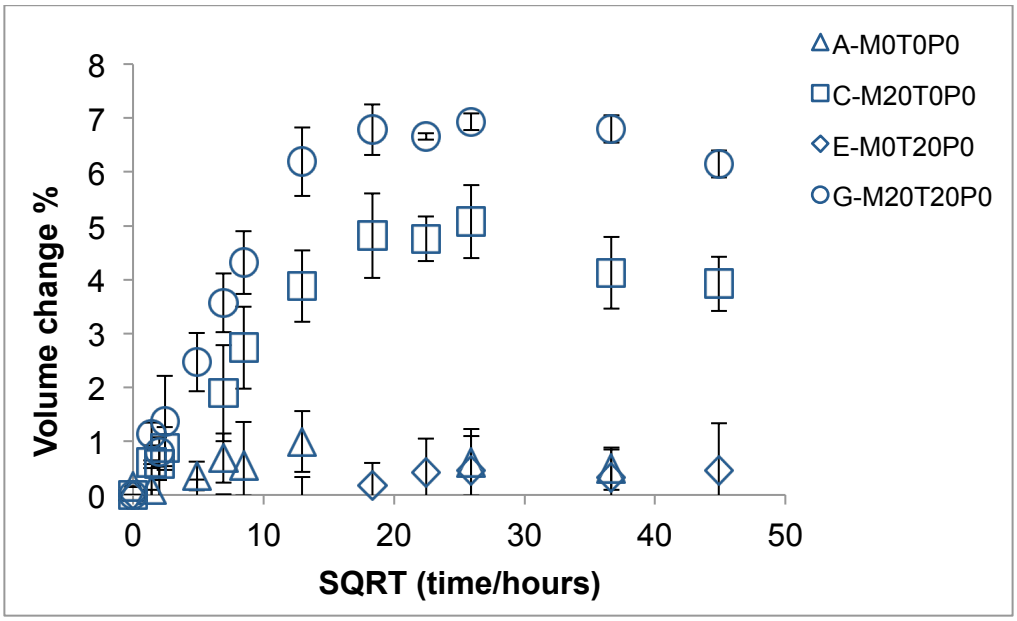

Graph a

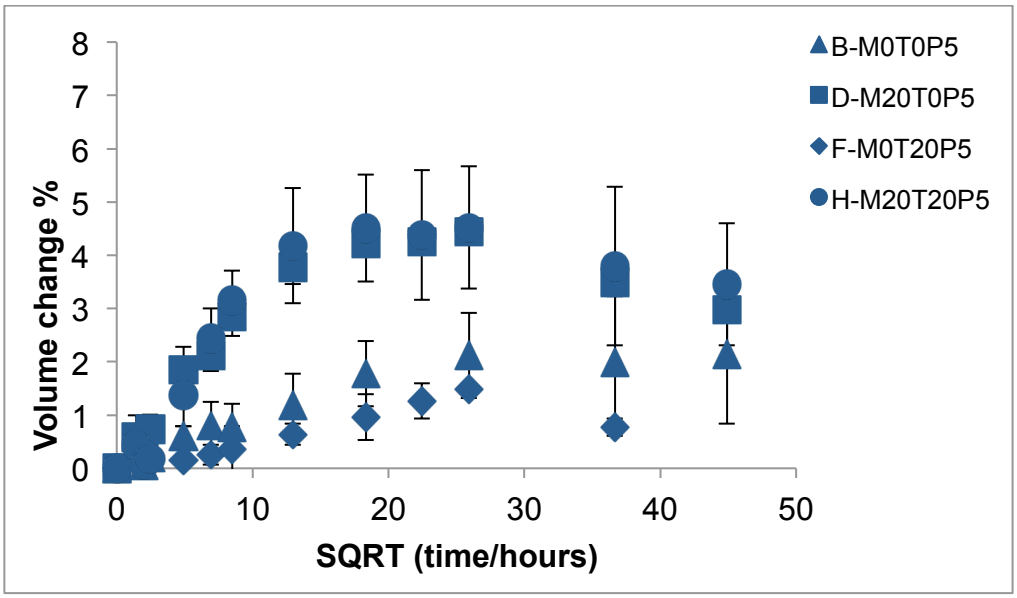

Graph b

Figure 3.30: Volume changes against SQRT (time/hours) of each formulation in SBF in different time periods at 37°C: a) formulations without EPL and b) with 5 wt% EPL during 12 weeks. Errors bars are 95% confidence interval, n=3.

Novel composite with 0% EPL:

Composites with 0% CaPs and 0% EPL (formula A ($M_0T_0P_0$)) showed the least increase in volume change during the 12 weeks. Composites containing 20% MCPM and lacking β-TCP and EPL (formula C ($M_{20}T_0P_0$)) showed more increase in volume compared to the control formula. Also formula C ($M_{20}T_0P_0$) showed more increase in volume change compared to the formula with 20 wt% β-TCP and lacking MCPM and EPL (formula E ($M_0T_{20}P_0$)). Composite containing 40% CaP (20% MCPM and 20% β-TCP) but lacking EPL (formula G ($M_{20}T_{20}P_0$)) showed the highest increase in volume change during the 12 weeks and reached the higher increase in volume of 6.8 % within 2 weeks (Figure 3.30 Graph a).

Novel composite with 5% EPL:

When EPL was combined at 5 wt% with the samples containing 0% CaP (formula B ($M_0T_0P_5$)) or 20% TCP (formula F ($M_0T_{20}P_5$)), the increase in volume change was low compared to other formulae with 5% EPL. Adding 20% MCPM showed more increase in the volume change (formula D ($M_{20}T_0P_5$)) and reached 4.2% increase within the second week. However, when EPL was incorporated with both CaP (20% MCPM and 20% β-TCP) (formula H ($M_{20}T_{20}P_5$)), this showed the highest increase in volume change and reached a maximum increase in the second week, of 4.5% ((Figure 3.30 Graph b).

Also, the increase in volume was higher during the early stages and reached the maximum increase within the first 2 weeks. Later on, the increase in volume started to level off in all the formulae.

Table 3.12 shows that the increase in volume change versus SQRT time during the early time (first 1 - 2 weeks) was higher compared to that at late time (last 10 weeks). Indeed, most of the samples showed a negative gradient for mass change versus SQRT time during the last 10 weeks of the experiment.

Also, samples containing MCPM and EPL showed higher early gradients. For example formulae G ($M_{20}T_{20}P_0$) and H ($M_{20}T_{20}P_5$) showed the highest gradient in the first 1 – 2 weeks (0.39 and 0.29 vol%/hr$^{0.5}$ respectively). On the other hand, formulae with 0%MCPM or 0%EPL but with or without TCP showed very low gradient during the early increase in volume change. Thus, there is difference between the initial gradient of formula A ($M_0T_0P_0$) when compared to formulae G ($M_{20}T_{20}P_0$) and H ($M_{20}T_{20}P_5$).

Formula	Gradient of increase in volume versus SQRT time (vol%/hr$^{0.5}$) ± SD	Square of the correlation coefficient (R^2)	Maximum increase in volume (%)	95% Confidence Interval (CI) of maximum increase in volume	Gradient of late increase in volume versus SQRT (vol%/hr$^{0.5}$)	Maximum increase in volume after 12 weeks (%)
A ($M_0T_0P_0$)	0.06 ± 0.04	0.58	0.8	0.04	- 0.01	0.4
B ($M_0T_0P_5$)	0.09 ± 0.01	0.96	1.8	0.01	0.01	2.1
C ($M_{20}T_0P_0$)	0.27 ± 0.02	0.99	4.8	0.02	- 0.17	1.5
D ($M_{20}T_0P_5$)	0.24 ± 0.04	0.95	4.2	0.04	- 0.06	3.0
E ($M_0T_{20}P_0$)	0.03 ± 0.02	0.42	0.2	0.02	- 0.00	0.5
F ($M_0T_{20}P_5$)	0.05 ± 0.01	0.93	1.0	0.01	- 0.04	0.8
G ($M_{20}T_{20}P_0$)	0.39 ± 0.05	0.96	6.8	0.06	- 0.02	6.2
H ($M_{20}T_{20}P_5$)	0.29 ± 0.05	0.92	4.5	0.06	- 0.05	3.5

Table 3.12: The novel composite maximum increase in volume and gradient (vol%/hr$^{0.5}$) during early (2 weeks) and late time (10 weeks) when immersed in SBF. Errors SD (n=3).

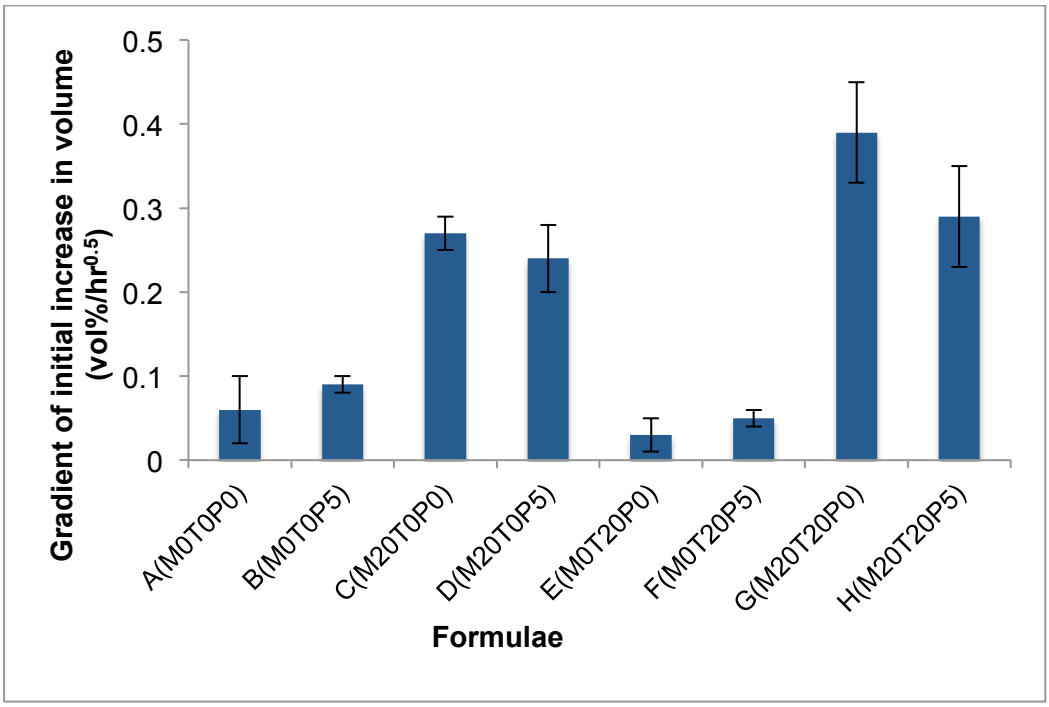

Figure 3.31: Gradient of initial increase in volume (2 weeks) for 8 formulae when immersed in SBF with 95% confidence interval error bars (n=3).

Statistically, TCP and EPL did not show any significant effect on the maximum increase in volume in SBF ($p>0.05$). (Appendix III (table 2)) Figure 3.31 shows the gradient of early increase in volume change versus SQRT time. The error bars in this graph are the 95% confidence intervals. Formulae with 0% MCPM showed low initial gradients compared to formulae with 20% MCPM. Thus, there is difference between the gradient of the initial increase in volume change between formula H ($M_{20}T_{20}P_5$) and A ($M_0T_0P_0$).

Volume Change increase after 12 weeks in distilled water:

In graphs a and b in figure 3.32, percentage change in volume for all formulations is plotted against square root of time. These formulations where kept in distilled water at 37°C during the experiment.

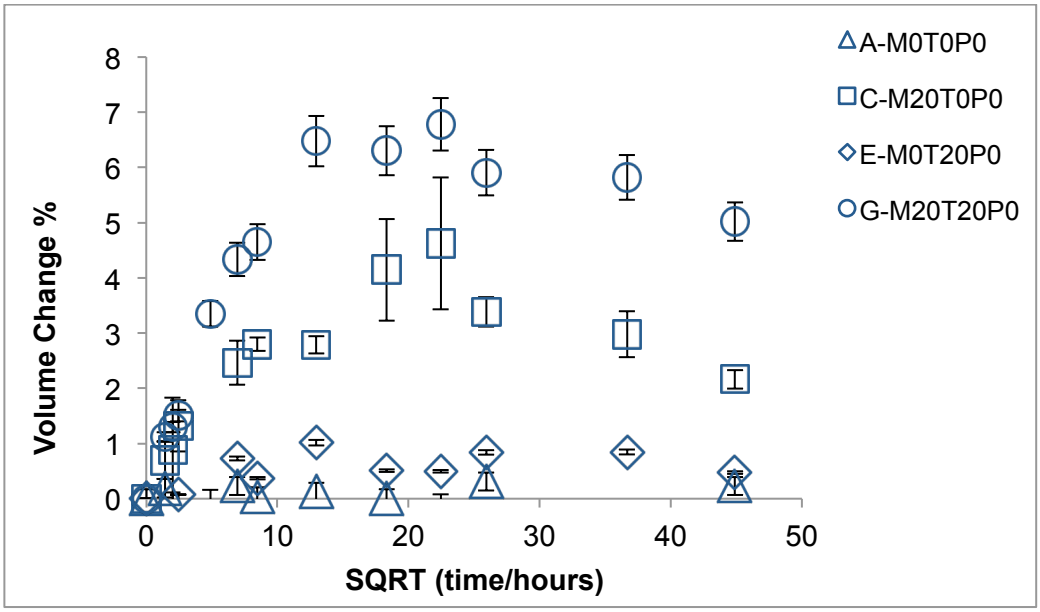

Graph a

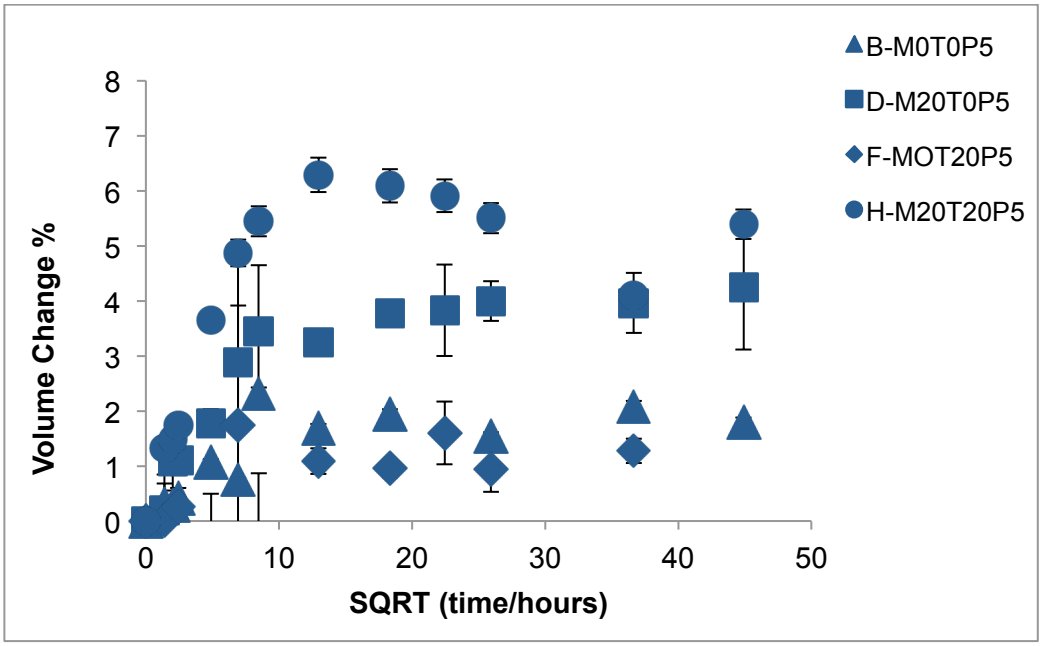

Graph b

Figure 3.32: Volume changes against SQRT (time/hours) of after immersion in distilled water at different time periods at 37°C: a) formulae without EPL and b) with 5 wt% EPL during 12 weeks. Errors bars are 95% confidence interval, n=3.

Novel composite with 0% EPL:

In figure 3.32 graph a shows the formulae containing 0% EPL when plotted against SQRT time. Composites without CaPs and EPL (formula A ($M_0T_0P_0$)) and composites containing 20 wt% β-TCP and lacking MCPM and EPL (formula E ($M_0T_{20}P_0$)) showed the least increase in volume change. But, composites containing 20% MCPM and without β-TCP or EPL (formula C ($M_{20}T_0P_0$)) showed more increase in volume compared to formulae A ($M_0T_0P_0$) and E ($M_0T_{20}P_0$) but less increase in volume when compared to formula G ($M_{20}T_{20}P_0$). Composites containing 40% CaP (20% MCPM and 20% β-TCP) but 0% EPL (formula G ($M_{20}T_{20}P_0$)) showed the highest increase in volume in all the samples containing 0% EPL. It reached the its greatest increase in the first week of 6.5% as shown in figure 3.32 (Graph a).

Novel composite with 5% EPL:

In figure 3.32 graph b, 5 wt% EPL addition (formula B ($M_0T_0P_5$)) but with 0% CaP showed low increase in volume change. Also this was seen when EPL was added with 20% β-TCP (formula F ($M_0T_{20}P_5$)). When EPL was included with 20% MCPM (formula D ($M_{20}T_0P_5$)), volume increased slightly more. However, once EPL was combined with both CaP (20% MCPM and 20% β-TCP) (formula H ($M_{20}T_{20}P_5$)), this volume percentage change was the highest and reached a maximum after 1 week of 6.3% (figure 3.32 Graph b).

So, when EPL was added with or without CaP, more increase in volume was noted. When both CaP was added with EPL the highest increase in volume change was seen and reached the maximum within the early period of immersion and started to level off within the full period of the immersion.

Considering figure 3.32 Graph a and b, the early volume change upon immersion in distilled water during the; first 2, 4, 6, 24, 48, and 72 hours was linear.

Formula	Gradient of increase in volume versus SQRT (vol%/hr$^{0.5}$) ± SD	Square of the correlation coefficient (R^2)	Maximum increase in volume (%)	Confidence Interval (CI) of maximum increase in volume	Gradient of late increase in mass versus SQRT (vol%/hr$^{0.5}$)	Volume increase after 12 weeks (%)
A ($M_0T_0P_0$)	0.00 ± 0.01	0.02	0.0	0.01	- 0.01	0.2
B ($M_0T_0P_5$)	0.11 ± 0.05	0.70	1.9	0.06	- 0.04	1.8
C ($M_{20}T_0P_0$)	0.20 ± 0.04	0.92	4.1	0.05	- 0.09	2.2
D ($M_{20}T_0P_5$)	0.21 ± 0.07	0.81	3.8	0.08	0.01	4.2
E ($M_0T_{20}P_0$)	0.09 ± 0.20	0.10	1.0	0.22	- 0.02	0.5
F ($M_0T_{20}P_5$)	0.07 ± 0.06	0.31	1.1	0.07	0.01	1.0
G ($M_{20}T_{20}P_0$)	0.37 ± 0.09	0.89	6.5	0.10	- 0.06	5.0
H ($M_{20}T_{20}P_5$)	0.51 ± 0.09	0.94	6.3	0.11	- 0.04	5.4

Table 3.13: The novel composite maximum increase in volume and gradient (vol%/hr$^{0.5}$) during early (2 weeks) and late time (10 weeks) when immersed in water. Errors SD (n=3).

Table 3.13 shows that the increase in volume change during the early time (first 1 - 2 weeks) was higher compared to the late time (last 10 weeks). Again, most of the samples showed negative gradient during the last 10 weeks of the experiment.

In addition, samples containing MCPM and EPL showed higher gradient in the early time of the increase in volume change. For example formula H ($M_{20}T_{20}P_5$) showed the highest gradient in the first 1 – 2 weeks (0.51 vol%/hr$^{0.5}$). On the other hand, formulae with 0%MCPM or 0%EPL but with or without TCP showed very low gradient of early increase in volume change. Thus, there is big difference between the initial gradient of formula A ($M_0T_0P_0$) when compared to formulae H ($M_{20}T_{20}P_5$).

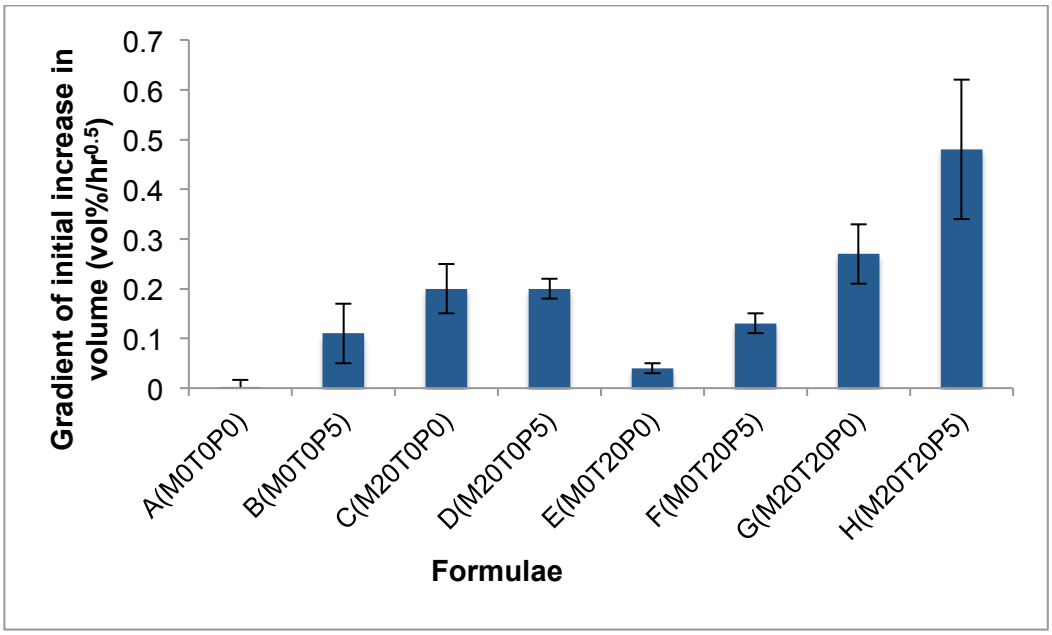

Figure 3.33: The initial gradient of early (2 weeks) increase in volume for 8 formulae when immersed in water with 95% confidence interval error bars (n=3).

Statistically, EPL did not show any significant effect on the maximum increase in volume when samples were immersed in water ($p>0.05$). (Appendix III (table 3)) Figure 3.33 shows the gradient in the early increase in volume change. The error bars in this graph are the 95% confidence interval. Formulae with 0% MCPM showed low initial gradients compared to formulae with 20% MCPM. Thus, there is difference between the gradient of the initial increase in volume change between formula H ($M_{20}T_{20}P_5$) and A ($M_0T_0P_0$).

Factorial analysis for volume change in SBF and water:

Factorial analysis showing the effect of the variables on the volume change in SBF or water after 12 weeks can be seen in figure 3.34.

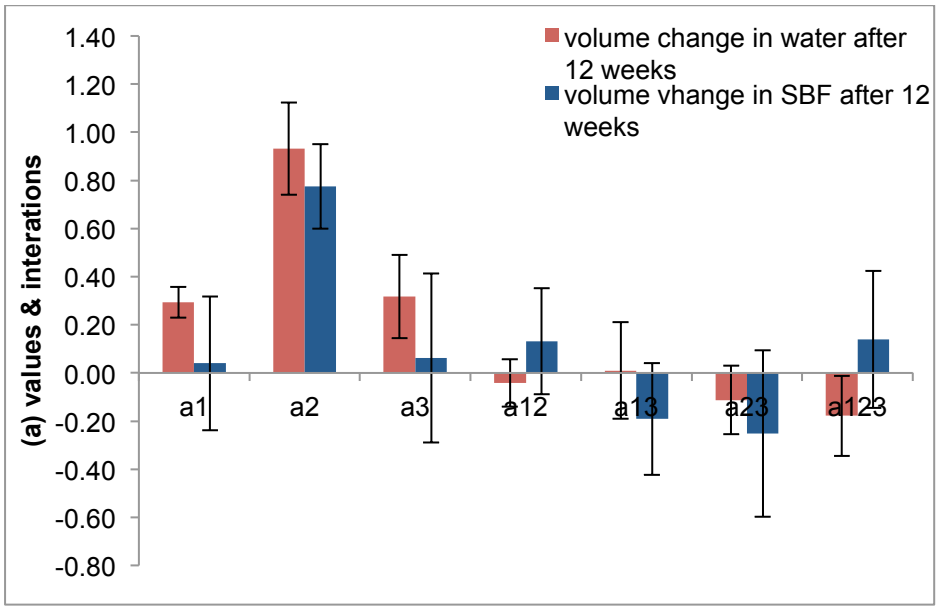

Figure 3.34: The factorial analysis of the effect of TCP, MCPM, and EPL on the increase in volume after 12 weeks for the samples when immersed in SBF and water, where: a_1 a_2 and a_3 indicate the level of effect of TCP, MCPM and EPL respectively. Errors SD (n=3).

In SBF:

On average MCPM highly affects the increase in the volume when the samples are immersed in SBF. According to equation (17), adding 20% MCPM increased the volume 79%. (Appendix VIII (figure 5)) The large interaction terms (a_{12} a_{13} a_{23}, and a_{123}) plus error bars crossing zero line means that the variables associated with a_1 and a_3 (TCP and EPL) have no significant effect.

In water:

According to figure 3.34, the variables associated with a_1 a_2 and a_3 do have a significant effect on volume increase. The small interaction terms $a_{12,}$ $a_{13,}$ $a_{23,}$ and a_{123} confirm that all the individual variables have an effect on the increase in volume change in water. According to equation (17), the volume increased in water with 20% TCP added was 44%. Addition of 20% MCPM and 5% EPL increased the volume by 85% and 47% respectively. (Appendix VIII (figure 6)) Thus, the increase in volume in water was affected by all three variables; TCP, MCPM, and EPL. MCPM, however, showed the highest effect.

Volume change difference between the two solutions:

After 12 weeks:

This section describes the impact of the added variables on the increase in volume after 12 weeks in both SBF and water. Figure 3.35 demonstrations the average effects of TCP, MCPM, and EPL on the increase in volume in the 2 solutions. The average effect of each variable was assessed using factorial analysis.

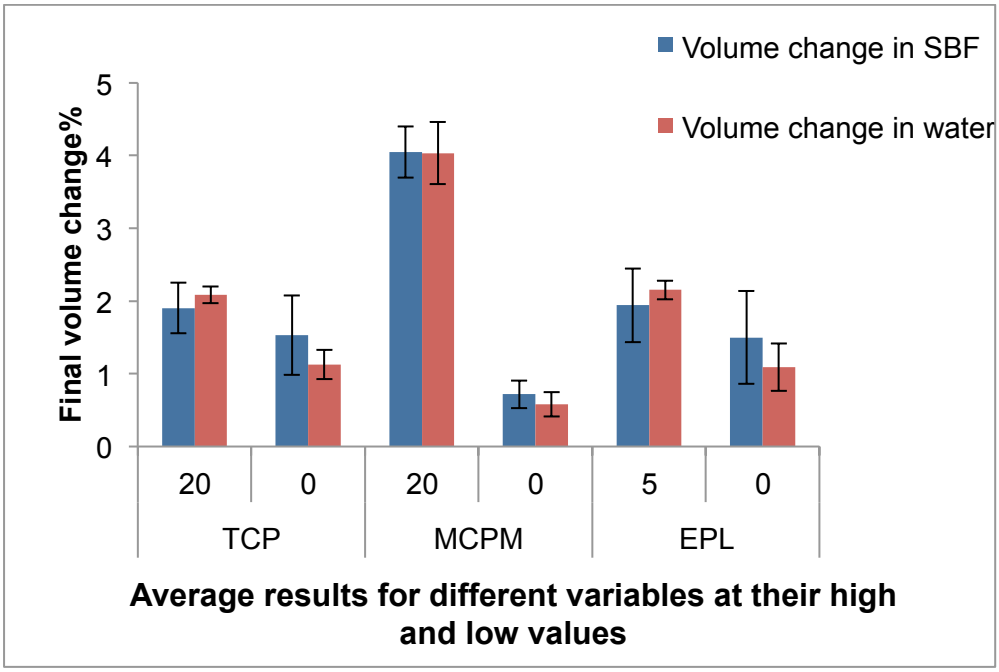

Figure 3.35: Average effects of TCP, MCPM and EPL on volume change in both water and SBF. Errors bars are 95% confidence interval, n=3.

The maximum volume change and the volume change after 12 weeks were significantly affected by MCPM and TCP. On the other hand, EPL and the storage medium (SBF or water) did not significantly affect the maximum and the final increase in volume change. (See Appendix III (table 1) and Appendix IV (table 2)) However, MCPM showed the highest effect.

On average, in SBF, the final volume change increased from 1.5 to 1.9 vol% with 20% TCP. Adding 20% MCPM and 5% EPL caused final volume change to increase from 0.4 to 4.1 vol% and 1.5 to 1.9 vol% respectively. However, in water, 20% TCP on average caused final increase from 1.1 to 2.1% in volume. 20% MCPM and 5% EPL increased the final volume from 0.6 to 4% and from 1.1 to 2.2% respectively.

The difference in volume change after 1 week:

This section includes assessing any significant difference in the volume of some samples when immersed for 1 week in SBF versus water. Referring to the microstructure analysis study explained earlier (section 3.1), formulae C ($M_{20}T_0P_0$), G ($M_{20}T_{20}P_0$), and H ($M_{20}T_{20}P_5$) showed calcium phosphate precipitation after 7 days in SBF (tables 3.3 and 3.4). Therefore, the difference in the increase in volume change between these formulae in SBF and water was plotted against time (hours) (see figure 3.36).

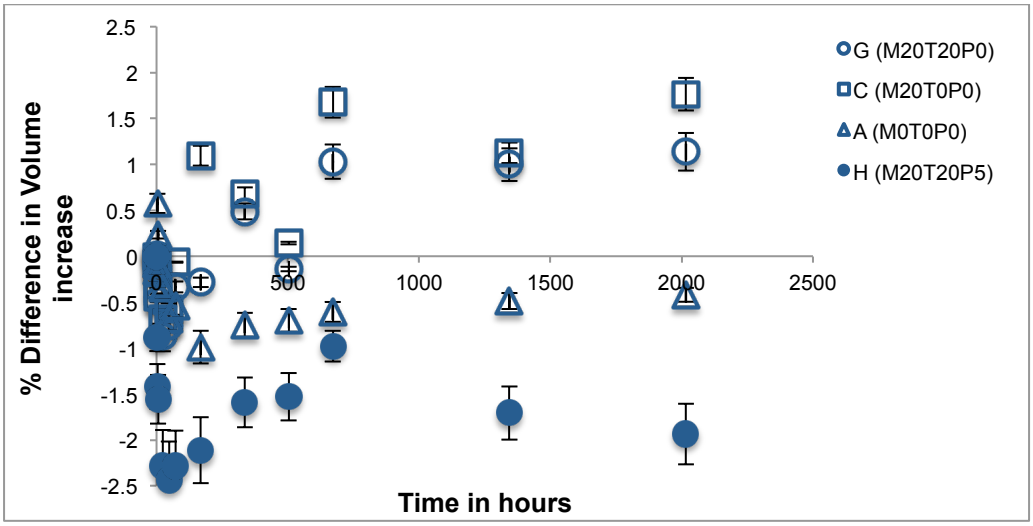

Figure 3.36: The % difference in volume increase in SBF vs. water during 12 weeks (Difference%= %volume in SBF - %volume in water).

Table 3.14 shows where there was significant difference between the volume increase in SBF vs. water and between formulations after 1-week (168 hours) immersion. There was significant difference in the volume change in formula H ($M_{20}T_{20}P_5$) between the 2 solutions (6.3-4.2 = 2.1%)

Volume increase after 1 week				
	H ($M_{20}T_{20}P_5$)	**G ($M_{20}T_{20}P_0$)**	**C ($M_{20}T_0P_0$)**	**A ($M_0T_0P_0$)**
In water	6.3% ± 0.64 (a)	6.5% ± 0.92 (a)	2.8% ± 0.2 (c,d)	1.4% ± 2.0 (g)
In SBF	4.2% ± 1.10(b,c)	6.2% ± 0.64 (a,b)	3.9% ± 0.7 (c)	1.0% ± 0.6 (d,g)

Table 3.14: The % volume increase of formulae A ($M_0T_0P_0$), C ($M_{20}T_0P_0$), G ($M_{20}T_{20}P_0$) and H ($M_{20}T_{20}P_5$) after 1 week in SBF or water. Same letters indicate no significant differences at p = 0.05. Errors SD (n=3) (Appendix I (tables 3 and 4)).

Summary:

Formulae C ($M_{20}T_0P_0$), D ($M_{20}T_0P_5$), F ($M_0T_{20}P_5$), G ($M_{20}T_{20}P_0$) and H ($M_{20}T_{20}P_5$) mass increase after 12 weeks is higher in SBF than in water. On the other hand, formulae B ($M_0T_0P_5$) and E ($M_0T_{20}P_0$) mass change is more in water than in SBF.

Volume change for formulae A ($M_0T_0P_0$) and E ($M_0T_{20}P_0$) were similar in both solutions but formulae B ($M_0T_0P_5$), C ($M_{20}T_0P_0$), and G ($M_{20}T_{20}P_0$) have higher volume in SBF than water. Conversely with formulae D ($M_0T_{20}P_5$), F ($M_0T_{20}P_5$) and H ($M_{20}T_{20}P_5$) volume change was higher in water than SBF.

The most important results concluded from the effect of adding calcium phosphate and polylysine on mass and volume in SBF and water was that mass and volume change is higher in formulae containing MCPM and EPL in both solutions. Mass and volume was higher at early time and reached the maximum increase generally during the first 1-2 weeks. So, there was a linear relation between the early increase in volume or mass and SQRT of time. Thus, the mass or volume change started to level off or decline after 1 – 2 weeks.

In addition, after 1 week, the difference in the increase in mass in SBF vs. water was significant for formulae C, G and H and insignificant for formula A. (Appendix I (tables 1 and 2)). On the other hand, after 1 week, the difference in the increase in volume in the 2 solutions was significant for formula H but insignificant for formulae G, C, and A. (Appendix I (tables 3 and 4)).

During the 12 weeks, the mass increase in SBF was affected by MCPM, TCP, and EPL. But MCPM and EPL showed more effect. Mass increase in water affected mainly by MCPM. Mass increase in samples with no MCPM was highly affected by EPL in both media. Mass increase in samples with MCPM was affected by all variables in both media and volume increase in SBF highly affected by MCPM. Finally, The volume change in water was affected by the 3 variables (TCP, MCPM, and EPL) but MCPM showed the highest effect.

3.3 Solubility and mass loss/Vol (mg/cc):

In general, MCPM and EPL significantly affected the solubility. On average TCP and the storage medium (SBF or water) effects on the solubility were not significant. (Appendix V (table 1)) Figure 3.37 shows the apparent solubility (%wt) of specimens of each formulation after submersion in simulated body fluid or water for 12 weeks. In formulae G and H the % solubility in water was higher than the solubility in SBF.

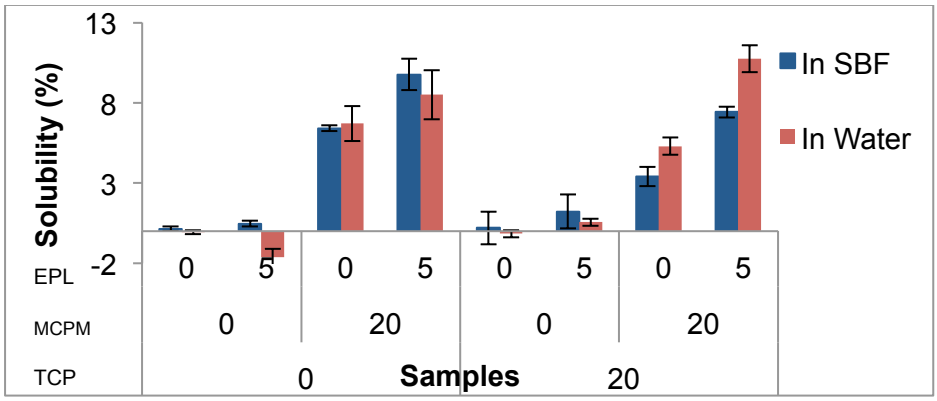

Figure 3.37: Mean of solubility % of experimental dental composites after 12 weeks in SBF and water. Samples from left to right are in alphabetical order A through to H. Errors bars are 95% confidence interval, n=3.

Solubility after 12 weeks in SBF:

The highest (9.8 wt%) was observed in formula D ($M_{20}T_0P_5$) followed by formula H ($M_{20}T_{20}P_5$) with 7.4% solubility. Formulae C ($M_{20}T_0P_0$), G ($M_{20}T_{20}P_0$), and F ($M_0T_{20}P_5$) showed percentages of 6.5 %, 3.4% and 1.5% respectively. Formula A ($M_0T_0P_0$), B ($M_0T_0P_5$), and E ($M_0T_{20}P_0$) showed very low solubility. On average MCPM addition causes the greatest increase in solubility. Addition of TCP reduces this solubility whilst EPL enhances it. According to equation (17), adding 20% MCPM increase the solubility by 95%. (Appendix VIII (figure 7))

Solubility after 12 weeks in distilled water:

After the submersion in distilled water for 12 weeks, the highest solubility (%wt) was observed in formula H ($M_{20}T_{20}P_5$) that is 10.8%, followed by formula D ($M_{20}T_0P_5$) of 8.5%. Formulae C ($M_{20}T_0P_0$) and G ($M_{20}T_{20}P_0$) showed solubilities of 6.7% and 5.3% respectively. Formula A ($M_0T_0P_0$), E ($M_0T_{20}P_0$), and F ($M_0T_{20}P_5$), showed very low solubility. However, formula B ($M_0T_0P_5$) showed mass gain of 1.6%. Referring to equation (17), adding 20% MCPM increase the solubility by 99%. (Appendix VIII (figure 8))

Figure 3.38 illustrates the mean of mass loss over volume in mg/cc of each formula after 12 weeks in simulated body fluid and water.

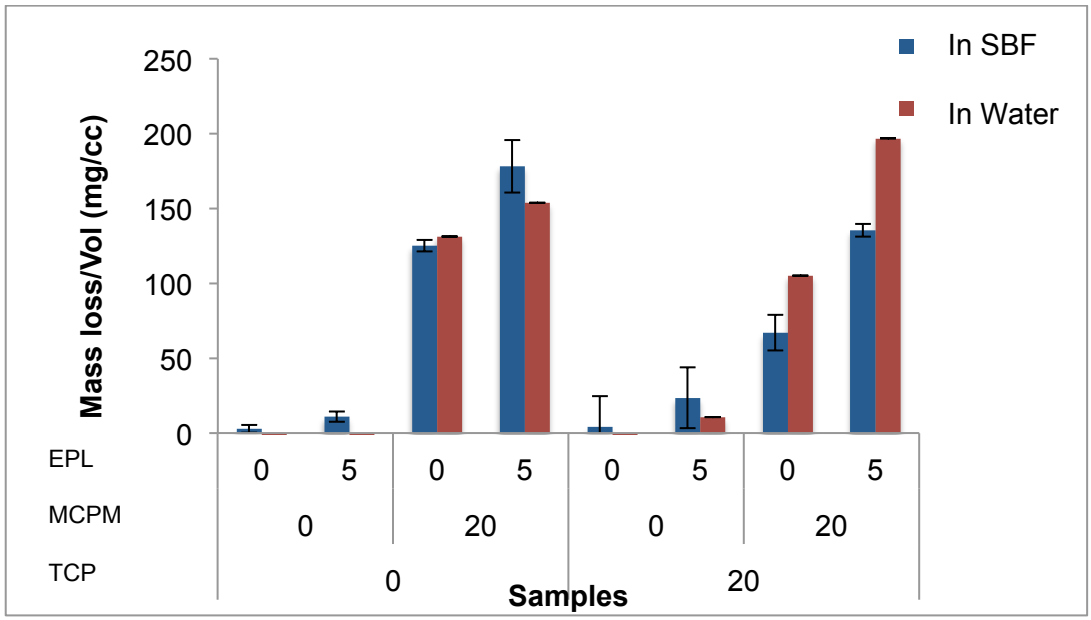

Figure 3.38: Mean of mass loss/ Vol (mg/cc) of experimental dental composites after 12 weeks in SBF and water. Samples from left to right are in alphabetical order. Errors bars are 95% confidence interval, n=3.

Mass loss/Vol (mg/cc) after 12 weeks in SBF:

Formula D ($M_{20}T_0P_5$) showed the highest amount of mass loss to volume of 178 (mg/cc) followed by formulae H ($M_{20}T_{20}P_5$), C ($M_{20}T_0P_0$), G ($M_{20}T_{20}P_0$), and F ($M_0T_{20}P_0$) of 136, 125, 67, and 24 (mg/cc) in order. Formulae A ($M_0T_0P_0$), B ($M_0T_0P_5$), and F ($M_0T_{20}P_5$) showed very low mass loss per unit volume. Over all, formulae with MCPM and EPL showed the highest mass loss between all the formulae. Adding both components induced a higher mass loss percentage.

Mass loss/Vol (mg/cc) after 12 weeks in distilled water:

Formula H ($M_{20}T_{20}P_5$) showed the highest amount of mass loss to volume of 197 (mg/cc) followed by formulae D ($M_{20}T_0P_5$), C ($M_{20}T_0P_0$), and G ($M_{20}T_{20}P_0$), of 154, 130, and 105 (mg/cc) orderly. Formulae A ($M_0T_0P_0$), B ($M_0T_0P_5$) and, E ($M_0T_{20}P_0$) showed almost 0 mass loss/Vol. And, formula F ($M_0T_{20}P_5$) showed mass loss per volume of around 11 mg/cc.

3.4 Water content:

The four different variables (MCPM, TCP, EPL, and medium) significantly affected the water content. (Appendix VI (table 1)) According to figure 3.39, samples B ($M_0T_0P_5$), C ($M_{20}T_0P_0$), and D ($M_{20}T_0P_5$) show higher water content in SBF than in water (See figure 3.39). However, the water content in formula H is higher in water than in SBF. It is around 13.8% in water 12.2% in SBF.

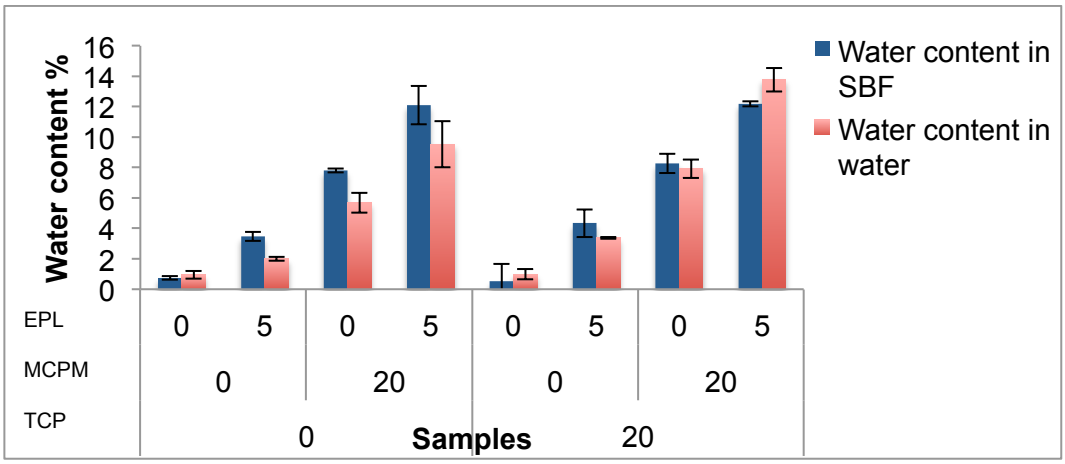

Figure 3.39: Mean of water sorption of experimental dental composites after 12 weeks in SBF and water. Samples from left to right are in alphabetical order. Errors bars are 95% confidence interval, n=3.

After 12 weeks in SBF:

TCP did not show significant effect in water content% of the samples in SBF. (Appendix VI (table 2)) Water contents of the formulae after 12 weeks in simulated body fluid are shown in figure 3.39. Formula D ($M_{20}T_0P_5$) and formula H ($M_{20}T_{20}P_5$) showed the highest water sorption percentages of 12.2%. Formulae G ($M_{20}T_{20}P_0$) and C ($M_{20}T_0P_0$) showed 8.3% and 7.8% water sorption. Formulae F ($M_0T_{20}P_5$), B ($M_0T_0P_5$), and A ($M_0T_0P_0$) showed water content of 4.3%, 3.5% and 0.8%. Formula E ($M_0T_{20}P_0$) showed only 0.5% of water content. Thus, formulae with MCPM and/or EPL showed more water content. Furthermore, Referring to equation (17), adding 20% MCPM and 5% EPL increased the water content by 84% and 67% respectively. (Appendix VIII (figure 9))

After 12 weeks in distilled water:

Water contents of the formulae after 12 weeks in distilled water are provided in figure 3.40. Formula H ($M_{20}T_0P_5$) and formula D ($M_{20}T_{20}P_5$) showed the highest water sorption percentages of about 13.8% followed by of 9.5% respectively. Formula G ($M_{20}T_{20}P_0$) and C ($M_{20}T_0P_0$) had 7.9% and 5.7% water sorption. Formulae F

($M_0T_{20}P_5$), B ($M_0T_0P_5$), E ($M_0T_{20}P_0$) and A ($M_0T_0P_0$) showed water content of 3.4%, 2.0%, 1.0% and 0.9% respectively. According to equation (17), the water content increased 82% and 54% by adding 20% MCPM and 5% EPL respectively. (Appendix VIII (figure 10))

Summary:

- Solubility in SBF and in water was significantly affected by all the variables. (Appendix V (tables 2 and 3))
- MCPM showed the highest effect in the increase in solubility in SBF and water.
- Generally, the solubility was not significantly affected by TCP. (Appendix V (table 1))
- There was no significant difference in the solubility between both solutions. (Appendix V (table 1))
- Water content was not significantly affected by TCP in SBF. (Appendix VI (table 2))
- Water content in both SBF and water was mainly affected by MCPM
- There was significant difference between the water content between the two media (SBF vs. water) (Appendix VI (table 1))
- Water content generally was affected by all the variables including the medium. (Appendix VI (table 1))

Comparisons between solubility and water content in SBF and water:

Figure 3.40 shows the difference between the water sorption percentage and the solubility in SBF. The difference in water content % was higher than solubility in all the formulae. The difference was particularly high in G ($M_{20}T_{20}P_0$), H ($M_{20}T_{20}P_5$), F ($M_0T_{20}P_5$) and B ($M_0T_0P_5$) and equal to 4.9%, 4.8%, 3.1%, and 3.0% respectively. However, in formulae D ($M_{20}T_0P_5$), C ($M_{20}T_0P_0$), A ($M_0T_0P_0$), and E ($M_0T_{20}P_0$) the difference was 2.3%, 1.4%, 0.6%, and 0.3% respectively.

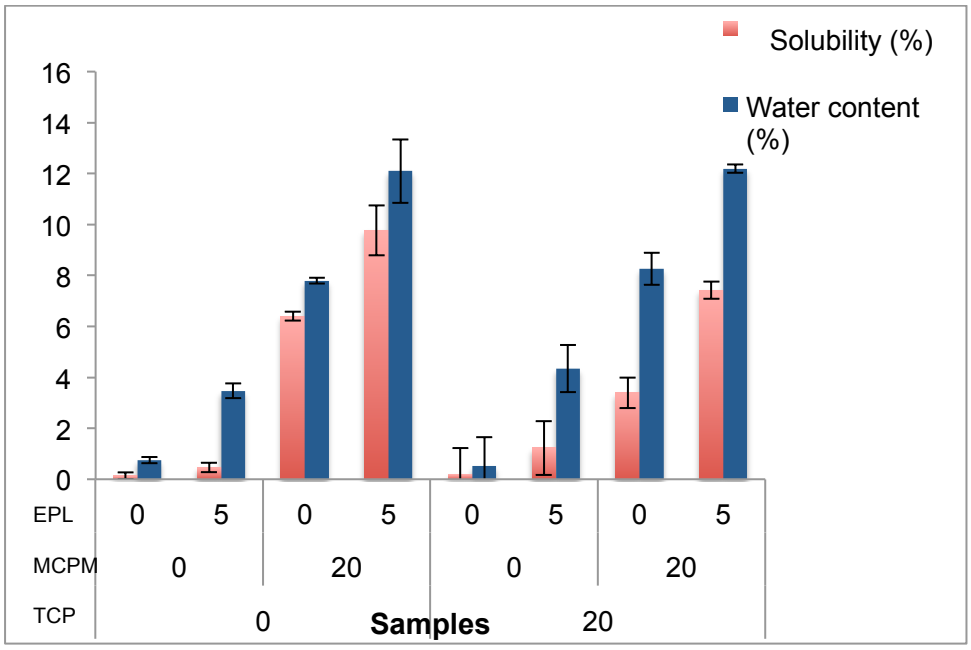

Figure 3.40: Mean water sorption % and solubility % of experimental dental composites after 12 weeks in SBF. Samples from left to right are in alphabetical order. Errors bars are 95% confidence interval, n=3.

Figure 3.41 shows the difference between the water sorption percentage and mass loss percentage of each formula after 12 weeks in distilled water. The difference in water content % and solubility % was variable in all the formulae. The difference was high in B ($M_0T_0P_5$), H ($M_{20}T_{20}P_5$), F ($M_0T_{20}P_5$) and G ($M_{20}T_{20}P_5$) to be around 3.6%, 3.0%, 2.8%, and 2.6%. However, in formulae A ($M_0T_0P_0$), D ($M_{20}T_0P_5$), and E ($M_0T_{20}P_0$) the difference is between 2.3%, 1.4%, 0.6%, and 0.3% correspondingly. On the other hand formula C ($M_{20}T_0P_0$) the difference was around -1.0%.

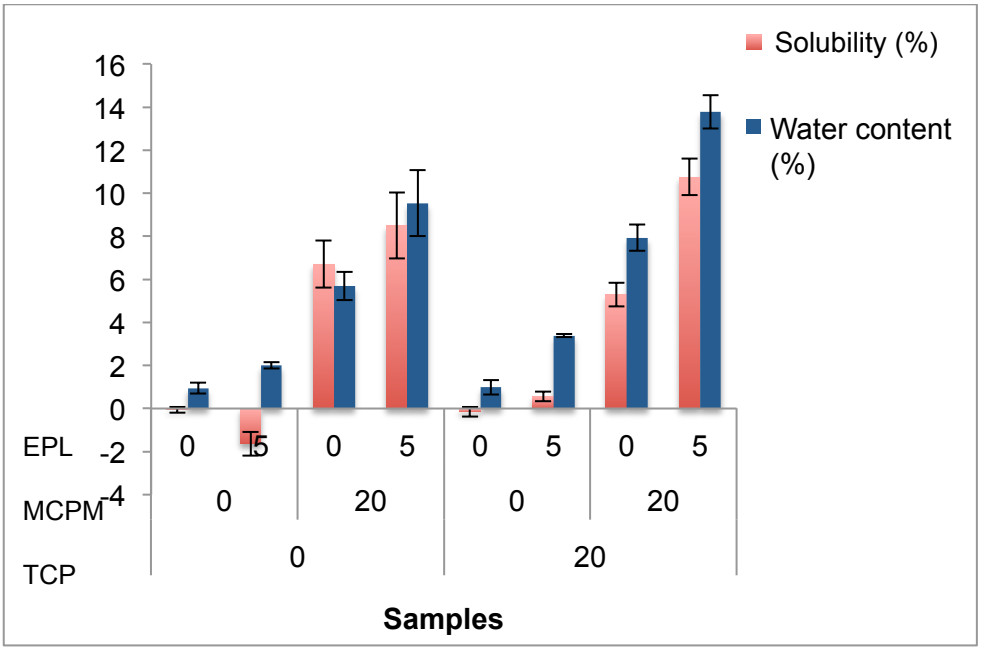

Figure 3.41: Mean of water sorption % and solubility % of experimental dental composites after 12 weeks in distilled water. Samples from left to right are in alphabetical order. Errors bars are 95% confidence interval, n=3.

3.5 Anti bacterial (polylysine release) study:

The distilled water of the formulae containing polylysine was analysed in this study. The 4 formulae are B ($M_0T_0P_5$), D ($M_{20}T_0P_5$), F ($M_0T_{20}P_5$) and H ($M_{20}T_{20}P_5$). Figure 3.42 shows the percentage release of polylysine from the novel composite at different time points during 12 weeks (3 months).

Statistically, there is no significant difference between the releases of the four samples. (Appendix VII (table 1)) However, throughout the 12 weeks, formula H ($M_{20}T_{20}P_5$), showed the highest polylysine release. The release was about 48% after 3 months. Formula D ($M_{20}T_0P_5$) was slightly less and approximately 45%. However, formulae F ($M_{20}T_{20}P_5$) and B ($M_{20}T_{20}P_5$) showed release around 42% and 39% respectively. See figure 3.42.

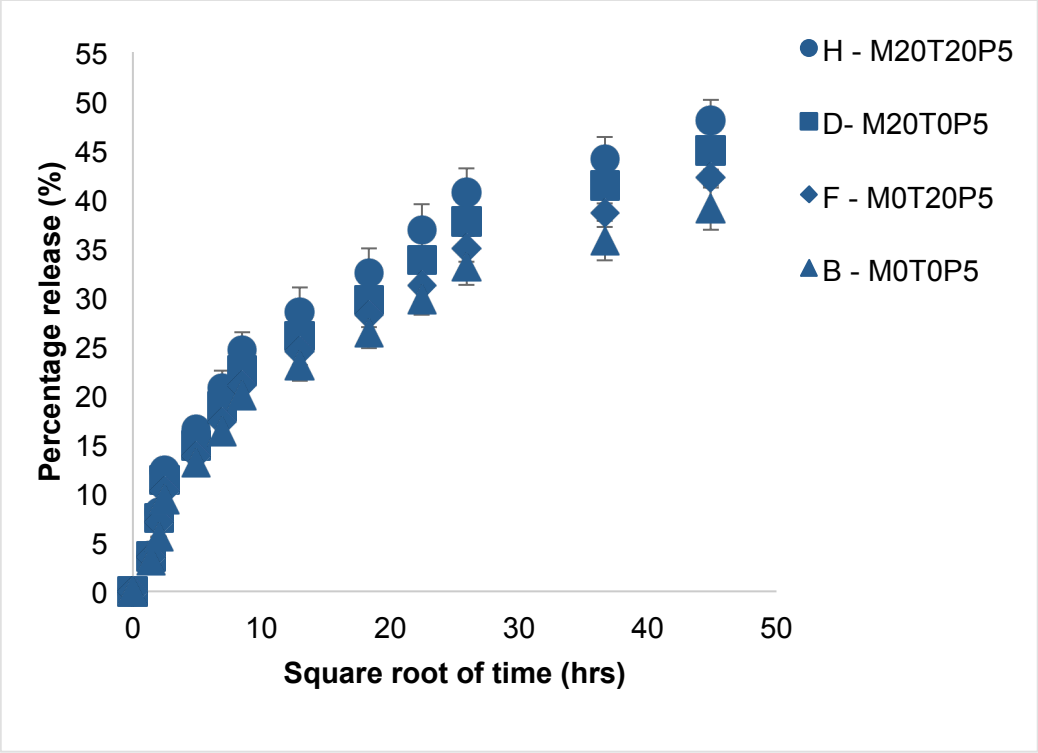

Figure 3.42: Polylysine release from novel composite containing 5% EPL during 3 months (12 weeks) in distilled water. Errors bars are 95% confidence interval, n=3.

Polylysine release during the first 2 weeks (18 SQRT time) in all the formulae was similar as seen in figure 3.42. Almost all the formulae showed similar range of release during the early time. However, formula H ($M_{20}T_{20}P_5$) showed always slightly higher release than the other formulations. In 2 weeks (18 SQRT time point), formula B showed 26% of release. Formulae F, D, and H showed 28%, 30%, and 33% amount of release correspondingly.

The release after 2 weeks and during the last 10 weeks (from 18 to 45 SQRT time) started to show some difference between the formulae. However, within this period a more noticeable difference between the formulae containing 0% or 40% CaP started to appear. So comparing the release of formula H ($M_{20}T_{20}P_5$) to formula B ($M_0T_0P_5$) the average release during the 3rd, 4th, 8th, and 12th week was almost 10% higher in all the time points. Therefore, comparing 0% CaP formula to 40% a higher release difference was noted in the later formula as seen in figure 3.42

As seen in table 3.15, the gradient of the initial release (from 0 to 2 weeks) of EPL was higher in all the formulae compared to the gradient of late release (from 2 to 10 weeks) of the experiment. For example, the initial gradient in formula B ($M_0T_0P_5$) is 1.43 wt%/hr$^{0.5}$ while in formula H ($M_{20}T_{20}P_5$) is 1.75 wt%/hr$^{0.5}$. Also, formulae with 20% MCPM and with/without TCP showed higher gradient compared to 0% MCPM.

Formula	Gradient of initial release (wt%/hr$^{0.5}$) ± SD	Square of the correlation coefficient (R^2)	% 2 weeks release	95% Confidence interval (CI) of initial release	Gradient of late release (wt%/hr$^{0.5}$) ± SD	Square of the correlation coefficient (R^2)	% Maximum release after 12 weeks	95% Confidence interval (CI) of late release
B ($M_0T_0P_5$)	1.43 ± 0.32	0.90	26.3	0.36	0.34 ±0.10	0.95	39.0	0.11
D ($M_{20}T_0P_5$)	1.59 ± 0.37	0.90	29.7	0.42	0.46 ±0.11	0.96	45.0	0.13
F ($M_0T_{20}P_5$)	1.51 ± 0.33	0.90	28.2	0.37	0.45 ±0.11	0.96	42.2	0.12
H ($M_{20}T_{20}P_5$)	1.75 ± 0.41	0.89	32.5	0.46	0.46 ±0.11	0.96	48.0	0.12

Table 3.15: The gradient of the early (from zero to 2 weeks) and late release (from 2 to 10 weeks) of polylysine versus SQRT time (hrs) from experimental composite upon immersion in water for 12 weeks. Errors SD (n=3).

Chapter IV

Discussion and Conclusions

4.1 Identification of new mineral phase on the surface and in the bulk of the Novel composite:

In this experiment the re-mineralising properties of composites that contain different calcium phosphates and polylysine were analysed. The individual and combined effect of the additive components was assessed using several analytical techniques.

In the oral cavity the existence of water from the saliva can make CaPs diffuse from the material and react with each other, resulting in different CaPs mineral formation some of which are of greater volume. The microscopic gaps that have formed by mechanical damage or polymerisation shrinkage can be filled as a result. This may aid in self- repair mechanisms and prevention of recurrent carries due to bacterial micro-leakage. Brushite, Monetite or both minerals can be formed according to the level of moisture. Although the strength and hardness can be less, chemically these minerals are quite similar to the mineralised tissue that constitutes 70% of dentine, hydroxyapatite (HA). Besides, Brushite may transform into HA in vivo (la Rubia García, 2012).

The study performed was used to provide evidence of crystal formation on and in the novel composites using SEM images and Raman analysis. EDX was also used to identify the Ca/P ratio of the new calcium precipitates. Apatite formation was confirmed by comparing the Raman spectra obtained with the standard Raman spectra of all the raw components.

Starting with the SEM analysis, selected images were provided so as to compare the effect of adding the variable components on the precipitation potential of the experimental composite. For example from SEM images of G ($M_{20}T_{20}P_0$) and H ($M_{20}T_{20}P_5$) samples immersed in SBF for 7 days, there was significant precipitation on the surface and in the core of the sample that could be confirmed by the average Raman spectra as hydroxyapatite and Brushite crystals. These results suggest that these formulations can release calcium and phosphate ions and promote the formation of apatite.

Comparing the SEM images between all the different samples, samples immersed in in SBF showed more significant calcium phosphate precipitations. For example, HA, Brushite, and Monetite precipitation were all seen in this solution. On the other hand, the dry samples, samples immersed in de-ionised water or in AS showed no or very minimal crystallisation. These results may be due to the difference in degree of

saturation between SBF, AS and distilled water, which then induced the precipitation of calcium phosphate. This finding suggested that dental composites formulae that contain both MCPM and TCP have re-mineralising potential by enabling higher degree of mineral saturation (DS) in the solution due to the release of ions (Dickens et al., 2003, Xu et al., 2007b).

The first part of this study is considered to be a qualitative study. Therefore, description of the obtained images and Raman spectrum was only performed. Also, to confirm the findings located in SEM images, Raman spectroscopy was under taken with these samples. Raman mapping can provide chemical characterisation and detailed chemical images. Also, the EDX method was employed in order to verify the composition of the precipitation on the surface and core of the samples. The aim of using the EDX method was to qualify the Ca/P ratios. Different and random points in the bulk and surface of selected formulae that showed significant precipitation using SEM only were studied by EDX. These included formulae G ($M_{20}T_{20}P_0$) and H ($M_{20}T_{20}P_5$) in saliva and SBF solutions. For these samples at least 10 random points were analysed using EDX in each sample to have a more representative analysis of what were inhomogeneous (on the micron scale) samples.

Formula A ($M_0T_0P_0$):

Samples containing no CaPs and only glass showed no significant or obvious features. This control demonstrates that without adding the re-mineralising agent, no precipitation is possible in any storage medium.

Formula B ($M_0T_0P_5$):

Formula B contained the anti-bacterial agent, polylysine (EPL) and glass only in the filler phase. It showed no significant crystal precipitations. This finding was confirmed by Raman analysis in all samples when immersed in the 3 different solutions. Unreacted EPL was seen in both the surface and core of the dry samples. Polylysine presence after 1 week was seen in SEM images and in Raman analysis but only in the core of this formula and not the surface in the other 3 solutions. This is because EPL is a soluble component and dissolved by the immersing solution. In conclusion the EPL cannot induce any precipitation on its own with any of the different media. EPL may therefore be considered an anti-bacterial but not a re-mineralising agent.

Formula C ($M_{20}T_0P_0$):

In formula C ($M_{20}T_0P_0$), precipitation was seen in the core of the sample when it was immersed in both AS and SBF. In addition, the surface of this formula in SBF showed Brushite in SEM and Raman analysis. A possible explanation to this; is that MCPM has the potential to transfer into Monetite or Brushite in buffered solutions with or without TCP. MCPM in the presence of water can give phosphoric acid and dicalcium phosphate (Dickens et al., 2003, Xu et al., 2007b). This dicalcium phosphate can then precipitate as Brushite/Monetite. Provided the phosphoric acid is removed by buffering more dicalcium phosphate may then form (Further in this section CaP equations are provided and can explain this reaction equation). So individually, MCPM has the potential to enhance the remineralisation process in a basic environment. Also, ions from the surrounding medium (AS or SBF) can help to neutralise the acid and enhance the conversion of MCPM into Monetite or Brushite (Aoba, 2004).

Formula E ($M_0T_{20}P_0$):

In this formula only TCP was added and no precipitation in any of the solutions was noted. The single explanation to this is that TCP has low solubility and is unable to transform to Brushite or Monetite on its own. SEM images and Raman spectroscopy confirmed no precipitation in any of the solutions in this formula.

Formula G ($M_{20}T_{20}P_0$):

Both calcium phosphates were added in equal amounts in formula G. This formula in the three solutions showed calcium phosphate precipitation. This suggests that when both TCP and MCPM were combined together they have more potential to encourage remineralisation. Therefore, this formula was assessed using 3 different analytical techniques (Reynolds, 2009).

TCP when added with MCPM it can react with it and enhance surface remineralisation. Also, TCP helps prevent MCPM dissolving out of the material bulk by transforming it to less soluble Monetite or Brushite (Dickens et al., 2003, Xu et al., 2007b).

SEM and Raman analysis showed calcium phosphate precipitation in SEM and Raman peaks of Brushite and Monetite. In addition, EDX was performed with this sample to confirm the kind of precipitation according to Ca/P ratio.

The EDX results of this formula in AS and SBF showed Ca/P ratios typical of: TCP, OCP, DCPA and DCPD. Also some points in the core of this formula showed ratios consistent with unreacted MCPM and polymer. Due to the fact that MCPM is a very soluble component the surface did not show any MCPM. This confirms that both calcium phosphates can react together in the presence of aqueous solution to enhance precipitation.

Formula H ($M_{20}T_{20}P_5$):

Finally, formula H ($M_{20}T_{20}P_5$) showed the most significant levels of precipitation. All the variable components were added here. The core of this formula showed calcium phosphate precipitations in water, AS, and SBF. The surface also showed crystallisation in AS and SBF. A different kind of calcium phosphate precipitation was noted in the surface when the sample was immersed in SBF. These crystals were different in structure to the previously detected crystals. Moreover, comparing the SEM images to previous work suggests apatite formation. Also Raman showed a single high peak at 960 cm^{-1}, which is similar to the standard HA peak in Raman spectroscopy. For further confirmation to the identity of these crystals, EDX was performed in the core and surface for this formula when it was kept in SBF and AS. According to EDX Ca/P of approximately 1.67 was noted in multiple areas in the surface in SBF. Also, almost all the MCPM in the surface when immersed in SBF has dissolved and possibly became a part of the crystallisation process.

It was also apparent that more precipitation was seen in sample H ($M_{20}T_{20}P_5$) than in G without EPL. A possible explanation is that Polylysine promotes water sorption into the dental composite, thus enhancing the release of ions. As a result, the polylysine or released polylysine on the surface may also enhance the HA crystallisation process.

To summarise, the surfaces and the cores of formulae A ($M_0T_0P_0$), B ($M_0T_0P_5$), and E ($M_0T_{20}P_0$) did not show any crystal precipitations under any conditions. But the surfaces and the cores of formulae C ($M_{20}T_0P_0$), G ($M_{20}T_{20}P_0$) and H ($M_{20}T_{20}P_5$) showed crystal precipitation when kept in AS or SBF. In addition the cores of formulae G ($M_{20}T_{20}P_0$) and H ($M_{20}T_{20}P_5$) in water also showed several different kinds of calcium phosphate reactions and precipitations.

Average effects of different additives on precipitations:

From SEM and Raman it was clear that only formulations containing MCPM (C, G, and H|) had precipitation whilst those without (A and B) had none. The change in calcium phosphate type with addition of EPL, TCP or components in the medium suggest interactions with the MCPM. In addition, TCP and EPL alone can't induce any precipitation in contrast to MCPM that is able to transfer into Monetite or Brushite (Dickens et al., 2003, Xu et al., 2007b).

Referring to table 3.1 and 3.2, MCPM, TCP and EPL were all visible and unreacted under dry conditions in the surfaces and cores of the experimental composites. Surface MCPM and EPL had dissolved, however, in all three solutions by 7 days. Conversely, in all three solutions, TCP was not dissolved from the surface of formula E ($M_0T_{20}P_0$). This is due to the fact that TCP is less soluble than MCPM and EPL. Also, some TCP was seen in the surface of formula G ($M_{20}T_{20}P_0$) when immersed in water but not when immersed in SBF or AS. This may be because precipitating layers in the media containing additional ions may hide it.

The following chemical equations give the different equilibria between various calcium phosphate species:

$$Ca_{10}(PO_4)_6(OH)_2 + 18\ H_2O \leftrightarrow 3\ Ca_3(PO_4)_2 + Ca(OH)_2 + 18\ H_2O$$

$$\leftrightarrow 6\ CaHPO_4 + 4\ Ca(OH)_2 + 12\ H_2O$$

$$\leftrightarrow 3\ Ca(H_2PO_4)_2 + 7\ Ca(OH)_2 + 6\ H_2O$$

$$\leftrightarrow 6\ H_3PO_4 + 10\ Ca(OH)_2$$

$$\leftrightarrow 6\ PO_4^{3-} + 10\ Ca^{2+} + 20\ OH^- + 18\ H^+$$

$$Ca(H_2PO_4)_2 + 2\ H_2O \leftrightarrow 2\ H_3PO_4 + Ca(OH)_2$$

$$3\ Ca_3(PO_4)_2 + 6\ H_2O \leftrightarrow 6\ CaHPO_4 + 3\ Ca(OH)_2$$

$$6\ CaHPO_4 + 4\ Ca(OH)_2 \leftrightarrow Ca_{10}(PO_4)_6(OH)_2 + 6\ H_2O$$

MCPM may disproportionate into Brushite or Monetite plus phosphoric acid. The acidic environment needs to be neutralised to enable the reaction to continue otherwise the reverse reaction would dissolve the Brushite again and convert it back to MCPM. Additives in AS and SBF help to drive this equilibrium towards Brushite formation. TCP and EPL can also help to drive this equilibrium. SBF has a stronger effect on this equilibrium than the AS. When there are sufficient basic and Calcium ions this reaction can be driven towards HA production as seen in the previous equations (Aoba, 2004).

Referring to figure 3.15, SEM images show the early possible apatite formation after 7 days immersion in SBF. Comparing it to images in figure 3.16, more mature formation of precipitation was seen after 4 weeks immersion in SBF. This indicates that other mature phases of calcium phosphate precipitations might form upon longer period of immersion.

To summarise, the formulations G ($M_{20}T_{20}P_0$) and H ($M_{20}T_{20}P_5$) when immersed in SBF show evidence of calcium phosphate reaction in the core and on the surface of the sample.

4.2 Effect of calcium phosphate and ε-poly (L-lysine) on composite mass and volume changes:

Sample mass and volume changes provide more quantitative data on composite properties than the SEM and Raman investigations but can be difficult to interpret due to them being affected by a range of different processes. These processes include water sorption, component adsorption and release, chemical interactions or reactions that can cause density changes.

The experimental composite was evaluated under wet conditions in order to mimic the oral conditions. Evaluating the water sorption helps to understand the physical and chemical properties of various formulae.

In this study, gravimetric analysis was used for mass change determination and Archimedes principle was used to measure the volume change. This is a commonly used method (Rüttermann et al., 2007, Rüttermann et al., 2011). An ISO standard method was modified for the above thesis study. Modifications included less diameter and longer storage time. The dimensions of the experimental composites were 1mm thickness and 10 mm diameter compared to ISO standards of 1mm thickness and 15 mm diameter. Also, the ISO standards for storage time are one week. However, 12 weeks was applied to this study in order to look at the long-term effect of the hydrophilic components over a prolonged period of storage.

Mass change and volume change:

Generally the addition of the more hydrophilic additives (MCPM and EPL in particular) caused an increase in mass and volume. This is due to water penetrating to try and balance osmotic pressure differences, which occur upon dissolution of these soluble components into the absorbed water. The relative effects of the two different calcium phosphates and EPL on both mass and volume change were complicated, however, by interactions between these components and additives in the storage solutions.

Mass and volume increase in the samples may be due to the absorbed water expanding the polymer. Mass increase without expansion occurs upon water filling the pores. Further complications arise when components are released or precipitate.

Early increase in mass and volume:

The increase in mass at early times is due to a delay between water sorption and subsequent ion and EPL component release. MCPM is more soluble than β-TCP, and as a result generally caused faster early water sorption. EPL had a lesser effect but typically added to this property. In most cases EPL increased the mass change but had lesser effect on the average volume changes. (See Figure 3.22, 3.24, 3.30 and 3.32) This suggests there may be increases in density upon water sorption when EPL is present.

A linear increase in mass and volume change versus the SQRT time is expected from Fick's laws of diffusion. A peak in some mass change plots could be due to water being pulled in and making the material temporarily denser before the EPL is released. These temporary peaks in plots are not as evident in the volume changes.

Linear regression analysis using the Linest functions on excel was done to enable quantitative comparison of the early increase in mass and volume in both solutions within the first 1-2 weeks (see Tables 3.9, 3.10, 3.12 and 3.13). The early gradients were always positive initially as mass gain due to water sorption always outweighed any loss due to component release.

With A ($M_0T_0P_0$), the initial gradient for mass and volume versus SQRT (time) in both media was very low in comparison with other composites in the literature (Boaro et al., 2013). A possible explanation is the very high conversion observed with the monomer system of this study enabling high crosslinking and preventing water sorption (Shami, 2014). The addition of EPL increased these gradients but the increase was less when MCPM was also present. This might suggest interaction between these two components. This interaction was more evident in the mass changes. This might be due to the high crosslinking density that would stop expansion but the high EPL hydrophilicity would still force water to be pulled in and increase mass more than volume. The MCPM had particularly large effect on these gradients when TCP was also present. This could be due to reaction between these two components preventing bulk ions being released and also binding the water in new calcium phosphate phases. Previous work has shown that this reaction can occur within MCPM and TCP containing composites within the first 24 hours after immersion in water (Mehdawi et al., 2009).

Late increase in mass and volume:

The maximum increase in mass and volume in both solutions occurred within the first 2 weeks. Later on, the polymer crosslinking will limit the amount of water that can get in and counteract the osmotic pressure that draws in the water. Therefore the increase started to level off after 2 weeks.

There could be slight decline in mass at later times when water sorption has largely reached equilibrium and there is a net loss of components such as EPL or calcium phosphate species.

Later time results are also complicated by competing component release and precipitation. Following the early increase in mass and volume there will be a slower diffusion of the Calcium and phosphate ions and also EPL from the polymer. Once these have gone or if there is reaction to form less soluble species such as Brushite and Monetite there is a possible reduction in osmotic pressure and some water may be expelled. When components have been released they may then re-precipitate on the material surfaces due to interactions with other components in solution.

Later increase of the mass and volume happens due to the fact that the dissolution of soluble components (MCPM and EPL) may cause super saturation of Ca and PO_4 ions in the solution leading to the observed later precipitation on the surface of the samples. Therefore, an increase in mass change in samples containing MCPM was seen. All in all, samples containing MCPM had increase in mass change due to its high solubility that induced more water sorption and apatite precipitation due to Ca and PO_4 ions saturation. On the other hand, TCP has a low solubility compared to MCPM and as a result samples with MCPM replaced by TCP induced less mass change.

In addition, volume changes are small at later times. So mass loss at this time is likely due to water replacing MCPM of higher density. Also the water and EPL may be expelled at later times from areas where EPL solutions were forced to be of higher density than expected from their pure densities. This would also decrease mass without affecting volume too much.

Moreover, EPL and water have similar density so replaced one by the other will have no effect. This is contrary to MCPM. As MCPM has higher density than water its replacement will cause a decrease in mass. Subsequently, however, the ions that are released re-precipitate with other ions to cause the increase in mass.

EPL-containing samples showed more increase in mass in both solutions. However, EPL caused more increase in volume change in water and not in SBF. As describes earlier, EPL causes the water to be pulled in and create regions of higher density than expected from the volumes of the individual components. This causes pressure in the materials that is released with the EPL expulsion from the material. This expulsion causes a period of decline in mass but no change in volume.

The diffusion coefficient is proportional to the gradient of increase in mass versus SQRT time divided by the final mass change all squared. Gradient divided by final value is smaller for formulae that contained EPL without MCPM. The EPL is encouraging water sorption but apparent diffusion is slower. This could be a consequence of the water replacing EPL. The mass change is also complicated by both increase due to water sorption and decrease due to EPL release.

Factorial analysis interpretation of increase in mass and volume:

Comparing the individual and combined effect of the variable components, the factorial analysis confirmed that soluble variable components could cause more significant increase in mass and volume in both solutions. The presence of both MCPM and EPL cause greater increase in water sorption and eventually more ion release and crystallisation potential.

Referring to figure 3.26, interaction effects make it difficult to understand the effects of the individual components. By taking the factor causing interactions out from the analysis it is easier to see which factors are having the bigger effects.

Therefore, in figure 3.27, medium and TCP only have an effect on mass change when MCPM is present. This is due to these components helping reduce the dissolution of the MCPM either by precipitation in the bulk or on the surface. Also, MCPM reduces the effect of the EPL on water sorption. This can be due to EPL reacting with MCPM to form less soluble products or MCPM causing the EPL to be released more quickly and thereby not allowing time for high water sorption.

The difference in mass and volume of the samples in both solutions:

Differences in mass change in water vs. SBF can give an estimate of the level of precipitation. Due to differing osmotic pressure, however, there may also be differences in water content of the samples in the two solutions. For this reason to separate the effects of differing water sorption the samples were dried at the end of the experiment.

The difference in mass change of samples in SBF versus water was provided in figure 3.29. In this graph the samples that showed precipitations; ie: C ($M_{20}T_0P_0$), G ($M_{20}T_{20}P_0$), H ($M_{20}T_{20}P_5$) and the control formula A ($M_0T_0P_0$) were plotted against time in hours. Looking at this graph the mass increase in SBF for these samples was higher in SBF compared to water. A possible explanation for this is that the difference in the mass is due to the mass of the precipitation layer in the sample. The difference in mass increase between the two solutions was particularly significant for all formulae with MCPM (C, G and H) as would be expected if precipitation is encouraged by MCPM release. In these samples mass in SBF is higher because the mass of them includes the mass of water filling the pores and the mass of the formed precipitation.

The difference in volume between SBF and water was plotted against time in hours in figure 3.36. In this graph, the volume of the samples that showed apatite precipitation in the microstructure study could be slightly higher or lower in water versus SBF. Strong interactions between the components might, however, cause factors affecting density and volume changes to be more complex than the mass changes.

The aim of this study is to reduce the recurrent caries, relieve the stress that might occur due to polymerisation shrinkage, and improve the longevity of the restoration by reducing the micro-leakage. As a result volumetric expansion can play an important role in achieving these properties.

The excessive increase in volume in some of the formulae, however, could potentially crack the tooth. Maximum expansion that would be acceptable would be around 4 vol percent. This increase in mass and volume change may contribute just enough to counteract the effect of polymerization shrinkage

Solubility and Mass loss/Vol (mg/cc):

Generally, the solubility in both solutions for formulae containing MCPM and/or EPL was high. This is because they are highly soluble. As seen in table 1.3, MCPM is very soluble and considered to be the most soluble calcium phosphate phase. EPL also has very high solubility in water (Hiraki, 2000). As a result when both components were combined together solubility was increased.

Comparing the solubility of the formulae in SBF and water figure 3.37, the solubility of formula H ($M_{20}T_{20}P_5$) that showed apatite precipitation was higher in water than in

SBF. Again this is because the crystals formed in SBF are less soluble. Also, the soluble components (MCPM and EPL) are trapped and became a part of crystallisation and possibly HA formation.

As stated by Gerritsen in 2010, dental hard structure is able to induce re-mineralisation and respond to the effect of demineralization caused by carious attacks when the surrounding environment is saturated with ions to induce precipitation (Gerritsen et al., 2010). So the more ions released to the surrounding solution the higher the possibility for precipitation

Mass loss/Vol (mg/cc) was also calculated, as it is required in the ISO standard. From this calculation, the amount of the soluble components that dissolves into water can be estimated. The mass loss into water provides an indication of the ions that will be released or the saturation of ions in the SBF. As a result, samples with more mass loss/Vol in water showed more precipitation in SBF.

The mass loss/Vol after 12 weeks in water for G and H with both TCP and MCPM were both higher than in SBF as expected with released mineral re-precipitation. A possible explanation as to why TCP is important factor could be that it becomes a part of the apatite phase and aids the MCPM re-precipitation. Also, sample C showed high mass loss due to the lost MCPM, which is high in density.

Water Content:

A composite that contains hydrophilic components (e.g MCPM and EPL) should absorb more water. As a result, this can help in inducing more anti-microbial and re-mineralising agent release. Furthermore, the swelling effect caused by water sorption can aid in polymerisation shrinkage compensation.

When calculating water content in SBF and water, the water content in SBF for formula H ($M_{20}T_{20}P_5$) was less than the water content of the sample in water (figure 3.39). Lower water sorption could be a consequence of reduced osmotic pressure difference. Lower water sorption with media containing ions has been previously observed when both MCPM and TCP are present in composites (Mehdawi et al., 2009).

Water is essential to form the Brushite that is the precursor of HA. The more basic the solution the higher is the ability to form HA. Thus, formulae containing the acidic MCPM and the basic TCP induced more water sorption and caused greater mineral precipitations.

The following chemical equation shows how HA formation may occur starting with phosphoric acid.

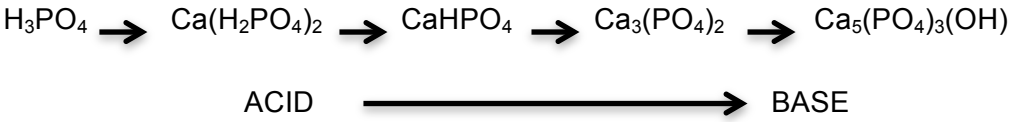

Water sorption is essential to compensate the polymerisation shrinkage. On the other hand, excess water sorption can adversely affect the mechanical properties of the sample. Diffusion controls the uptake of water in dental composites (Örtengren et al., 2001). It is decreased with raised crosslinking of the matrix or reduction in hydrophilic components and hence can be adjusted to exactly compensate for the polymerization shrinkage.

Upon immersion in aqueous solution, resin based materials have the potential to absorb water. This property is more controlled by the resin phase in the commercial materials (Boaro et al., 2013, Sideridou et al., 2004). Various changes can occur to the material when water is absorbed into its structure. For example, the chemical, biological and physic-chemical properties might be altered.

Unreacted monomer can be released from the specimens so the mechanical properties can be deteriorated as a result of excess water sorption (Øysæd and Ruyter, 1986, Örtengren et al., 2001, Drummond, 2008). Also, (Reichl et al., 2006) reported that upon water sorption, the resin based restorative material could induce cytotoxic effects by releasing the unreacted monomers. In addition, the growth of cariogenic bacteria can be promoted consequently, plasticization, decline in the mechanical properties and hydrolytic degradation can occur in excessive water sorption events. However, referring to the control formula A, the results show conversion is very high and so monomer release highly unlikely.

Comparisons between solubility and water content in SBF and water:

As seen in figure 3.40 and 3.41, the water content in almost all the formulae is higher than the solubility (mass loss) in both solutions. The difference between the water content and the solubility provides some indication of how much water was expanding the polymer matrix phase.

For example formula H ($M_{20}T_{20}P_5$) in both SBF and water showed high difference but even the difference was higher in SBF. Referring to figure 3.40, TCP is reducing the MCPM solubility in SBF due to it helping re-precipitation. Also, all the samples

containing EPL, the water is being drawn in and bound. In addition, negative solubility of formula B suggests that it was difficult to fully dry off all the water content.

Figure 3.41 showed that TCP enhanced MCPM solubility in water when EPL was present, therefore, aiding the precipitation potential of the sample.

4.3 Polylysine release:

Polylysine was added to this composite as an anti-bacterial agent. All the samples contained 5% polylysine in the powder phase by weight and therefore 4% of the total. Its inclusion in the sample may reduce the demineralisation by killing the bacteria that produce acid.

The release of any component is affected by many factors. For example, a study done in 2008 showed that all of the anti-bacterial chlorhexidine included in a Brushite cement could be released in a few days due to cement high porosity (Young and Ho, 2008). Significant drug entrapment, however, is more commonly observed in composites and drug release relies upon high water sorption. Interaction between the matrix and the drug and its solubility in the matrix versus surrounding medium can play an important role in the release potential of the material (Ginebra et al., 2006).

In this study, the composites showed high percentages of polylysine release. The amount of release was higher at early times. Samples with MCPM and greater water sorption had only slightly increased EPL release. This is contrary to what has been observed with other less water-soluble drugs such as chlorhexidine (Leung et al., 2005, Mehdawi et al., 2009). A possible explanation is that the very high water solubility of the EPL draws in high levels of water causing pressure within the composite that drive the EPL out.

4.4 Conclusions:

The aim of this project was to produce a dental composite that is capable of optimising re-mineralisation and provide anti-bacterial release to help inhibit bacterial micro-leakage.

Adding both calcium phosphates (MCPM and TCP) and the anti-bacterial agent (EPL) into the powder phase of the experimental composites enhanced the formation of apatite.

Water sorption was higher in the composite that contained the soluble components (MCPM and EPL).

The anti-bacterial release (Polylysine) was slightly higher in the formulae that contained both calcium phosphates (MCPM and TCP). However, this was not significant.

Novel EPL-releasing calcium phosphate-filled methacrylate-based dental materials have been developed that could be used as a permanent filling in dentistry with the following superior properties:

- Re-mineralising properties and possibly apatite formation.
- Able to compensate for polymerisation shrinkage by water sorption ability
- Potentially have the ability to release the antibacterial agent EPL.

Microstructure and re-mineralistation study:

Adding both calcium phosphates (MCPM and TCP) and the antibacterial agent (EPL) into the powder phase of the experimental composites enhanced the formation of apatite. This was seen when the experimented composite was immersed in SBF. SEM, Raman spectroscopy, and EDX confirmed that calcium phosphate apatite was formed in the surface and on the bulk of the novel composite.

Water sorption study:

Water sorption was higher in the composite that contained the soluble components (MCPM and EPL). These encouraged more water sorption therefore enhanced the precipitation of calcium phosphate and increased the mass and volume changes. Swelling may compensate for the polymerisation shrinkage and eventually may

reduce the bacterial microleakage and enhance the tooth-restoration interface stability.

Drug release study:

The antibacterial release (Polylysine) was slightly higher in the formulae that contained both calcium phosphates (MCPM and TCP). However, this was not significant. Further work is needed to confirm the antibacterial potential of EPL release.

Chapter V

Future work and Summary

5.1 Future work:

- ***Adhesion properties of the experimental composite:***

Adhesion can be mechanical, physical, and chemical adhesion (Van Noort and Barbour, 2013). Looking at the adhesion properties of the composite is highly important. This can be done using various tests (Van Meerbeek et al., 2003). For example, push out, tensile, shear, micro-shear, and micro-tensile tests can be used (Scherrer et al., 2010, Fusayama et al., 1979). A possible future study can be done to look at the adhesion properties of this composite containing the variable components. As reported earlier, EPL has the potential to form ionic bonds with collagen and might improve the adhesion properties. So it is interesting to look at the individual and combined effect of these variable components on the adhesion properties. Improving this property can add to preventing the micro-leakage and enhancing the bonding of the filling material to the dentine.

- ***Mechanical properties:***

Several factors can affect the mechanical strength of composites. For example, the addition of the re-mineralising agent might have effect in reducing the strength or toughness of the composite. Also, several SEM images showed porosities. This might initiate cracks and stress concentration that can lead to failure. No mechanical studies were performed on this experimental composite. However, it was reported previously that excessive water sorption could affect the mechanical properties of the composite (Øysæd and Ruyter, 1986, Örtengren et al., 2001, Drummond, 2008). Therefore further studies to look at this area are essential. For example the modulus of elasticity, biaxial strength, surface hardness, and toughness should all be assessed.

- ***Degree of conversion:***

It was shown and proven that uncured monomer can cause harm to dental pulp tissue due to the fact that un-polymerised resin components diffuse across the permeable hybrid layer and dentinal tubules and reach the pulp cells (Gerzina and Hume, 1996, Ulker and Sengun, 2009). Therefore, the degree of conversion is an important property that highly influences the performance of the dental material. It can fundamentally affect the mechanical, physical, and biological properties of the material. So, studies to look at this this property are important.

- ***Shelf life of the monomer:***

Assessing the cure profile at several time points and temperatures will give us an idea about the stability and shelf life of the monomer. This might justify the use of PPGDMA instead of TEGDMA as diluent monomer and NTG-GMA-Na instead of DMPT as accelerator.

- ***Aesthetics properties of the composite:***

Good aesthetic properties for dental restorative materials are in demand. So, it is essential to look at this property. For example, assessing the colour change in the different formulae when immersed in tooth discolouration solutions (ie; wine, tea, or coffee) can give an idea of the colour stability of the experimented composite.

- ***Biocompatibility:***

Biocompatibility contributes to a significant portion of the possible future work plan. These novel composite formulations can be tested to demonstrate the biocompatibility-using cell culturing techniques as a future work. The growth of the bacteria on the surface of the materials should also be quantified and compared to commercial composite. A measure of the bacterial micro leakage will also be beneficial.

De Souza Costa et al did a study in 2001 aimed to assist the human pulp response to dental materials such as self-etching bonding agent and calcium hydroxide (de Souza Costa et al., 2001). Moreover, a study done by Ulker et al, in 2009 evaluated the effect of different self-etched dental composite resin materials on the cell viability of dental papilla-derived cells. The cytotoxicity of the different types of the composite was analysed using a three-dimensional (3D) pulp cell cultures by dentine barrier test device and determining cell survival by MTT assay (Ulker and Sengun, 2009).

According to Schedle et al in 1998, cell-culture studies demonstrated that resin composites' components are hazardous when they are in direct contact with the fibroblasts. Therefore, he illustrated that "Drawing comparisons between the cytotoxicity of composite materials, bonding agents and other dental materials is complex and would necessitate development of standardized test systems in vitro"(Schedle et al., 1998).

So it is essential that an ideal dental material should be biocompatible, have little interaction with body tissues and fluids, have non-toxic properties, and no allergic

potentials (El-Mowafy, 2001, Ulker and Sengun, 2009, Craig, 1997).

- ***Microstructure study of the novel composite:***

There are various limitations to the microstructure study done in this thesis. Firstly, the areas included may not be fully representative because the surfaces are far from homogeneous. In some cases not all the surface area was covered with the precipitations. This study attempted to focus upon the main precipitation regions but this will not have been quantitative. Some regions with different precipitation types may have been missed. Secondly these samples where only investigated after 7 days of immersion. If these samples were analysed after a longer period of immersion more significant precipitation might have been noted.

Thus, qualitative assessment of the microstructure of the experimented composite was only done. So, further analysis needs to be done to quantify the re-mineralising potential of this composite. Also, quantifying the amount of porosities due to the addition of polylysine in order to understand the effect on the drug release property is needed. Also, analysis may have focussed on the Brushite and not looked at the surface layer covering the whole sample. Therefore, modification to the performed microstructure study can be done in several parameters:

- Broader the area analysed and assessed in the experimental composite.
- Increase the time of immersion.
- Quantify the amount of precipitation by measuring the thickness of the layer formed.
- Immersing in simulated dentinal fluids instead of simulated body fluid and assess any precipitation.
- Modify the percentages of the added components and assess any precipitation.

- ***Water sorption study:***

Further studies are required to idealise the maximum expansion that can occur due to water sorption. The volumetric expansion of some of the formulae might be considered excessive according to the ISO. So, further consideration should be done to allow for reasonable expansion of the composite in a way that will not affect the mechanical and physical properties. Also, the limitation of the study done was that there was no quantifying for the amount of the calcium or phosphate released.

Further work might include analysis of the storage medium by ion chromotography to compare and calculate the release of the ions from the different solutions. This can also help in quantifying the re-mineralising abilities of the formulae in various solutions.

- ***Anti-bacterial study:***

This study showed that Polylysine was released from the experimental composite. However, it is essential to look if the polylysine released has a significant effect as an anti-bacterial agent. For example, assessing if the concentration of ε-polylysine released from the experimental composite was adequate for minimum inhibitory concentration required to exert an anti-bacterial action. The limitation in the study done may include that there was no significant difference in the release of the polylysine in all the formulae. This might necessitate the future work of adding the polylysine in variable percentages to assess the effect of the amount of release according to the incorporated added polylysine.

- ***Comparison to commercial composite:***

More studies are needed to compare the developed composite with the other commercial composite. However, the current experimental composite has no or limited anti-bacterial properties. Also, the re-mineralising properties are considered an advantage but their mechanical impact on the strength of the composite was not assessed and compared to commercial composites. In addition, the water sorption of this composite is considered excessive therefore idealisation of the final composition of the experimented composite is essential. The final formulation should have the superior properties stated earlier in addition to considering the negative impact they can cause. For example, the mechanical, physical, biological, and aesthetic should be accounted.

- ***Final composition of the experimental composite:***

More studies are needed to finalise the composition of the final composite. Raman mapping and mechanical testing for composite with modified percentages should be done. The final composition should have the potential to re-mineralise, compensate for polymerisation shrinkage, release anti-bacterial agents, and also exhibit good mechanical strength. Also, future research has to be done to idealise the proper mixing technique in order to minimise the porosities.

5.2 Summary

Forming dental composites that are able to enhance remineralisation and provide antibacterial release would be beneficial for many dental situations. This project aim was to produce such a material. It could be beneficial for many patients especially children and anxious adults because less teeth preparation may be needed.

So, this thesis describes the aetiology and histopathology of dental caries. As well it included a description of dental management of caries, restorative materials, and commercial composite. A brief summary of the procedures and work done to formulate the new composite materials that is able to re-mineralise, compensate for polymerisation shrinkage, and has antibacterial potential. Therefore, it describes how these new formulae will be the future of both caries elimination in a conservative manner and a more durable antibacterial re-mineralising restorative material with superior properties than any other conventional materials.

Chapter VI

References

Agras, S., Sylvester, D. & Oliveau, D. 1969. The epidemiology of common fears and phobia. *Comprehensive psychiatry,* 10**,** 151-156.

Ahmad Salimi, M. N. 2013. *Systematic investigations of calcium phosphates produced by wet chemistry method and supercritical processing techniques.* University of Birmingham.

Ambjörnsson, H. A., Schenzel, K. & Germgård, U. 2013. Carboxymethyl cellulose produced at different mercerization conditions and characterized by NIR FT Raman spectroscopy in combination with multivariate analytical methods. *BioResources,* 8**,** 1918-1932.

Andor.com,. 'Raman Spectroscopy - An Introduction To Raman Spectroscopy'. N.p., 2015. Web. 18 Sept. 2015.

Antonucci, J. M., Fowler, B. O., Weir, M. D., Skrtic, D. & Stansbury, J. W. 2008. Effect of ethyl-α-hydroxymethylacrylate on selected properties of copolymers and ACP resin composites. *Journal of Materials Science: Materials in Medicine,* 19**,** 3263-3271.

Anusavice, K. J., Phillips, R. W., Shen, C. & Rawls, H. R. 2012. *Phillips' science of dental materials*, Elsevier Health Sciences.

Aoba, T. 2004. Solubility properties of human tooth mineral and pathogenesis of dental caries. *Oral diseases,* 10**,** 249-257.

Arsov, L. D., Kormann, C. & Plieth, W. 1991. In situ Raman spectra of anodically formed titanium dioxide layers in solutions of H 2 SO 4, KOH, and HNO 3. *Journal of The Electrochemical Society,* 138**,** 2964-2970.

Becker, P. 1989. *Phosphates and phosphoric acid: raw materials, technology, and economics of the wet process. revised and expanded*, Marcel Dekker, Inc.

Benji 2008. Study on the Antimicrobial Activity of ε-Polylysine and Application on Livestock Products Preservation. *In:* Sung, L. (ed.) *Agricultural Products Processing and Storage Engineering.* Sichuan Agricultural University.

Berkovitz, B. K. B., Holland, G. R. & Moxham, B. J. 2002. *Oral anatomy, embryology and histology*, Mosby.

Bermudez, O., Boltong, M., Driessens, F. & Planell, J. 1994a. Development of some calcium phosphate cements from combinations of α-TCP, MCPM and CaO. *Journal of Materials Science: Materials in Medicine,* 5**,** 160-163.

Bermudez, O., Boltong, M., Driessens, F. & Planell, J. 1994b. Optimization of a calcium orthophosphate cement formulation occurring in the combination of monocalcium phosphate monohydrate with calcium oxide. *Journal of Materials Science: Materials in Medicine,* 5**,** 67-71.

Bernardo, M., Luis, H., Martin, M. D., Leroux, B. G., Rue, T., Leitão, J. & DeRouen, T. A. 2007. Survival and reasons for failure of amalgam versus composite posterior restorations placed in a randomized clinical trial. *J Am Dent Assoc,* 138**,** 775-83.

Berry, T. G., Summitt, J. B., Chung, A. K. & Osborne, J. W. 1998. Amalgam at the new millennium. *The Journal of the American Dental Association,* 129**,** 1547-1556.

Bjorndal, L., Darvann, T. & Lussi, A. 1999. A computerized analysis of the relation between the occlusal enamel caries lesion and the demineralized dentin. *European journal of oral sciences,* 107**,** 176-182.

Bjørndal, L. & Thylstrup, A. 2007. A structural analysis of approximal enamel caries lesions and subjacent dentin reactions. *European Journal of Oral Sciences,* 103**,** 25-31.

Boaro, L. C., Gonçalves, F., Guimarães, T. C., Ferracane, J. L., Pfeifer, C. S. & Braga, R. R. 2013. Sorption, solubility, shrinkage and mechanical properties of "low-shrinkage" commercial resin composites. *Dental Materials,* 29**,** 398-404.

Bolin, A.-K. 1996. Children's dental health in Europe. An epidemiological investigation of 5-and 12-year-old children from eight EU countries. *Swedish dental journal. Supplement,* 122**,** 1-88.

Brown, P. W. 1987. *Cements Research Progress: 1986*.

Burke, F., Cheung, S. W., Mjör, I. & Wilson, N. 1999. Restoration longevity and analysis of reasons for the placement and replacement of restorations provided by vocational dental practitioners and their trainers in the United Kingdom. *Quintessence international (Berlin, Germany: 1985),* 30**,** 234-242.

Carrier, D. & Pézolet, M. 1984. Raman spectroscopic study of the interaction of poly-L-lysine with dipalmitoylphosphatidylglycerol bilayers. *Biophysical journal,* 46**,** 497.

Carvalho, J. C., Thylstrup, A. & Ekstrand, K. R. 1992. Results after 3 years of non-operative occlusal caries treatment of erupting permanent first molars. *Community dentistry and Oral Epidemiology,* 20**,** 187-192.

Cheng, L., Weir, M. D., Limkangwalmongkol, P., Hack, G. D., Xu, H. H., Chen, Q. & Zhou, X. 2012a. Tetracalcium phosphate composite containing quaternary ammonium dimethacrylate with anti-bacterial properties. *Journal of Biomedical Materials Research Part B: Applied Biomaterials,* 100**,** 726-734.

Cheng, L., Weir, M. D., Xu, H. H., Antonucci, J. M., Kraigsley, A. M., Lin, N. J., Lin-Gibson, S. & Zhou, X. 2012b. Anti-bacterial amorphous calcium phosphate nanocomposites with a quaternary ammonium dimethacrylate and silver nanoparticles. *Dental Materials,* 28**,** 561-572.

Cheng, L., Weir, M. D., Xu, H. H., Kraigsley, A. M., Lin, N. J., Lin-Gibson, S. & Zhou, X. 2012c. Anti-bacterial and physical properties of calcium–phosphate and calcium–fluoride nanocomposites with chlorhexidine. *Dental Materials,* 28**,** 573-583.

Combes, C. & Rey, C. 2010. Amorphous calcium phosphates: synthesis, properties and uses in biomaterials. *Acta biomaterialia,* 6**,** 3362-3378.

Craig, R. G. 1997. *Restorative Dental Materials: Edited [and Selected] by Robert G. Craig, Marcus L. Ward*, Mosby.

Craig, R. G., William Joseph, O. B. & Powers, J. M. 2004. *Dental materials: properties and manipulation*, Mosby.

Crall, J. & Bjerga, J. 1987. Effects of DCPD/APF application and prolonged exposure to fluoride on caries-like lesion formation in vitro. *Journal of Oral Pathology & Medicine,* 16**,** 488-491.

de Souza Costa, C. A., Lopes do Nascimento, A. B., Teixeira, H. M. & Fontana, U. F. 2001. Response of human pulps capped with a self-etching adhesive system. *Dental Materials,* 17**,** 230-240.

Dickens, S. H., Flaim, G. M. & Takagi, S. 2003. Mechanical properties and biochemical activity of remineralizing resin-based Ca–PO< sub> 4</sub> cements. *Dental Materials,* 19**,** 558-566.

Dickens, S. H., Kelly, S. R., Flaim, G. M. & Giuseppetti, A. A. 2004. Dentin adhesion and micro-leakage of a resin-based calcium phosphate pulp capping and basing cement. *European journal of oral sciences,* 112**,** 452-457.

Dorozhkin, S. V. 2007. Calcium orthophosphates. *Journal of materials science,* 42**,** 1061-1095.

Dorozhkin, S. V. 2009. Nanodimensional and nanocrystalline apatites and other calcium orthophosphates in biomedical engineering, biology and medicine. *Materials,* 2**,** 1975-2045.

Drummond, J. L. 2008. Degradation, fatigue, and failure of resin dental composite materials. *Journal of Dental Research,* 87**,** 710-719.

El Briak-BenAbdeslam, H., Ginebra, M., Vert, M. & Boudeville, P. 2008. Wet or dry mechanochemical synthesis of calcium phosphates? Influence of the water content on DCPD–CaO reaction kinetics. *Acta biomaterialia,* 4**,** 378-386.

El-Mowafy, O. 2001. The use of resin cements in restorative dentistry to overcome retention problems. *Journal-canadian dental association,* 67**,** 97-102.

Elliott, J. C. 1994. Structure and chemistry of the apatites and other calcium orthophosphates. *Studies in organic chemistry*.

Fazel-Rezai, R. 2011. Biomedical Engineering–Frontiers and Challenges. InTech publisher, Rijeka, Croatia.

Featherstone, J. 2009. Remineralization, the natural caries repair process—the need for new approaches. *Advances in Dental Research,* 21**,** 4-7.

Fejerskov, O., Manji, F. & Bader, J. D. 1990. Risk assessment in dental caries. *Risk Assessment in Dentistry. Chapel Hill, University of North Carolina Dental Ecology***,** 215-217.

Fejerskov, O. & Thylstrup, A. 1994. Different concepts of dental caries and their implications. *Textbook of clinical cariology,* 2.

Feng, W., Mu-Sen, L., Yu-Peng, L. & Yong-Xin, Q. 2005. A simple sol–gel technique for preparing hydroxyapatite nanopowders. *Materials Letters,* 59**,** 916-919.

Ferraz, M., Monteiro, F. & Manuel, C. 2004. Hydroxyapatite nanoparticles: A review of preparation methodologies. *Journal of Applied Biomaterials and Biomechanics,* 2**,** 74-80.

Floyd, C. J. E. & Dickens, S. H. 2006. Network structure of Bis-GMA-and UDMA-based resin systems. *Dental Materials,* 22**,** 1143-1149.

Furuse, A. Y., Mondelli, J. & Watts, D. C. 2011. Network structures of Bis-GMA/TEGDMA resins differ in DC, shrinkage-strain, hardness and optical properties as a function of reducing agent. *Dental Materials,* 27**,** 497-506.

Fusayama, T., Nakamura, M., Kurosaki, N. & Iwaku, M. 1979. Non-pressure adhesion of a new adhesive restorative resin. *Journal of dental research,* 58**,** 1364-1370.

Gao, X., Fan, Y., Kent, R., Van Houte, J. & Margolis, H. 2001. Association of caries activity with the composition of dental plaque fluid. *Journal of dental research,* 80**,** 1834-1839.

Garcia, C. S., Abedin, M. N., Sharma, S. K., Misra, A. K., Ismail, S., Singh, U. N., Refaat, T. F., Elsayed-Ali, H. E. & Sandford, S. P. Remote pulsed laser Raman spectroscopy system for detecting water, ice, and hydrous minerals. SPIE Optics+ Photonics, 2006. International Society for Optics and Photonics, 630215-630215-7.

Gerritsen, A. E., Allen, P. F., Witter, D. J., Bronkhorst, E. M. & Creugers, N. 2010. Tooth loss and oral health-related quality of life: a systematic review and meta-analysis. *Health Qual Life Outcomes,* 8**,** 552.

Gerzina, T. M. & Hume, W. R. 1996. Diffusion of monomers from bonding resin-resin composite combinations through dentine< i> in vitro</i>. *Journal of dentistry,* 24**,** 125-128.

Ginebra, M., Fernandez, E., De Maeyer, E., Verbeeck, R., Boltong, M., Ginebra, J., Driessens, F. & Planell, J. 1997. Setting reaction and hardening of an apatitic calcium phosphate cement. *Journal of dental research,* 76**,** 905-912.

Ginebra, M., Traykova, T. & Planell, J. 2006. Calcium phosphate cements as bone drug delivery systems: a review. *Journal of Controlled Release,* 113**,** 102-110.

Gregory, T. 1974. Solubility of β-Ca_3 (PO_4) _2 in the system Ca (OH) _2-H_3PO_4-H_2O at 5, 15, 25, and 37°C. *J Res Nat Bur Stand,* 78**,** 667-674.

Grotzky, A., Manaka, Y., Fornera, S., Willeke, M. & Walde, P. 2010. Quantification of α-polylysine: a comparison of four UV/Vis spectrophotometric methods. *Analytical Methods,* 2**,** 1448-1455.

Görücü, J., Tiritoglu, M. & Ozgünaltay, G. 1997. Effects of preparation designs and adhesive systems on retention of class II amalgam restorations. *The Journal of prosthetic dentistry,* 78**,** 250-254.

Hai-tao, N. Q.-y. L. Y. Z. 2008. Study on Anti-bacterial Action of ε-Poly-L-lysine and Its Application in Preservation of Sliver Carp Surimi. *the food science,* 29**,** 9.

Hench, L. L., Wilson, J., McLaren, M. & Niesz, D. 1993. *An introduction to bioceramics*, World Scientific Singapore.

Hiraki 2000. ε-Polylysine, its development and utilization. *Fine chem,* 29**,** 18-25.

Hiraki, J. & Suzuki, E. 1999. Process for producing ε-poly-L-lysine with immobilized Streptomyces albulus. Google Patents.

Hirayama, C., Sakata, M., Nakamura, M., Ihara, H., Kunitake, M. & Todokoro, M. 1999. Preparation of poly (ε-lysine) adsorbents and application to selective removal of lipopolysaccharides. *Journal of Chromatography B: Biomedical Sciences and Applications,* 721**,** 187-195.

Holmen, L., Thylstrup, A., Øgaard, B. & Kragh, F. 1985. A polarized light microscopic study of progressive stages of enamel caries in vivo. *Caries Research,* 19**,** 348-354.

Huang, C., Tay, F., Cheung, G., Kei, L., Wei, S. & Pashley, D. 2002. Hygroscopic expansion of a compomer and a composite on artificial gap reduction. *Journal of dentistry,* 30**,** 11-19.

Huang, G. T. J. 2011. Dental Pulp and Dentin Tissue Engineering and Regeneration–Advancement and Challenge. *Frontiers in Bioscience (Elite Edition),* 3**,** 788.

Imazato, S. 2003. Anti-bacterial properties of resin composites and dentin bonding systems. *Dental Materials,* 19**,** 449-457.

Innes, N., Evans, D. & Stirrups, D. 2011. Sealing caries in primary molars randomized control trial, 5-year results. *Journal of dental research,* 90**,** 1405-1410.

Ismail, A. I., Sohn, W., Tellez, M., Amaya, A., Sen, A., Hasson, H. & Pitts, N. B. 2007. The International Caries Detection and Assessment System (ICDAS): an integrated system for measuring dental caries. *Community dentistry and oral epidemiology,* 35**,** 170-178.

Jalota, S., Tas, A. C. & Bhaduri, S. B. 2005. Synthesis of HA-Seeded TTCP (Ca4 (PO4) 2O) Powders at 1230° C from Ca (CH3COO) 2· H2O and NH4H2PO4. *Journal of the American Ceramic Society,* 88**,** 3353-3360.

Jandt, K., Mills, R., Blackwell, G. & Ashworth, S. 2000. Depth of cure and compressive strength of dental composites cured with blue light emitting diodes (LEDs). *Dental Materials,* 16**,** 41-47.

Johnson, N. W., Taylor, B. R. & Berman, D. S. 1969. The response of deciduous dentine to caries studied by correlated light and electron microscopy. *Caries Research,* 3**,** 348-368.

Jurado, J., Vargas-Hernández, C. & Vargas, R. 2012. Raman and structural studies on the high-temperature regime of the KH2PO4-NH4H2PO4 system. *Rev. Mex. Fis,* 58**,** 411-416.

Kidd, E. A. M. & Fejerskov, O. 2004. What constitutes dental caries? Histopathology of carious enamel and dentin related to the action of cariogenic biofilms. *Journal of dental research,* 83**,** C35-C38.

Kirkevang, L.-L., Væth, M. & Wenzel, A. 2011. Incidence of caries lesions in approximal surfaces: A radiographic study of a general adult Danish population. *Caries research,* 45**,** 538-546.

Koulourides, T., Keller, S. E., Manson-Hing, L. & Lilley, V. 1980. Enhancement of fluoride effectiveness by experimental cariogenic priming of human enamel. *Caries research,* 14**,** 32-39.

Koutsoukos, P. & Nancollas, G. 1981. Crystal growth of calcium phosphates-epitaxial considerations. *Journal of crystal Growth,* 53**,** 10-19.

la Rubia García, C. G. 2012. SPEED OF SOUND MEASUREMENTS IN AMMONIA AND IONIC LIQUIDS.

LARSEN, M. J. & FEJERKOV, O. 1989. Chemical and structural challenges in remineralization of dental enamel lesions. *European Journal of Oral Sciences,* 97**,** 285-296.

Lee, D. D., Tofighi, A., Aiolova, M., Chakravarthy, P., Catalano, A., Majahad, A. & Knaack, D. 1999. [alpha]-BSM (R): A Biomimetic Bone Substitute and Drug Delivery Vehicle. *Clinical orthopaedics and related research,* 367**,** S396-S405.

Lee, S. Y., Regnault, W., Antonucci, J. & Skrtic, D. 2007. Effect of particle size of an amorphous calcium phosphate filler on the mechanical strength and ion release of polymeric composites. *Journal of Biomedical Materials Research Part B: Applied Biomaterials,* 80**,** 11-17.

Lee, T. Y., Guymon, C. A., Jönsson, E. S. & Hoyle, C. E. 2004. The effect of monomer structure on oxygen inhibition of (meth) acrylates photopolymerization. *Polymer,* 45**,** 6155-6162.

LeGeros, R. & LeGeros, J. Dense hydroxyapatite, Hench LL, Wilson J., An introduction to bioceramics, 1993, 139-180. World Scientific, Singapore.

LeGeros, R. Z. 1985. Preparation of octacalcium phosphate (OCP): a direct fast method. *Calcified tissue international,* 37**,** 194-197.

LeGeros, R. Z. 1990. Calcium phosphates in oral biology and medicine. *Monographs in oral science,* 15**,** 1-201.

Leung, D., Spratt, D. A., Pratten, J., Gulabivala, K., Mordan, N. J. & Young, A. M. 2005. Chlorhexidine-releasing methacrylate dental composite materials. *Biomaterials,* 26**,** 7145-7153.

Levine, R. S. 1974. The microradiographic features of dentine caries. Observations on 200 lesions. *British Dental Journal,* 137**,** 301-306.

Li, X., Wang, Q., Sun, X., Fan, X. & Han, X. 2012. The hydrophilic finishing of wool fabric via mTGase-catalyzed grafting of?-PLL. *International Journal of Clothing Science and Technology,* 24**,** 317-327.

Lu, X. & Leng, Y. 2005. Theoretical analysis of calcium phosphate precipitation in simulated body fluid. *Biomaterials,* 26**,** 1097-1108.

Lynn, A. & Bonfield, W. 2005. A novel method for the simultaneous, titrant-free control of pH and calcium phosphate mass yield. *Accounts of chemical research,* 38**,** 202-207.

Manji, F., Fejerskov, O., Nagelkerke, N. J. D. & Baelum, V. 1991. A random effects model for some epidemiological features of dental caries. *Community dentistry and oral epidemiology,* 19**,** 324-328.

Marculescu, L. 1974. Impurity-induced Raman spectra of KCl: Pb crystals. *Journal of Physics C: Solid State Physics,* 7**,** 2387.

Massler, M. 1967. Pulpal reactions to dental caries. *International dental journal,* 17**,** 441.

McKnight-Hanes, C. & Whitford, G. 1992. Fluoride release from three glass ionomer materials and the effects of varnishing with or without finishing. *Caries research,* 26**,** 345-350.

Mehdawi, I., Neel, E. A. A., Valappil, S. P., Palmer, G., Salih, V., Pratten, J., Spratt, D. A. & Young, A. M. 2009. Development of remineralizing, anti-bacterial dental materials. *Acta Biomaterialia,* 5**,** 2525-2539.

Mehdawi, I. & Young, A. 2012. Anti-bacterial composite restorative materials for dental applications. *Non-Metallic Biomaterials for Tooth Repair and Replacement***,** 270-293.

Mejdoubi, E., Lacout, J., Heughebaert, J. & Michaud, P. 1994. Optimization of a hydraulic calcium phosphate cement. *Advanced Materials Research,* 1**,** 163-172.

Melo, M. A., Guedes, S. F., Xu, H. H. & Rodrigues, L. K. 2013. Nanotechnology-based restorative materials for dental caries management. *Trends in biotechnology,* 31**,** 459-467.

Mercuryconvention.org,. 'Minamata Convention On Mercury > Home'. N.p., 2015. Web. 13 July 2015.

Miao, X., Hu, Y., Liu, J. & Wong, A. 2004. Porous calcium phosphate ceramics prepared by coating polyurethane foams with calcium phosphate cements. *Materials Letters,* 58**,** 397-402.

Mirtchi, A. A., Lemaître, J. & Munting, E. 1990. Calcium phosphate cements: study of the β-tricalcium phosphate—dicalcium phosphate—calcite cements. *Biomaterials,* 11**,** 83-88.

Mitchell, L. & Mitchell, D. A. 2009. *Oxford handbook of clinical dentistry*, OUP Oxford.

Mjor, I. A. & Toffenetti, F. 2000. Secondary caries: a literature review with case reports. *Quintessence international-english edition-,* 31**,** 165-180.

Morra, M. 1993. Acid-base properties of adhesive dental polymers. *Dental Materials,* 9**,** 375-378.

Moszner, N. & Salz, U. 2007. Recent developments of new components for dental adhesives and composites. *Macromolecular Materials and Engineering,* 292**,** 245-271.

Nelson, S. J. 2009. *Wheeler's Dental Anatomy, Physiology and Occlusion-E-Book*, Saunders.

Nicholson, J. W. 2007. Polyacid-modified composite resins ("compomers") and their use in clinical dentistry. *Dental materials,* 23**,** 615-622.

O'Neil, M. J. 2013. *The Merck index: an encyclopedia of chemicals, drugs, and biologicals*, RSC Publishing.

Odian, G. G. & Odian, G. 2004. *Principles of polymerization*, Wiley-Interscience New York.

Oliveira, C., Ferreira, A. & Rocha, F. 2007. Dicalcium phosphate dihydrate precipitation: characterization and crystal growth. *Chemical Engineering Research and Design,* 85**,** 1655-1661.

Örtengren, U., Wellendorf, H., Karlsson, S. & Ruyter, I. 2001. Water sorption and solubility of dental composites and identification of monomers released in an aqueous environment. *Journal of Oral Rehabilitation,* 28**,** 1106-1115.

Øysæd, H. & Ruyter, I. 1986. Water sorption and filler characteristics of composites for use in posterior teeth. *Journal of Dental Research,* 65**,** 1315-1318.

Pierre, P. S. 1955. The Preparation of Dicalcium Phosphate Dihydrate and Calcium Pyrophosphate. *Journal of the American Chemical Society,* 77**,** 2197-2198.

Piwowarczyk, A., Ottl, P., Lauer, H. C. & Büchler, A. 2002. Laboratory strength of glass ionomer cement, compomers, and resin composites. *Journal of Prosthodontics,* 11**,** 86-91.

Poorsattar Bejeh Mir, A. & Poorsattar Bejeh Mir, M. 2012. How does duration of curing affect the radiopacity of dental materials? *Imaging science in dentistry,* 42**,** 89-93.

Ratledge, D. K., Kidd, E. A. M. & Beighton, D. 2001. A clinical and microbiological study of approximal carious lesions. Part 2: Efficacy of caries removal following tunnel and Class II cavity preparations. *Caries Research,* 35**,** 8-11.

Regnault, W. F., Icenogle, T. B., Antonucci, J. M. & Skrtic, D. 2008. Amorphous calcium phosphate/urethane methacrylate resin composites. I. Physicochemical characterization. *Journal of Materials Science: Materials in Medicine,* 19**,** 507-515.

Reichl, F.-X., Simon, S., Esters, M., Seiss, M., Kehe, K., Kleinsasser, N. & Hickel, R. 2006. Cytotoxicity of dental composite (co) monomers and the amalgam component Hg2+ in human gingival fibroblasts. *Archives of toxicology,* 80**,** 465-472.

Reynolds, E. 2009. Casein phosphopeptide-amorphous calcium phosphate: the scientific evidence. *Advances in Dental Research,* 21**,** 25-29.

Rhee, S.-H. 2002. Synthesis of hydroxyapatite via mechanochemical treatment. *Biomaterials,* 23**,** 1147-1152.

Ricketts, D., Kidd, E., Innes, N. & Clarkson, J. E. 2006. Complete or ultraconservative removal of decayed tissue in unfilled teeth. *The Cochrane Library*.

Rugg-Gunn, A. 2013. Dental Caries: Strategies to control this preventable disease. *Acta medica academica,* 42**,** 117.

Rüttermann, S., Alberts, I., Raab, W. H. & Janda, R. R. 2011. Physical properties of self-, dual-, and light-cured direct core materials. *Clinical oral investigations,* 15**,** 597-603.

Rüttermann, S., Krüger, S., Raab, W. H.-M. & Janda, R. 2007. Polymerization shrinkage and hygroscopic expansion of contemporary posterior resin-based filling materials—a comparative study. *Journal of dentistry,* 35**,** 806-813.

Sakaguchi, R. & Powers, J. 2012a. Restorative materials–ceramics. *Craig's restorative dental materials (13th ed.), Elsevier Mosby, Philadelphia***,** 253-275.

Sakaguchi, R. L. & Powers, J. M. 2012b. *Craig's restorative dental materials*, Elsevier Health Sciences.

Schedle, A., Franz, A., Rausch-Fan, X., Spittler, A., Lucas, T., Samorapoompichit, P., Sperr, W. & Boltz-Nitulescu, G. 1998. Cytotoxic effects of dental composites, adhesive substances, compomers and cements. *Dental Materials,* 14**,** 429-440.

Scherrer, S. S., Cesar, P. F. & Swain, M. V. 2010. Direct comparison of the bond strength results of the different test methods: a critical literature review. *Dental Materials,* 26**,** e78-e93.

Schmalz, G. & Arenholt-Bindslev, D. 2009. *Biocompatibility of dental materials*, Springer.

Scully, C. & Al-Bayaty, H. 2002. *Oxford handbook of applied dental sciences*, Oxford University Press.

Shami, a. a. a. 2014. *DEVELOPMENT OF A NOVEL ANTI-BACTERIAL AND REMINERALISING DENTAL COMPOSITE FOR PAEDIATRIC DENTISTRY.* ddent, university college london.

Sheiham, A. 2005. Oral health, general health and quality of life. *Bulletin of the World Health Organization,* 83**,** 644-644.

Sheiham, A. 2006. Dental caries affects body weight, growth and quality of life in pre-school children. *British dental journal,* 201**,** 625-626.

Shelton, R., Liu, Y., Cooper, P., Gbureck, U., German, M. & Barralet, J. 2006. Bone marrow cell gene expression and tissue construct assembly using octacalcium phosphate microscaffolds. *Biomaterials,* 27**,** 2874-2881.

Shi, D. 2004. *Biomaterials and tissue engineering*, 清华大学出版社有限公司.

Shih, I.-L., Shen, M.-H. & Van, Y.-T. 2006. Microbial synthesis of poly(ε-lysine) and its various applications. *Bioresource Technology,* 97**,** 1148-1159.

Shukla, S. C., Singh, A., Pandey, A. K. & Mishra, A. 2012a. Review on production and medical applications of ε-polylysine. *Biochemical Engineering Journal,* 65**,** 70-81.

Shukla, S. C., Singh, A., Pandey, A. K. & Mishra, A. 2012b. Review on production and medical applications of ε-polylysine. *Biochemical Engineering Journal,* 65**,** 70-81.

Sideridou, I., Achilias, D. S., Spyroudi, C. & Karabela, M. 2004. Water sorption characteristics of light-cured dental resins and composites based on Bis-EMA/PCDMA. *Biomaterials,* 25**,** 367-376.

Sigmaaldrich.com,. 'Methyl 4-Hydroxybenzoate, Food And Flavor Ingredient, FEMA No 2710 | Sigma-Aldrich'. N.p., 2015. Web. 13 July 2015.

Silverstone, L. M. 1973. Structure of carious enamel, including the early lesion. *Oral sciences reviews,* 3**,** 100.

Skrtic, D. & Antonucci, J. 2007. Dental composites based on amorphous calcium phosphate—resin composition/physicochemical properties study. *Journal of biomaterials applications,* 21**,** 375-393.

Skrtic, D., Antonucci, J. & Eanes, E. 2003. AMORPHOUS CALCIUM PHOSPHATE-BASED BIOACTIVE POLYMERIC COMPOSITES FOR MINERALISED TISSUE REGENERATION. *JOURNAL OF RESEARCH-NATIONAL INSTITUTE OF STANDARDS AND TECHNOLOGY,* 108**,** 167-182.

Skrtic, D., Antonucci, J., Eanes, E. & Eidelman, N. 2004. Dental composites based on hybrid and surface-modified amorphous calcium phosphates. *Biomaterials,* 25**,** 1141-1150.

Skrtic, D., Antonucci, J. M. & Eanes, E. D. 1996. Improved properties of amorphous calcium phosphate fillers in remineralizing resin composites. *Dental Materials,* 12**,** 295-301.

Sonoda, K., Furuzono, T., Walsh, D., Sato, K. & Tanaka, J. 2002. Influence of emulsion on crystal growth of hydroxyapatite. *Solid State Ionics,* 151**,** 321-327.

Sun, L., Berndt, C. C., Gross, K. A. & Kucuk, A. 2001. Material fundamentals and clinical performance of plasma-sprayed hydroxyapatite coatings: A review. *Journal of biomedical materials research,* 58**,** 570-592.

Takagi, S., Chow, L. & Ishikawa, K. 1998. Formation of hydroxyapatite in new calcium phosphate cements. *Biomaterials,* 19**,** 1593-1599.

Theilade, J., Fejerskov, O. & Hørsted, M. 1976. A transmission electron microscopic study of 7-day old bacterial plaque in human tooth fissures. *Archives of oral biology,* 21**,** 587-598.

Thylstrup, A., Bruun, C. & Holmen, L. 1994. In vivo caries models-mechanisms for caries initiation and arrestment. *Advances in Dental Research,* 8**,** 144-157.

Thylstrup, A. & Qvist, V. 1987. Principal enamel and dentine reactions during caries progression. *Dentine and Dentine Reactions in the Oral Cavity. IRL Press.| Oxford***,** 3-16.

Tsujita, T., Sumiyoshi, M., Takaku, T., Momsen, W. E., Lowe, M. E. & Brockman, H. L. 2003. Inhibition of lipases by ε-polylysine. *Journal of lipid research,* 44**,** 2278-2286.

Ulker, H. E. & Sengun, A. 2009. Cytotoxicity evaluation of self adhesive composite resin cements by dentin barrier test on 3D pulp cells. *European journal of dentistry,* 3**,** 120.

Updated by: Ilona Fotek, and the A.D.A.M. Editorial team. 'Tooth Anatomy: Medlineplus Medical Encyclopedia Image'. *Nlm.nih.gov*. N.p., 2015. Web. 13 July 2015.

Uriarte, L. M., Dubessy, J., Boulet, P., Baonza, V. G., Bihannic, I. & Robert, P. 2015. Reference Raman spectra of synthesized CaCl2· nH2O solids (n= 0, 2, 4, 6). *Journal of Raman Spectroscopy*.

Vallittu, P. 2012. *Non-metallic biomaterials for tooth repair and replacement*, Elsevier.

Van Landuyt, K. L., Snauwaert, J., De Munck, J., Peumans, M., Yoshida, Y., Poitevin, A., Coutinho, E., Suzuki, K., Lambrechts, P. & Van Meerbeek, B. 2007. Systematic review of the chemical composition of contemporary dental adhesives. *Biomaterials,* 28**,** 3757-3785.

Van Meerbeek, B., De Munck, J., Mattar, D., Van Landuyt, K. & Lambrechts, P. 2002. Microtensile bond strengths of an etch&rinse and self-etch adhesive to enamel and dentin as a function of surface treatment. *Operative Dentistry,* 28**,** 647-660.

Van Meerbeek, B., De Munck, J., Yoshida, Y., Inoue, S., Vargas, M., Vijay, P., Van Landuyt, K., Lambrechts, P. & Vanherle, G. 2003. Adhesion to enamel and dentin: current status and future challenges. *OPERATIVE DENTISTRY-UNIVERSITY OF WASHINGTON-,* 28**,** 215-235.

Van Noort, R. & Barbour, M. E. 2013. *Introduction to Dental Materials4: Introduction to Dental Materials*, Elsevier Health Sciences.

Vassend, O. 1993. Anxiety, pain and discomfort associated with dental treatment. *Behaviour Research and Therapy,* 31**,** 659-666.

Walter, N. 2015. *RE:* Novel dental restorative materials foNovel dental restorative materials for prevention of micro-leakage*; Anti-microbial, re-mineralising composites with high strength and toughness and low shrinkage.* PhD Thesis in Progress

Wimpenny, J. W. T. 1994. The spatial organisation of biofilm. *Bacterial biofilms and their control in medicine and industry. Wimpenny J, Nichols W, Stickler D, Lappin-Scott H, editors. Bioline***,** 1-5.

Xu, H., Weir, M., Sun, L., Takagi, S. & Chow, L. 2007a. Effects of calcium phosphate nanoparticles on Ca-PO4 composite. *Journal of dental research,* 86**,** 378-383.

Xu, H. H., Sun, L., Weir, M. D., Takagi, S., Chow, L. C. & Hockey, B. 2007b. Effects of incorporating nanosized calcium phosphate particles on properties of whisker-reinforced dental composites. *Journal of Biomedical Materials Research Part B: Applied Biomaterials,* 81**,** 116-125.

Yagci, Y., Jockusch, S. & Turro, N. J. 2010. Photoinitiated polymerization: advances, challenges, and opportunities. *Macromolecules,* 43**,** 6245-6260.

Yengopal, V., Harneker, S. Y., Patel, N. & Siegfried, N. 2009. Dental fillings for the treatment of caries in the primary dentition. *Cochrane Database Syst Rev,* 15.

Yin, X., Stott, M. & Rubio, A. 2003. α-and β-tricalcium phosphate: a density functional study. *Physical Review B,* 68**,** 205205.

Yip, K. & Smales, R. 2012. Oral diagnosis and treatment planning: part 2. Dental caries and assessment of risk. *British dental journal,* 213**,** 59-66.

Young, A. M. & Ho, S. M. 2008. Drug release from injectable biodegradable polymeric adhesives for bone repair. *Journal of Controlled Release,* 127**,** 162-172.

Young, A. M., Rafeeka, S. A. & Howlett, J. A. 2004. FTIR investigation of monomer polymerisation and polyacid neutralisation kinetics and mechanisms in various aesthetic dental restorative materials. *Biomaterials,* 25**,** 823-833.

Zhang, H., Wang, Y., Yan, Y. & Li, S. 2003. Precipitation of biocompatible hydroxyapatite whiskers from moderately acid solution. *Ceramics international,* 29**,** 413-418.

Zhao, J., Liu, Y., Sun, W. & Zhang, H. 2011. Amorphous calcium phosphate and its application in dentistry. *Chem Cent J,* 5**,** 40.

Zimmerli, B., Strub, M., Jeger, F., Stadler, O. & Lussi, A. 2009. Composite materials: composition, properties and clinical applications. A literature review. *Schweizer Monatsschrift fur Zahnmedizin= Revue mensuelle suisse d'odonto-stomatologie= Rivista mensile svizzera di odontologia e stomatologia/SSO,* 120**,** 972-986.

Chapter VII

Appendices

Appendix I

Tables 1 and 2 show the multiple comparison test indicating the significant difference between the mean increase in mass for formulae A, C, G, and H when immersed in SBF and water for 1 week.

Dependent Variable	TEST	(I) group	(J) group	Mean Difference (I-J)	Std. Error	Sig.	95% Confidence Interval	
							Lower Bound	Upper Bound
Mass after 1 week	Bonferroni	G water	G SBF	-1.42000*	.24077	.001	-2.3204	-.5196
			H water	-1.32667*	.24077	.001	-2.2271	-.4262
			H SBF	-2.80000*	.24077	.000	-3.7004	-1.8996
			C water	3.34000*	.24077	.000	2.4396	4.2404
			C SBF	1.74000*	.24077	.000	.8396	2.6404
			A water	4.09667*	.24077	.000	3.1962	4.9971
			A SBF	3.44000*	.24077	.000	2.5396	4.3404
		G SBF	G water	1.42000*	.24077	.001	.5196	2.3204
			H water	.09333	.24077	1.000	-.8071	.9938
			H SBF	-1.38000*	.24077	.001	-2.2804	-.4796
			C water	4.76000*	.24077	.000	3.8596	5.6604
			C SBF	3.16000*	.24077	.000	2.2596	4.0604
			A water	5.51667*	.24077	.000	4.6162	6.4171
			A SBF	4.86000*	.24077	.000	3.9596	5.7604
		H water	G water	1.32667*	.24077	.001	.4262	2.2271
			G SBF	-.09333	.24077	1.000	-.9938	.8071
			H SBF	-1.47333*	.24077	.000	-2.3738	-.5729
			C water	4.66667*	.24077	.000	3.7662	5.5671
			C SBF	3.06667*	.24077	.000	2.1662	3.9671
			A water	5.42333*	.24077	.000	4.5229	6.3238
			A SBF	4.76667*	.24077	.000	3.8662	5.6671
		H SBF	G water	2.80000*	.24077	.000	1.8996	3.7004
			G SBF	1.38000*	.24077	.001	.4796	2.2804
			H water	1.47333*	.24077	.000	.5729	2.3738
			C water	6.14000*	.24077	.000	5.2396	7.0404
			C SBF	4.54000*	.24077	.000	3.6396	5.4404
			A water	6.89667*	.24077	.000	5.9962	7.7971
			A SBF	6.24000*	.24077	.000	5.3396	7.1404

*. The mean difference is significant at the 0.05 level.

Table 1

Dependent Variable	TEST	(I) group	(J) group	Mean Difference (I-J)	Std. Error	Sig.	95% Confidence Interval	
							Lower Bound	Upper Bound
Mass after 1 week	Bonferroni	C water	G water	-3.34000*	.24077	.000	-4.2404	-2.4396
			G SBF	-4.76000*	.24077	.000	-5.6604	-3.8596
			H water	-4.66667*	.24077	.000	-5.5671	-3.7662
			H SBF	-6.14000*	.24077	.000	-7.0404	-5.2396
			C SBF	-1.60000*	.24077	.000	-2.5004	-.6996
			A water	.75667	.24077	.176	-.1438	1.6571
			A SBF	.10000	.24077	1.000	-.8004	1.0004
		C SBF	G water	-1.74000*	.24077	.000	-2.6404	-.8396
			G SBF	-3.16000*	.24077	.000	-4.0604	-2.2596
			H water	-3.06667*	.24077	.000	-3.9671	-2.1662
			H SBF	-4.54000*	.24077	.000	-5.4404	-3.6396
			C water	1.60000*	.24077	.000	.6996	2.5004
			A water	2.35667*	.24077	.000	1.4562	3.2571
			A SBF	1.70000*	.24077	.000	.7996	2.6004
		A water	G water	-4.09667*	.24077	.000	-4.9971	-3.1962
			G SBF	-5.51667*	.24077	.000	-6.4171	-4.6162
			H water	-5.42333*	.24077	.000	-6.3238	-4.5229
			H SBF	-6.89667*	.24077	.000	-7.7971	-5.9962
			C water	-.75667	.24077	.176	-1.6571	.1438
			C SBF	-2.35667*	.24077	.000	-3.2571	-1.4562
			A SBF	-.65667	.24077	.418	-1.5571	.2438
		A SBF	G water	-3.44000*	.24077	.000	-4.3404	-2.5396
			G SBF	-4.86000*	.24077	.000	-5.7604	-3.9596
			H water	-4.76667*	.24077	.000	-5.6671	-3.8662
			H SBF	-6.24000*	.24077	.000	-7.1404	-5.3396
			C water	-.10000	.24077	1.000	-1.0004	.8004
			C SBF	-1.70000*	.24077	.000	-2.6004	-.7996
			A water	.65667	.24077	.418	-.2438	1.5571

*. The mean difference is significant at the 0.05 level.

Table 2

Tables 3 and 4 show the multiple comparison test indicating the significant difference between the mean increase in volume for formulae A, C, G, and H when immersed in SBF and water for 1 week.

Dependent Variable	TEST	(I) group	(J) group	Mean Difference (I-J)	Std. Error	Sig.	95% Confidence Interval	
							Lower Bound	Upper Bound
Volume after 1 week	Bonferroni	G water	G SBF	.28333	.55305	**1.000**	-1.7850	2.3517
			H water	.18000	.55305	1.000	-1.8883	2.2483
			H SBF	2.29667*	.55305	.021	.2283	4.3650
			C water	3.67333*	.55305	.000	1.6050	5.7417
			C SBF	2.60667*	.55305	.007	.5383	4.6750
			A water	6.34000*	.55305	.000	4.2717	8.4083
			A SBF	5.50667*	.55305	.000	3.4383	7.5750
		G SBF	G water	-.28333	.55305	1.000	-2.3517	1.7850
			H water	-.10333	.55305	1.000	-2.1717	1.9650
			H SBF	2.01333	.55305	.062	-.0550	4.0817
			C water	3.39000*	.55305	.000	1.3217	5.4583
			C SBF	2.32333*	.55305	.019	.2550	4.3917
			A water	6.05667*	.55305	.000	3.9883	8.1250
			A SBF	5.22333*	.55305	.000	3.1550	7.2917
		H water	G water	-.18000	.55305	1.000	-2.2483	1.8883
			G SBF	.10333	.55305	1.000	-1.9650	2.1717
			H SBF	2.11667*	.55305	.042	.0483	4.1850
			C water	3.49333*	.55305	.000	1.4250	5.5617
			C SBF	2.42667*	.55305	.013	.3583	4.4950
			A water	6.16000*	.55305	.000	4.0917	8.2283
			A SBF	5.32667*	.55305	.000	3.2583	7.3950
		H SBF	G water	-2.29667*	.55305	.021	-4.3650	-.2283
			G SBF	-2.01333	.55305	.062	-4.0817	.0550
			H water	-2.11667*	.55305	.042	-4.1850	-.0483
			C water	1.37667	.55305	.677	-.6917	3.4450
			C SBF	.31000	.55305	1.000	-1.7583	2.3783
			A water	4.04333*	.55305	.000	1.9750	6.1117
			A SBF	3.21000*	.55305	.001	1.1417	5.2783

*. The mean difference is significant at the 0.05 level.

Table 3

Dependent Variable	TEST	(I) group	(J) group	Mean Difference (I-J)	Std. Error	Sig.	95% Confidence Interval	
							Lower Bound	Upper Bound
Volume after 1 week	Bonferroni	C water	G water	-3.67333*	.55305	.000	-5.7417	-1.6050
			G SBF	-3.39000*	.55305	.000	-5.4583	-1.3217
			H water	-3.49333*	.55305	.000	-5.5617	-1.4250
			H SBF	-1.37667	.55305	.677	-3.4450	.6917
			C SBF	-1.06667	.55305	1.000	-3.1350	1.0017
			A water	2.66667*	.55305	.005	.5983	4.7350
			A SBF	1.83333	.55305	.123	-.2350	3.9017
		C SBF	G water	-2.60667*	.55305	.007	-4.6750	-.5383
			G SBF	-2.32333*	.55305	.019	-4.3917	-.2550
			H water	-2.42667*	.55305	.013	-4.4950	-.3583
			H SBF	-.31000	.55305	1.000	-2.3783	1.7583
			C water	1.06667	.55305	1.000	-1.0017	3.1350
			A water	3.73333*	.55305	.000	1.6650	5.8017
			A SBF	2.90000*	.55305	.002	.8317	4.9683
		A water	G water	-6.34000*	.55305	.000	-8.4083	-4.2717
			G SBF	-6.05667*	.55305	.000	-8.1250	-3.9883
			H water	-6.16000*	.55305	.000	-8.2283	-4.0917
			H SBF	-4.04333*	.55305	.000	-6.1117	-1.9750
			C water	-2.66667*	.55305	.005	-4.7350	-.5983
			C SBF	-3.73333*	.55305	.000	-5.8017	-1.6650
			A SBF	-.83333	.55305	1.000	-2.9017	1.2350
		A SBF	G water	-5.50667*	.55305	.000	-7.5750	-3.4383
			G SBF	-5.22333*	.55305	.000	-7.2917	-3.1550
			H water	-5.32667*	.55305	.000	-7.3950	-3.2583
			H SBF	-3.21000*	.55305	.001	-5.2783	-1.1417
			C water	-1.83333	.55305	.123	-3.9017	.2350
			C SBF	-2.90000*	.55305	.002	-4.9683	-.8317
			A water	.83333	.55305	1.000	-1.2350	2.9017

*. The mean difference is significant at the 0.05 level.

Table 4

Appendix II

Table 1 shows the Univariate Analysis of Variance indicating the significant effect of the variables (MCPM, TCP, EPL, and medium) on the maximum increase in mass after 2 weeks.

Source	Type III Sum of Squares	Mean Square	Sig.
Corrected Model	198.506[a]	13.234	.000
tcp	26.403	26.403	.000
mcpm	110.413	110.413	.000
epl	32.341	32.341	.000
medium	7.680	7.680	.000
tcp * mcpm	15.641	15.641	.000
tcp * epl	.030	.030	.496
tcp * medium	.241	.241	.060
mcpm * epl	.000	.000	1.000
mcpm * medium	4.688	4.688	.000
epl * medium	.163	.163	.118
tcp * mcpm * epl	.521	.521	.007
tcp * mcpm * medium	.213	.213	.076
tcp * epl * medium	.101	.101	.216
mcpm * epl * medium	.068	.068	.310
tcp * mcpm * epl * medium	.003	.003	.820
Error	2.027	.063	
Corrected Total	200.533		

a. R Squared = .990 (Adjusted R Squared = .985)

Table 1

Table 2 shows the Univariate Analysis of Variance indicating the significant effect of the variables (MCPM, TCP, EPL) on the maximum increase in mass when immersed in SBF.

Source	Type III Sum of Squares	Mean Square	Sig.
Corrected Model	115.073[a]	16.439	.000
tcp	10.800	10.800	.000
mcpm	80.300	80.300	.000
epl	13.954	13.954	.000
tcp * mcpm	9.754	9.754	.000
tcp * epl	.010	.010	.644
mcpm * epl	.034	.034	.410
tcp * mcpm * epl	.220	.220	.046
Error	.753	.047	
Corrected Total	115.826		

a. R Squared = .993 (Adjusted R Squared = .991)

Table 2

Table 3 shows the Univariate Analysis of Variance indicating the significant effect of the variables (MCPM, TCP, EPL) on the maximum increase in mass when immersed in water.

Source	Type III Sum of Squares	Mean Square	Sig.
Corrected Model	75.753[a]	10.822	.000
tcp	15.844	15.844	.000
mcpm	34.800	34.800	.000
epl	18.550	18.550	.000
tcp * mcpm	6.100	6.100	.000
tcp * epl	.120	.120	.236
mcpm * epl	.034	.034	.524
tcp * mcpm * epl	.304	.304	.068
Error	1.273	.080	
Corrected Total	77.026		

a. R Squared = .983 (Adjusted R Squared = .976)

Table 3

Appendix III

Table 1 shows the Univariate Analysis of Variance indicating the significant effect of the variables (MCPM, TCP, EPL, and medium) on the maximum increase in voume after 2 weeks.

Source	Type III Sum of Squares	Mean Square	Sig.
Corrected Model	259.967[a]	17.331	.000
tcp	6.453	6.453	.000
mcpm	224.468	224.468	.000
epl	.001	.001	.960
medium	.030	.030	.765
tcp * mcpm	13.021	13.021	.000
tcp * epl	1.021	1.021	.088
tcp * medium	3.000	3.000	.005
mcpm * epl	8.003	8.003	.000
mcpm * medium	.608	.608	.184
epl * medium	.908	.908	.107
tcp * mcpm * epl	.083	.083	.619
tcp * mcpm * medium	.188	.188	.456
tcp * epl * medium	.368	.368	.299
mcpm * epl * medium	.963	.963	.097
tcp * mcpm * epl * medium	.853	.853	.118
Error	10.560	.330	
Corrected Total	270.527		

a. R Squared = .961 (Adjusted R Squared = .943)

Table 1

Table 2 shows the Univariate Analysis of Variance indicating the significant effect of the variables (MCPM, TCP, EPL) on the maximum increase in volume when immersed in SBF.

Source	Type III Sum of Squares	Mean Square	Sig.
Corrected Model	116.012[a]	16.573	.000
tcp	.327	.327	.349
mcpm	100.860	100.860	.000
epl	.482	.482	.258
tcp * mcpm	5.042	5.042	.002
tcp * epl	1.307	1.307	.071
mcpm * epl	7.260	7.260	.000
tcp * mcpm * epl	.735	.735	.167
Error	5.607	.350	
Corrected Total	121.618		

a. R Squared = .954 (Adjusted R Squared = .934)

Table 2

Table 3 shows the Univariate Analysis of Variance indicating the significant effect of the variables (MCPM, TCP, EPL) on the maximum increase in volume when immersed in water.

Source	Type III Sum of Squares	Mean Square	Sig.
Corrected Model	143.925[a]	20.561	.000
tcp	9.127	9.127	.000
mcpm	124.215	124.215	.000
epl	.427	.427	.258
tcp * mcpm	8.167	8.167	.000
tcp * epl	.082	.082	.615
mcpm * epl	1.707	1.707	.032
tcp * mcpm * epl	.202	.202	.431
Error	4.953	.310	
Corrected Total	148.878		

a. R a. R Squared = .967 (Adjusted R Squared = .952)

Table 3

Appendix IV

Table 1 shows the Univariate Analysis of Variance indicating the significant effect of the variables (MCPM, TCP, EPL, and medium) on the increase in mass after 12 weeks.

Source	Type III Sum of Squares	Mean Square	Sig.
Corrected Model	152.860[a]	10.191	.000
tcp	30.720	30.720	.000
mcpm	5.603	5.603	.000
epl	39.968	39.968	.000
medium	9.541	9.541	.000
tcp * mcpm	36.750	36.750	.000
tcp * epl	2.521	2.521	.000
tcp * medium	.001	.001	.943
mcpm * epl	6.308	6.308	.000
mcpm * medium	18.008	18.008	.000
epl * medium	.270	.270	.202
tcp * mcpm * epl	.701	.701	.044
tcp * mcpm * medium	.068	.068	.519
tcp * epl * medium	1.080	1.080	.014
mcpm * epl * medium	1.203	1.203	.010
tcp * mcpm * epl * medium	.120	.120	.391
Error	5.087	.159	
Corrected Total	157.947		

a. R Squared = .968 (Adjusted R Squared = .953)

Table 1

Table 2 shows the Univariate Analysis of Variance indicating the significant effect of the variables (MCPM, TCP, EPL, and medium) on the increase in volume after 12 weeks.

Source	Type III Sum of Squares	Mean Square	Sig.
Corrected Model	168.146[a]	11.210	.000
tcp	5.672	5.672	.008
mcpm	120.017	120.017	.000
epl	2.297	2.297	.083
medium	.035	.035	.826
tcp * mcpm	12.100	12.100	.000
tcp * epl	5.135	5.135	.012
tcp * medium	1.435	1.435	.167
mcpm * epl	6.675	6.675	.005
mcpm * medium	.005	.005	.933
epl * medium	8.927	8.927	.001
tcp * mcpm * epl	.585	.585	.373
tcp * mcpm * medium	.017	.017	.879
tcp * epl * medium	.130	.130	.673
mcpm * epl * medium	5.005	5.005	.013
tcp * mcpm * epl * medium	.110	.110	.698
Error	22.987	.718	
Corrected Total	191.133		

a. R Squared = .880 (Adjusted R Squared = .823)

Table 2

Appendix V

Table 1 shows the Univariate Analysis of Variance indicating the significant effect of the variables (MCPM, TCP, EPL, and medium) on the solubility.

Source	Type III Sum of Squares	Mean Square	Sig.
Corrected Model	755.531[a]	50.369	.000
tcp	.542	.542	.324
mcpm	621.360	621.360	.000
epl	42.752	42.752	.000
medium	.200	.200	.547
tcp * mcpm	10.360	10.360	.000
tcp * epl	9.992	9.992	.000
tcp * medium	10.547	10.547	.000
mcpm * epl	37.630	37.630	.000
mcpm * medium	10.735	10.735	.000
epl * medium	1.050	1.050	.173
tcp * mcpm * epl	.317	.317	.449
tcp * mcpm * medium	4.625	4.625	.006
tcp * epl * medium	4.260	4.260	.008
mcpm * epl * medium	.775	.775	.240
tcp * mcpm * epl * medium	.385	.385	.405
Error	17.293	.540	
Corrected Total	772.825		

a. R Squared = .978 (Adjusted R Squared = .967)

Table 1

Table 2 shows the Univariate Analysis of Variance indicating the significant effect of the variables (MCPM, TCP, EPL) on the solubility when immersed in SBF.

Source	Type III Sum of Squares	Mean Square	Sig.
Corrected Model	299.732[a]	42.819	.000
tcp	7.935	7.935	.001
mcpm	234.375	234.375	.000
epl	28.602	28.602	.000
tcp * mcpm	14.415	14.415	.000
tcp * epl	.602	.602	.272
mcpm * epl	13.802	13.802	.000
tcp * mcpm * epl	.002	.002	.953
Error	7.433	.465	
Corrected Total	307.165		

a. R Squared = .976 (Adjusted R Squared = .965)

Table 2

Table 3 shows the Univariate Analysis of Variance indicating the significant effect of the variables (MCPM, TCP, EPL) on the solubility when immersed in water.

Source	Type III Sum of Squares	Mean Square	Sig.
Corrected Model	455.600[a]	65.086	.000
tcp	3.154	3.154	.038
mcpm	397.720	397.720	.000
epl	15.200	15.200	.000
tcp * mcpm	.570	.570	.350
tcp * epl	13.650	13.650	.000
mcpm * epl	24.604	24.604	.000
tcp * mcpm * epl	.700	.700	.302
Error	9.860	.616	
Corrected Total	465.460		

a. R Squared = .979 (Adjusted R Squared = .970)

Table 3

Appendix VI

Table 1 shows the Univariate Analysis of Variance indicating the significant effect of the variables (MCPM, TCP, EPL, and medium) on the water content.

Source	Type III Sum of Squares	Mean Square	Sig.
Corrected Model	899.470[a]	59.965	.000
tcp	15.413	15.413	.000
mcpm	693.120	693.120	.000
epl	146.301	146.301	.000
medium	4.941	4.941	.004
tcp * mcpm	4.563	4.563	.005
tcp * epl	3.101	3.101	.018
tcp * medium	8.501	8.501	.000
mcpm * epl	11.801	11.801	.000
mcpm * medium	.521	.521	.315
epl * medium	.480	.480	.335
tcp * mcpm * epl	.101	.101	.657
tcp * mcpm * medium	4.941	4.941	.004
tcp * epl * medium	1.203	1.203	.131
mcpm * epl * medium	3.630	3.630	.011
tcp * mcpm * epl * medium	.853	.853	.201
Error	16.027	.501	
Corrected Total	915.497		

a. R Squared = .982 (Adjusted R Squared = .974)

Table 1

Table 2 shows the Univariate Analysis of Variance indicating the significant effect of the variables (MCPM, TCP, EPL) on the water content when immersed in SBF.

Source	Type III Sum of Squares	Mean Square	Sig.
Corrected Model	450.266[a]	64.324	.000
tcp	.510	.510	.339
mcpm	365.820	365.820	.000
epl	81.770	81.770	.000
tcp * mcpm	.004	.004	.934
tcp * epl	.220	.220	.526
mcpm * epl	1.170	1.170	.155
tcp * mcpm * epl	.770	.770	.243
Error	8.393	.525	
Corrected Total	458.660		

a. R Squared = .982 (Adjusted R Squared = .974)

Table 2

Table 3 shows the Univariate Analysis of Variance indicating the significant effect of the variables (MCPM, TCP, EPL) on the water content when immersed in water.

Source	Type III Sum of Squares	Mean Square	Sig.
Corrected Model	444.263[a]	63.466	.000
tcp	23.404	23.404	.000
mcpm	327.820	327.820	.000
epl	65.010	65.010	.000
tcp * mcpm	9.500	9.500	.000
tcp * epl	4.084	4.084	.010
mcpm * epl	14.260	14.260	.000
tcp * mcpm * epl	.184	.184	.544
Error	7.633	.477	
Corrected Total	451.896		

a. R Squared = .983 (Adjusted R Squared = .976)

Table 3

Appendix VII

Table 1 shows the Univariate Analysis of Variance indicating the significant effect of the variables (MCPM and TCP) on the EPL release when immersed in water.

Source	Type III Sum of Squares	Mean Square	Sig.
Corrected Model	2389.776[a]	796.592	.044
tcp	708.482	708.482	.094
mcpm	685.669	685.669	.099
tcp * mcpm	329.840	329.840	.238
Error	2325.322	211.393	
Corrected Total	4715.097		

a. R Squared = .507 (Adjusted R Squared = .372)

Table 1

Appendix VIII

Figures 1 and 2 show the factorial analysis of the increase in mass change indicating the percentage effect of each variable. Where V1 is the effect of TCP, V2 is the medium and V3 is the EPL.

Figure 1 is for formula without MCPM, while figure 2 is for formulae with MCPM.

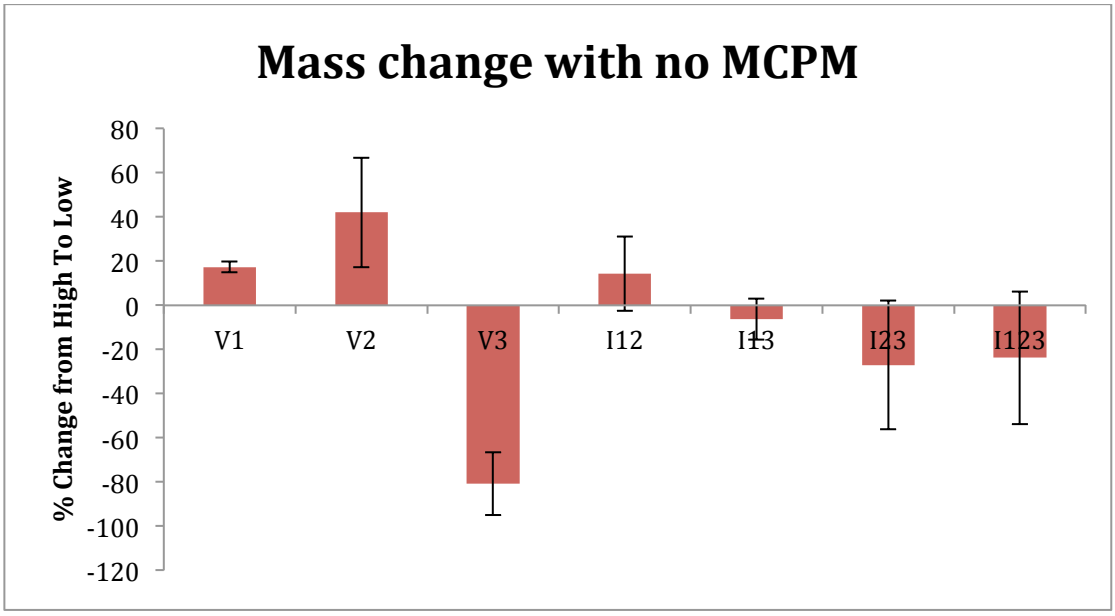

Figure 1

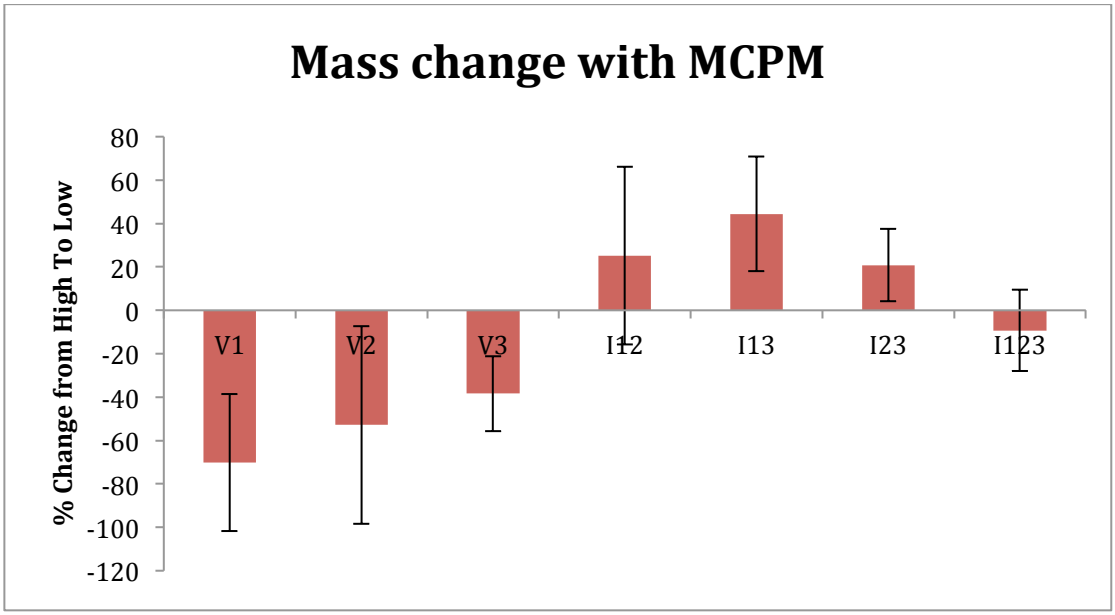

Figure 2

Figures 3 and 4 show the factorial analysis of the increase in mass change indicating the percentage effect of each variable. Where V1 is the effect of TCP, V2 is the MCPM and V3 is the EPL.

Figure 3 is for formula immersed in SBF, while figure 4 is for formulae immersed in water.

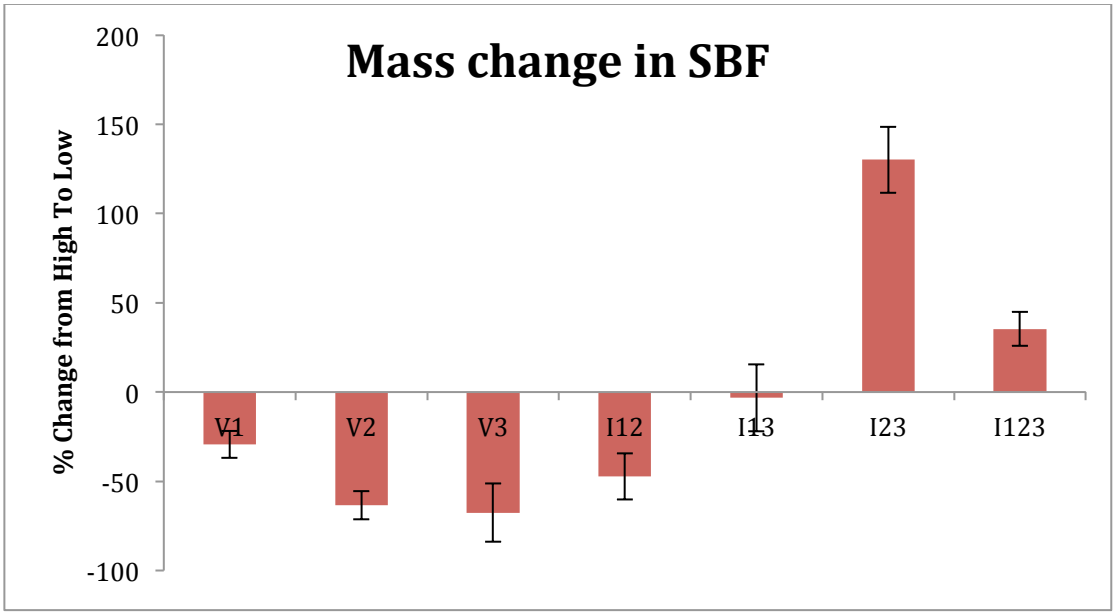

Figure 3

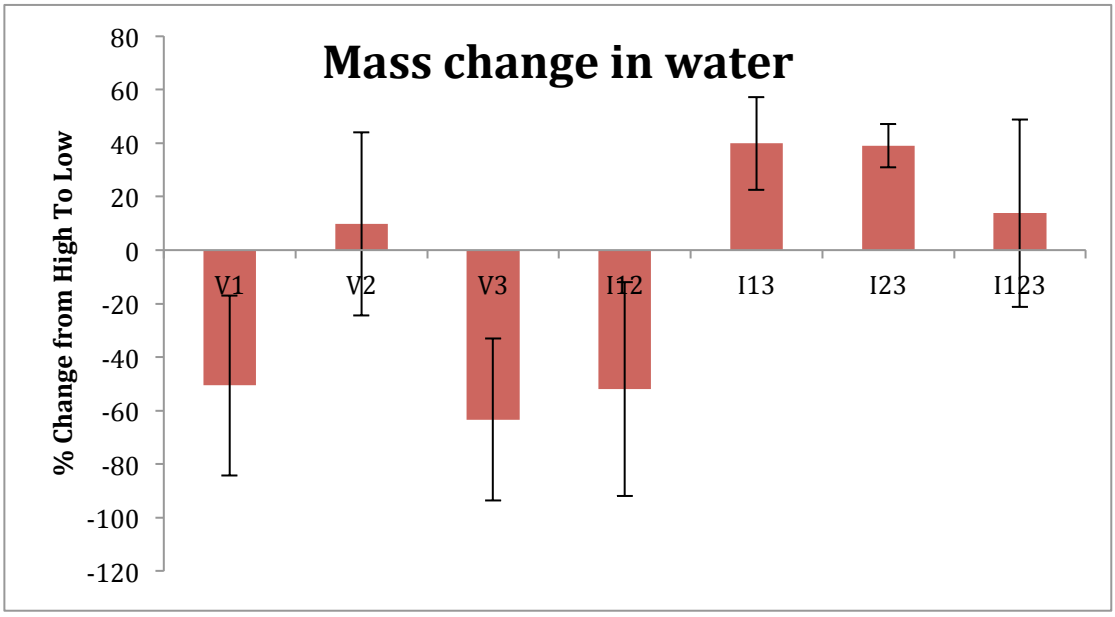

Figure 4

Figures 5 and 6 show the factorial analysis of the increase in volume change indicating the percentage effect of each variable. Where V1 is the effect of TCP, V2 is the MCPM and V3 is the EPL.

Figure 5 is for formula immersed in SBF, while figure 6 is for formulae immersed in water.

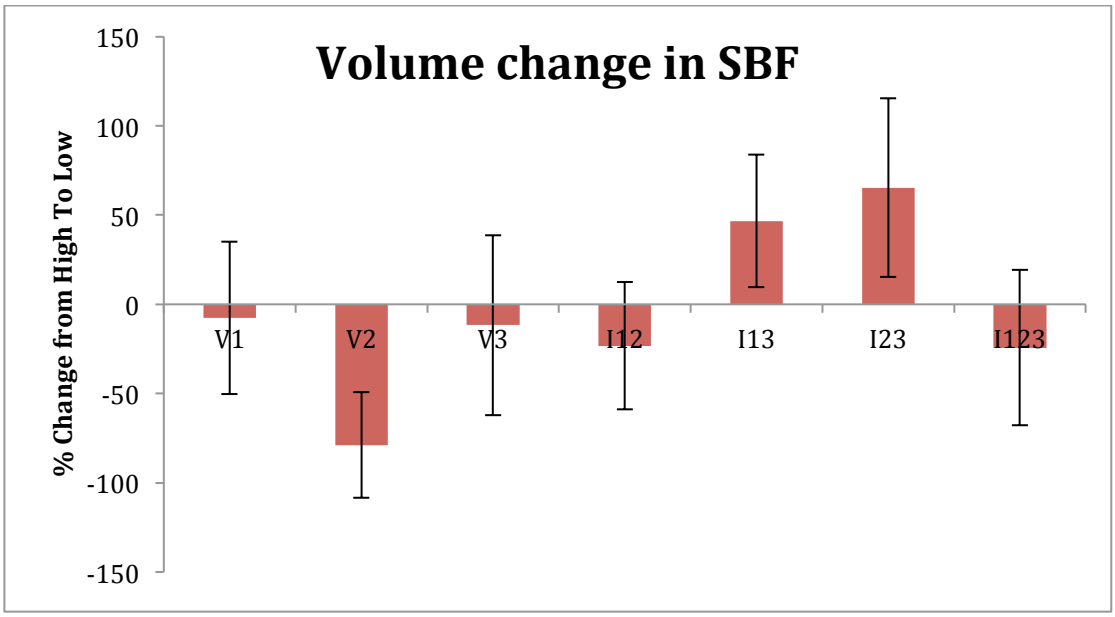

Figure 5

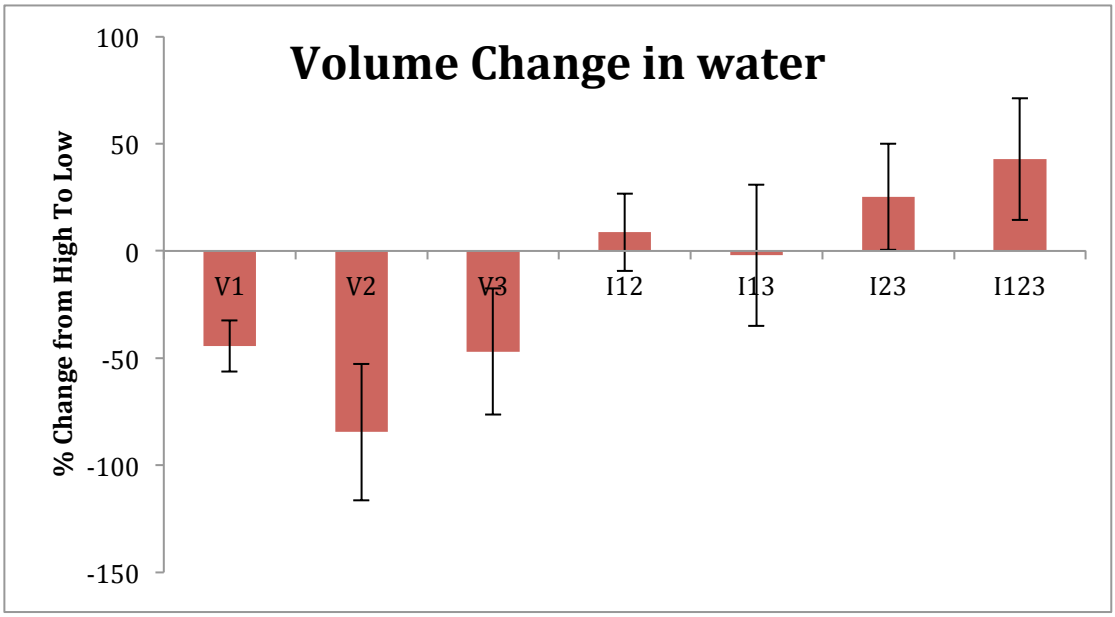

Figure 6

Figures 7 and 8 show the factorial analysis of the solubility of the samples indicating the percentage effect of each variable. Where V1 is the effect of TCP, V2 is the MCPM and V3 is the EPL.

Figure 7 is for formula immersed in SBF, while figure 8 is for formulae immersed in water.

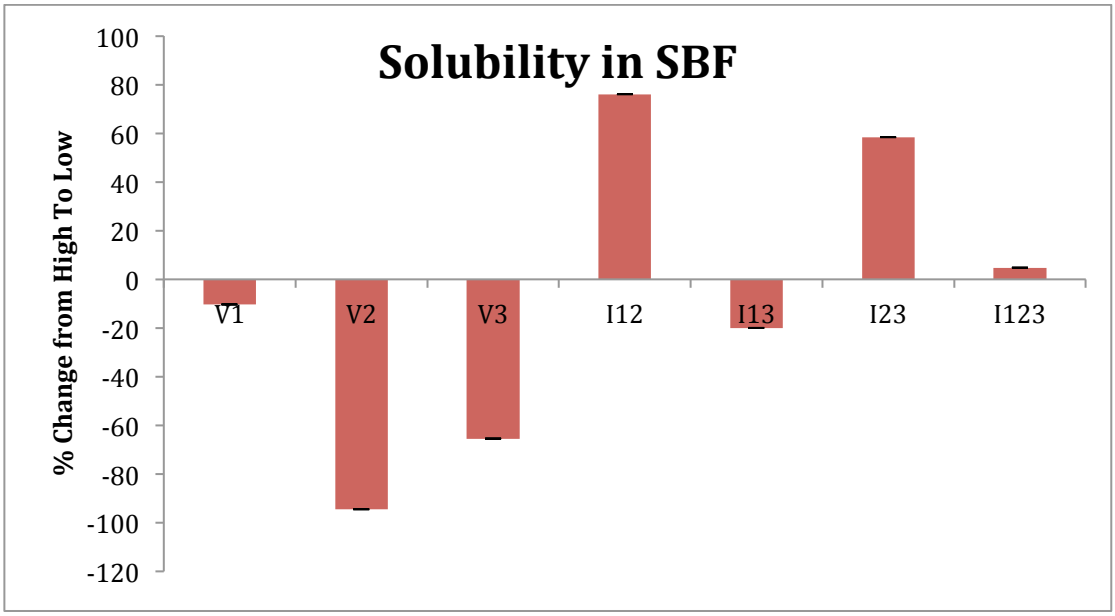

Figure 7

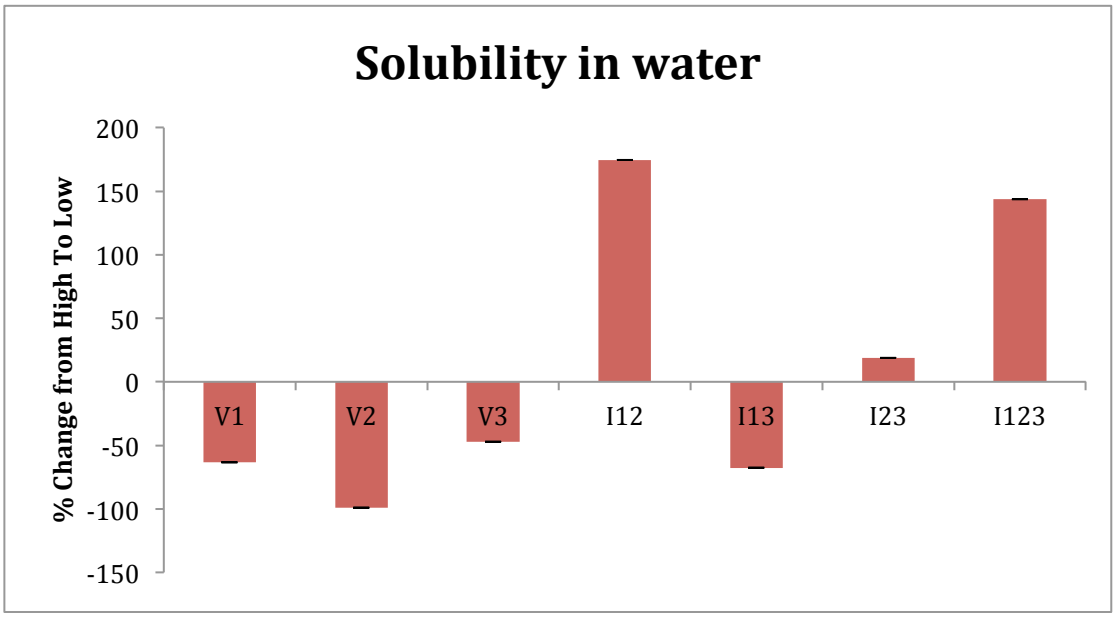

Figure 8

Figures 9 and 10 show the factorial analysis of the water content of the samples indicating the percentage effect of each variable. Where V1 is the effect of TCP, V2 is the MCPM and V3 is the EPL.

Figure 9 is for formula immersed in SBF, while figure 10 is for formulae immersed in water.

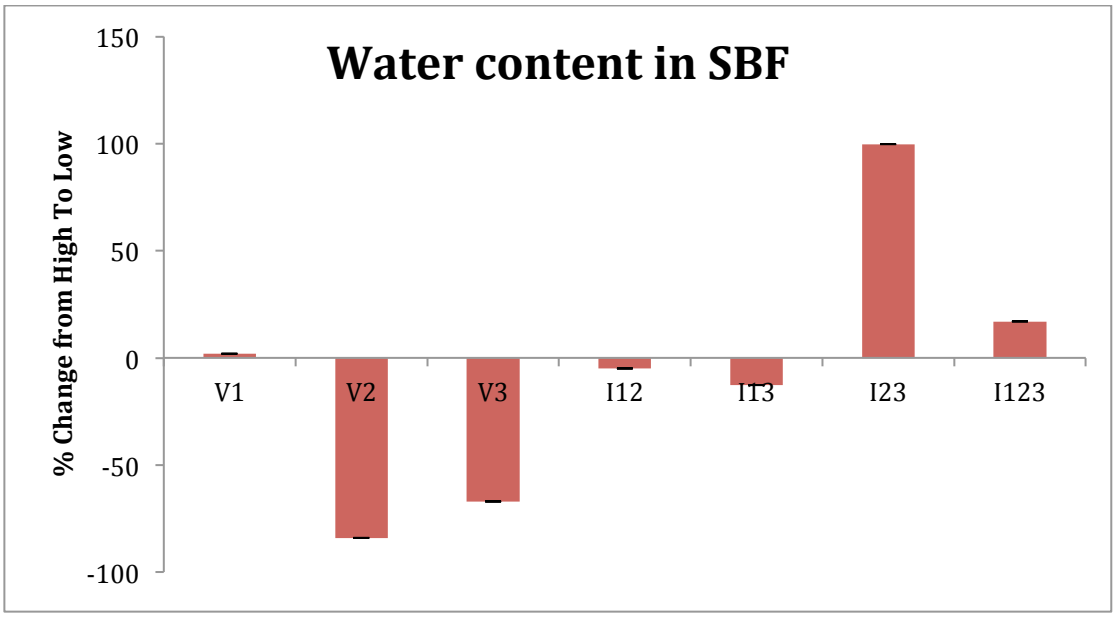

Figure 9

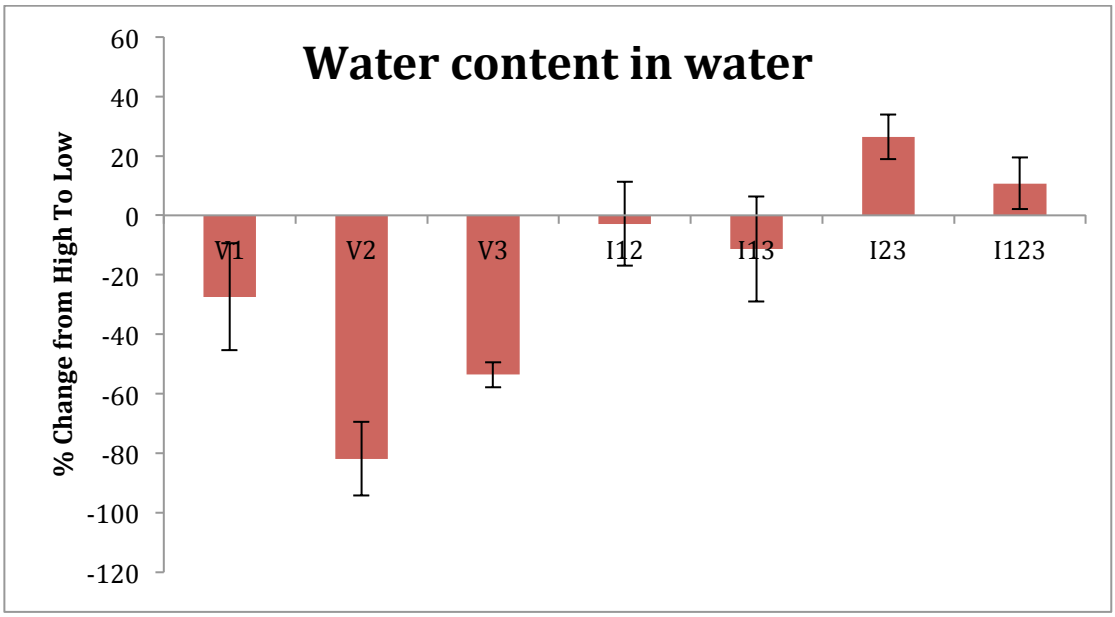

Figure 10